

Universidad Tecnológica de Pereira

Doctor of Engineering Program

Doctoral thesis:

Development of a methodology to construct driving cycles based on fuel
consumption and vehicle emissions

Author:

LUIS FELIPE QUIRAMA LONDOÑO

PEREIRA
2020

Development of a methodology to construct driving cycles based on fuel
consumption and vehicle emissions

LUIS FELIPE QUIRAMA LONDOÑO

A thesis submitted in fulfillment on the requirements for the degree of Doctor
of Engineering

Director: Juan Esteban Tibaquirá Giraldo, Ph.D.
Universidad Tecnológica de Pereira

Co-director: José Ignacio Huertas Cardozo, D.Sc.
Instituto Tecnológico y de Estudios Superiores de Monterrey

UNIVERSIDAD TECNOLÓGICA DE PEREIRA
Doctor of Engineering Program
PEREIRA
2020

Acceptance note

Director

Co-director

Jury

Jury

Jury

March 26th, 2020
Pereira

INSCRIPTION

To my wife, my parents, my sister, and my brother.

Luis Felipe Quirama Londoño

ACKNOWLEDGEMENT

Special acknowledgement to all the people who participate directly and indirectly in the ideation, planning and execution of this study.

Special acknowledgement to the Doctor of Engineering Program and to the Energy Management research group of Universidad Tecnológica de Pereira for hosting my doctoral studies.

Special acknowledgement to the research group on Energy and Climate Change of the Tecnológico de Monterrey for its guidance and for facilitating the database required for the development of this research.

Finally, a special acknowledgement to the MINCIENCIAS, COLFUTURO and the national doctorate program of call 727 of 2015 for the financial support provided during the development of the studies.

Luis Felipe Quirama Londoño.

Resumen

Este trabajo presenta el desarrollo de una metodología para construir ciclos locales de conducción utilizando el consumo de combustible y las emisiones del vehículo como criterios para evaluar su representatividad. Actualmente, el proceso para construir ciclos locales de conducción solo garantiza la representatividad en términos de los parámetros característicos (CPs). Los CPs a su vez están orientados a describir únicamente los patrones de manejo de la región de estudio y no el consumo de combustible ni las emisiones de los vehículos. Inicialmente se realizó una revisión del estado del arte acerca de los ciclos de conducción desarrollados en el mundo y su relevancia para desarrollar estrategias efectivas que busquen optimizar la operación de los vehículos disminuyendo su impacto energético y ambiental. En segundo lugar, se identificó que i) la cantidad y calidad de los datos de viajes monitoreados, ii) el método de construcción de los ciclos de conducción, y iii) los criterios usados para evaluar los ciclos de conducción son los factores principales que afectan su representatividad. Para mejorar la representatividad de los ciclos locales de conducción en términos del consumo de combustibles y las emisiones se desarrollaron, en este trabajo, un método determinístico denominado Fuel-based (FB) y un método estocástico denominado Energy-based Micro-trips (EBMT). El desempeño de los métodos desarrollados fue comparado con el de los métodos Micro-trips y Cadenas de Markov Monte Carlo, los cuales han sido tradicionalmente utilizados en la construcción de ciclos de conducción [1]–[3]. En segundo lugar, este trabajo analizó los criterios históricamente utilizados para evaluar la representatividad de los ciclos de conducción. Se concluyó que el porcentaje de tiempo en ralentí, la desviación de la aceleración, la velocidad promedio, la intensidad cinemática y la potencia específica del vehículo son los criterios de evaluación que garantizan ciclos de conducción con mayores niveles de representatividad. En tercer lugar, se identificó que el tiempo de duración del ciclo de conducción puede ser usado como un factor el cual influye en la representatividad de los ciclos generados. Se analizaron ciclos de conducción con tiempos de duración entre 5 y 120 minutos, concluyendo que ciclos de conducción muy cortos no representan los patrones de manejo de la región de estudio. Finalmente, este estudio presenta el desarrollo de un equipo de telemetría para monitorear el consumo de combustible, la velocidad y el tiempo de operación de un vehículo liviano de pasajeros. El desarrollo de este equipo fue necesario dado que los dispositivos disponibles comercialmente están diseñados principalmente hacia a la gestión y logística de una flota de vehículos, y por ende no facilitan el cálculo del impacto energético y ambiental del vehículo. Las variables registradas por este equipo y su frecuencia de muestreo corresponden a las condiciones requeridas por el EBMT para desarrollar ciclos de conducción que representen los patrones de manejo de una región, al igual que su consumo de combustible y las emisiones vehiculares.

Abstract

This work presents the development of a methodology to construct local driving cycles using fuel consumption and vehicle emissions as assessment criteria to evaluate the representativeness of the driving cycle. Currently, the process for constructing local driving cycles only guarantees representativeness in terms of the characteristic parameters (CPs). At the same time, the CPs are aimed to describe only the driving patterns and not the fuel consumption nor emissions of the vehicles. A review of the state of the art was carried out on the driving cycles developed in the world and their relevance to develop strategies to optimize the operation of vehicles, reducing their energy and environmental impact. We identified that i) the quantity and quality of the vehicle operation data, ii) the method to construct the driving cycles, and iii) the criteria used to assess the representativeness of the driving cycles, are the main factors that affect their representativeness. To improve the local driving cycles in terms of fuel consumption and emissions, a deterministic method defined as the Fuel-based (FB) method and a stochastic method defined as the Energy-based Micro-trips (EBMT) method were developed. The performance of the developed methods was compared with Micro-trips and Markov Monte Carlo Chain methods, which have traditionally been used in the construction of driving cycles [1]–[3]. Additionally, in this work is analyzed the criteria commonly used to assess the representativeness of driving cycles. We concluded that the percentage of time in idling, the standard deviation of acceleration, the average speed, the kinetic intensity and the vehicle specific power are the assessment criteria that guarantee driving cycles with high levels of representativeness respect to the driving patterns. Also, the time duration of the driving cycle was identified as a factor which influences their representativeness. Driving cycles with time duration between 5 and 120 minutes were analyzed. It was concluded that very short driving cycles do not represent the driving patterns of the region under study. Finally, this study presents the development of a telemetry equipment to register the fuel consumption, speed and operating time of a light-duty vehicle. The development of this equipment was necessary due to the available devices are oriented to the management and logistics of a vehicle fleets and they are not designed to determine the energetic and environmental impacts. The variables recorded by the telemetry equipment and its sampling frequency correspond to the inputs required by the EBMT to develop driving cycles that represent the driving patterns of a region, as well as its fuel consumption and vehicle emissions.

Table of contents

Resumen.....	6
Abstract.....	7
Table of contents.....	8
Figure list.....	11
Table list.....	13
1 Introduction.....	15
1.1 The importance of driving cycles in the energy efficiency of road transport	15
1.2 Thesis objectives	18
1.3 Structure of this document	19
2 Driving Cycles Based on Fuel Consumption.....	21
2.1 Introduction	22
2.2 Material and Methods	24
2.2.1 Regions of Study	24
2.2.2 Vehicles.....	26
2.2.3 Instrumentation	26
2.2.4 Data Collection	27
2.2.5 Assessment Methodology	27
2.3 Results and Discussion.....	28
2.3.1 Description of Driving Patterns	28
2.3.2 The SFC Distribution	29
2.3.3 Similitude of CPs and SAFDs.....	30
2.4 Conclusions	33
2.5 Appendix A	34
2.6 Appendix B	35
3 Comparison of three methods for constructing real driving cycles	37
3.1 Introduction	38
3.2 Materials and Methods.....	40
3.2.1 Selected regions	40
3.2.2 Monitored vehicles and instrumentation.....	41
3.2.3 Vehicle monitoring campaign	43
3.2.4 Implementation of the MT, MCMC and FB Methods	43
3.2.5 Test to Verify the Correct Implementation of the DC Construction Method ..	44
3.2.6 Methodology used to compare the MT, MCMC and FB methods	45

3.3	Results and discussion	48
3.4	Conclusions	53
3.5	Appendix A - Analysis of variation of the characteristic parameters in stochastic methods	54
4	Driving cycles that reproduce driving patterns, energy consumptions and tailpipe emissions	60
4.1	Introduction	61
4.2	Materials and methods	64
4.2.1	Route selection	65
4.2.2	Vehicle fleet and instrumentation	65
4.2.3	Monitoring campaign	67
4.2.4	Driving cycle construction method and assessment criteria	68
4.2.5	Assessment of representativeness of the driving cycles obtained by each method	69
4.2.6	Empirical results	71
4.2.7	Summary and conclusions	75
5	Main characteristic parameters to describe driving patterns	78
5.1	Introduction	79
5.2	Materials and methods	81
5.2.1	Selected regions	82
5.2.2	Vehicle fleet	82
5.2.3	Instrumentation	83
5.2.4	Monitoring campaign and data quality analysis.....	83
5.2.5	Method to identify the set of CPs that best describes driving patterns	84
5.3	Results	86
5.4	Conclusions	90
6	Relationship between the time duration of a driving cycle and its representativeness result.....	93
6.1	Introduction	94
6.2	Materials and methods	96
6.2.1	Region selection	96
6.2.2	Instrumented vehicles	96
6.2.3	Monitoring campaign	97
6.2.4	Comparison of the time DCs duration results	97
6.3	Results	99
6.4	Conclusions	104

7	Development of telemetry equipment for monitoring fuel consumption and vehicle operating variables	106
7.1	Introduction	107
7.2	Materials and method.....	109
7.2.1	Description of the telemetry equipment	109
7.2.2	Elements integrated into the telemetry equipment.....	112
7.2.3	Used vehicle to test the telemetry equipment	113
7.2.4	Method to validate the speed signals	113
7.2.5	Method for validating energy consumption records	114
7.3	Results	116
7.4	Conclusions	124
8	General discussion	126
	References	131

Figure list

Figure 1.1 Difference between the energy consumption results during the type approval (TA) test respect to the vehicle user perception [15].	16
Figure 1.2 Local driving cycles developed in cities or regions around the world. Figure built based on [18], [19], [28]–[32], [20]–[27].	17
Figure 2.1 Frequency distribution of the FCs measured of all trips considered in this study.	30
Figure 2.2 Average relative differences (ARD) of common characteristic parameters (CPs) used to describe driving cycles (DC) as a function of the number of trips sampled and the type of regions used in this study. (a) positive kinetic energy (PKE); (b) average speed; (c) percentage of time with positive acceleration; (d) percentage of idling time.	31
Figure 2.3 Comparison of the speed-acceleration probability distribution (SAPD) obtained for: (a) The sampled trips and, (b) The SFC closest to the average measured SFC of the sampled trips; (c) <i>QoF</i> as a function of the number of sampled trips.	32
Figure 2.4 Average relative differences (ARD) of characteristic parameters (CPs) commonly used to describe driving cycles (DC) as a function of the number of trips sampled and the type of regions used in this study. (a) maximum speed; (b) percentage of time in cruising; (c) percentage of time with positive acceleration; (d) average deceleration; (e) number of accelerations per kilometer; (f) root mean square and (g) percentage of time in deceleration.	34
Figure 3.1 Relative differences of the values reported by manufacturers with respect to the real fuel consumption or real CO ₂ emissions as function of the vehicles' model year. Sources: (a) [9], (b) [10], (c) [11], (d) [12], (e) [13], (f) [14], (g) [15], and (h) [16]. Dotted line shows the tendency obtained from data of reference (f) which are shown as red dots. References e-h include diesel and gasoline.	38
Figure 3.2 Illustration of the methodology followed to compare three alternatives to construct representative driving cycles	40
Figure 3.3 Illustration of the test used to verify the correct implementation of the methods to construct DCs. Artificial trips used (left side) and DCs (right side) obtained by (a) the MCMC and (b) the MT methods.	45
Figure 3.4 ARDi and their confidence intervals for some CPs with different number of runs. (a) Speed related CPs when applied MT. (b) Operation mode related CPs when applied MCMC.	48
Figure 3.5 Boxplots of the relative differences (RDi) of the CPs that describe the DCs obtained by the (a) MT, (b) MCMC, and (c) FB methods in the general region after 500 iterations. The ARDi are shown as blue dots, the IQRi by boxes, and the outliers by red “+” signs. The CPs used by each method as criteria for the construction of the DC are marked with (*).	50
Figure 3.6 Boxplots of the relative differences (RDi) of the CPs that describe the DCs obtained by the (a) MT, (b) MCMC, and (c) FB methods in the Urban 1, Urban 2 and Mountain regions after 500 iterations. The ARDi are shown as blue dots, the IQRi by boxes, and the outliers by red “+” signs. The CPs used by each method as the criteria for the construction of the DC are marked with (*).	52
Figure 3.7 Driving cycles calculated from the same set of trips data and using a stochastic method.	55

Figure 4.1 Proposed methodology to evaluate the representativeness of the driving cycles constructed following the EBMT method.....	64
Figure 4.2 Box and whisker plots of the RDi after 1000 iterations obtained by the MT method using as assessment criteria a.) Average speed and % idling, b.) SFC, d.) SFC, Average speed and % idling, and d.) SFC, average speed, % idling and EI of CO ₂ , CO and NO _x for the case of Urban 1 region.	73
Figure 4.2 Illustrative results for ARDi (blue dots), IQRi (boxes) and outliers (red “+”) obtained after constructing 1000 times DCs by the MT method and using as assessment parameters a.) SD a+, % idl, and the Ave s which is one of the best combination, and b.) SD a+, Ave a+ and Max a+, which is an arbitrary selected combination. The CPs used by each method as criteria for the construction of the DC are marked with (green “*”).....	88
Figure 6.1 Time duration and average speed for driving cycles developed for different regions or cities. * Correspond to driving cycles for motorcycles.....	95
Figure 6.2 (a) Average ARD and average IQR of characteristic parameters for different driving cycle time duration. (b) Average ARD and average IQR of emissions for different driving cycle time duration, for the region Urban 1.....	100
Figure 6.3 (a) Average ARD and average IQR of characteristic parameters for different driving cycle time duration. (b) Average ARD and average IQR of emissions for different driving cycle time duration, for the region Urban 2.....	104
Figure 7.1 Control methodology of the telemetry equipment.....	111
Figure 7.2 Components of the telemetry equipment.....	113
Figure 7.3 Comparison between the speed register by the equipment and the driving cycle data	117
Figure 7.4 Coefficient of determination analysis between the telemetry equipment and gravimetric test results	117
Figure 7.5 ARD and the IQR of the CPs for different time lengths of driving cycles	121
Figure 7.6 Five driving cycles proposed for Pereira	124
Figure 8.1 Methodology and main outputs of the thesis by chapter	130

Table list

Table 2.1 Characteristics of the roads considered in this work.	24
Table 2.2 Technical characteristics of the instruments used in this study.	27
Table 2.3 Characteristic parameters (CPs) that describe the driving patterns followed by drivers during the monitoring campaigns at every region considered in this study.....	29
Table 3.1 Description of the regions considered in this work. Taken from Huertas et al. [54]	41
Table 3.2 Technical characteristics of the instruments used in this work.....	42
Table 3.3 Input parameters used in the three methods of constructing DC.	44
Table 3.4 CPs that describe the driving patterns, fuel consumption and emission of pollutants, observed in regions G (General), U1 (Urban 1), U2 (Urban 2) and M (Mountain). Average relative differences (in percentage) observed between CPs of driving pattern and driving cycle, after 500 iterations. Boxes highlighted in green correspond to CPs with average relative differences below 10%. The numbers highlighted in italic and blue, indicates that the corresponding CP was used by the specified method as the assessment criteria for the construction of the DC. N/A: Not applicable.	47
Table 4.1 Some relevant driving cycles and the methods used for their construction.....	62
Table 4.2 Characteristics of routes considered in this work.	65
Table 4.3 Technical characteristics of the vehicles used in this study.....	66
Table 4.4 Technical characteristics of the instruments used in this study	67
Table 4.5 Characteristic parameters (CPs) used in this study to describe driving patterns and driving cycles	70
Table 4.6 Characteristic parameters that describe the driving patterns in Urban 1 and Urban 2 regions. ARDi for each CP	72
Table 4.7 <i>ARD</i> and <i>IQR</i> obtained for the different sets of assessment criteria after replicating the EBMT method 1000 times.....	74
Table 5.1 Construction methods and CPs used as assessment parameters in some DCs.....	80
Table 5.2 Description of the regions considered in this study.	82
Table 5.3 Technical characteristics of the instruments used in this study.	83
Table 5.4 Characteristic parameters used to describe driving patterns.....	86
Table 5.5 Top 15 out 1140 combinations of CPs that, when used as assessment parameters in the MT method, produce DCs that best represent driving patterns and best reproduce fuel consumption and tailpipe emissions in 2 urban regions in Mexico.	89
Table 6.1 Characteristics of the selected region.....	96
Table 6.2 Characteristics parameters used to describe the driving cycles in this study.....	99
Table 6.3 <i>ARD</i> results of the DCs characteristic parameters for the Urban 1 region.....	101
Table 6.4 <i>ARD</i> results of the DCs characteristic parameters for the Urban 2 region.....	102
Table 7.1 Measured and calculated signals through the telemetry equipment.	109
Table 7.2 Technical datasheet of the used vehicle	113
Table 7.3 Verification of values reported by the scale using mass.....	114

Table 7.4 Set of driving conditions used to test the telemetry equipment	115
Table 7.5 Comparison between the fuel consumption reported by the telemetry equipment respect to gravimetric test results	118
Table 7.6 Characteristic parameters used to describe driving patterns.	119
Table 7.7 Sets of assessment criteria with lowest values of <i>ARD</i>	120
Table 7.8 <i>ARD</i> and the <i>IQR</i> number results for different time lengths of driving cycles .	122
Table 7.9 Characteristic parameters of the five local driving cycles and driving patterns .	123

1 Introduction

1.1 The importance of driving cycles in the energy efficiency of road transport

Road transport of people and goods is one of the anthropogenic activities with the greatest environmental and energy impact. In 2018, the European environmental agency indicated that transportation generated nearly 60% of nitrogen dioxide (NO_x) emissions and 46% of particulate matter (PM₁₀) [4]. At global level, it is estimated that 74% of carbon dioxide emissions (5.2 Gt CO₂) come from this sector [5]. In terms of energy, road transport activities consume 35% of global energy resources, of which 91% is consumed by road transport [6].

In the Colombian context, road transport consumes 44% of energy resources, of which 95% is of fossil origin [7]. Private passenger vehicles are the largest energy consumers, followed by freight transport and public passenger transport vehicles [7]. On the other hand, in Colombia, road transport is one of the main sources of air pollutants. For instance, in Bogota, transport is responsible of 78% of the pollutant emission [8].

To reduce the environmental and energy impact produced from the operation of vehicles, countries and regions have implemented policies to monitor and control the energy consumption and emissions of vehicles that enter to the fleet. The implementation of these policies and a type approval test have shown that the technological improvement of vehicles has led to the gradual reduction of energy consumption and vehicle emissions. At the same time, these results have evidenced the difference between the energy consumption and vehicle emissions values reported by vehicle manufacturers through type approval tests, in comparison with values perceived by users under real driving conditions. Different authors have studied this difference obtaining different magnitudes. The authors of references [9]–[16] reported that vehicles users, according to the model and technology of the vehicle, observed between 9% to 60% more energy consumption than that reported by the vehicle manufacturer.

The type approval tests carried out by vehicle manufacturers to determine the energy consumption and emissions of different vehicle models are developed under controlled laboratory conditions. In this test, the vehicle is located on a roller dynamometer for simulating the restrictive forces that occur on the road related with a predetermined driving routine called the driving cycle. Driving cycles are generally expressed as time series of vehicle speed and they seek to represent the driving patterns of a city or region. Driving patterns are the way people drive their vehicles in a specific city or region. In some states of the United States, the driving cycles most used in the type approval tests are the FTP 75 and its supplementary cycles US06 used for higher speed, higher acceleration and aggressive driving behavior, HWFET used for driving under highway conditions, and SC03 represents the engine load and the emission associated with the use of air conditioning. Until 2017, in Europe, the type approval tests were performed using the New European Driving Cycle

(NEDC). This cycle presents steady speeds, acceleration and load, which hardly represent the real operating conditions of a vehicle. Then, the European regulations made the transition to a transient driving cycle called Worldwide harmonized Light vehicles Test Cycles (WLTC). The WLTC features high acceleration-speed and high RPM-power ranges, which even covers the limited NEDC ranges [17]. The WLTC presents operation characteristics similar to those that a vehicle can have under normal operating conditions. A similar path was adopted by Japan by replacing its JP 10-15 steady state driving cycle used until 2011, with JC-08 transient driving cycle.

Many of the vehicle operational conditions presented under real driving conditions are not represented by the approval tests. The author of reference [15] developed an analysis of the factors that increase the difference between the energy consumption value reported by the automakers and the one perceived by the user. Figure 1.1 summarizes these factors.

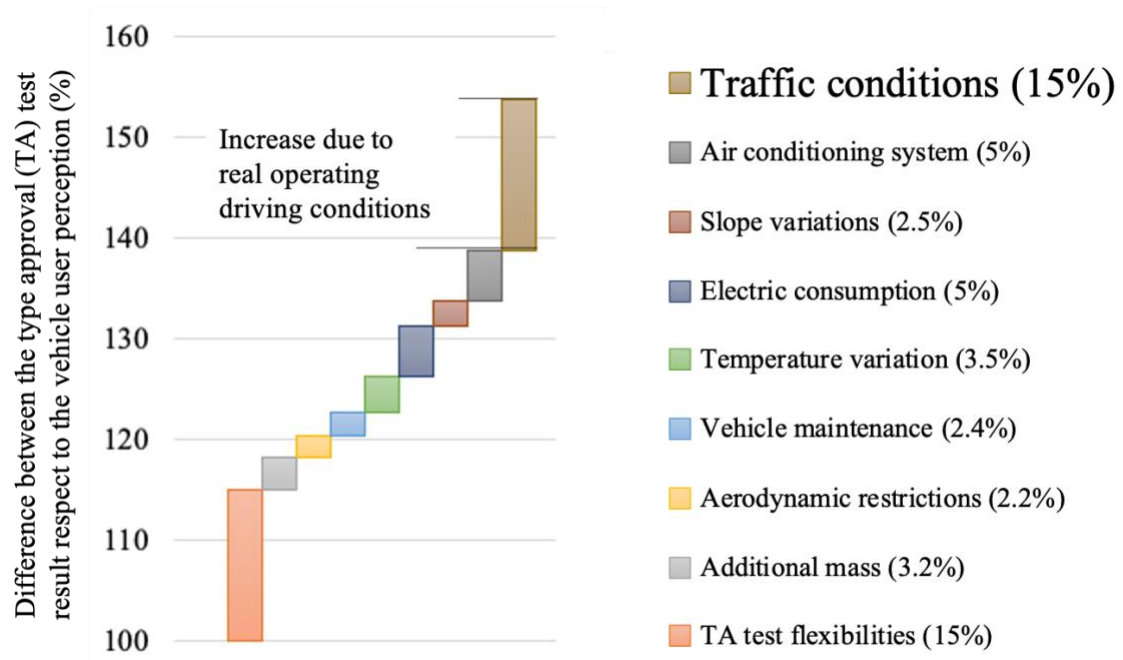


Figure 1.1 Difference between the energy consumption results during the type approval (TA) test respect to the vehicle user perception [15].

The Figure 1.1 indicates that within the procedures of the type approval test, the enlistment and the measurement of the mechanical, energetic and environmental performances of the vehicle, could present flexibilities and tolerances that increase the vehicle energy consumption up to 15%. Externalities such as the additional mass to the one considered in the homologation test, aerodynamic restrictions, the condition and maintenance of the vehicle, variations in the ambient temperature and changes in the slope of the road can generate increases in vehicle energy consumption up to 14%. The electrical consumption of the systems of the vehicle, such as lighting and entertainment, and the use of the air conditioning system, could increase energy consumption up to 10%. Finally, the traffic conditions and the driving patterns typical of the region, which have not been represented in the driving cycles used in the homologation test, could increase the energy consumption of around 15%.

The driving cycles commonly used in the type approval tests allow to verify the compliance with emission and energy consumption standards of different vehicle models under a consistent and unbiased framework. However, these cycles represent a small range of the driving patterns that could occur in a city or region, which could produce an underestimation of the energy consumption and emissions. Therefore, an inaccuracy in estimating the energy and environmental impact of the transport sector in the region of study is caused. Therefore, there is a need to study how the driving patterns of a given city or a region varies from the standard cycles.

As an alternative, local driving cycles have been developed to represent specific driving patterns of given cities or regions. Some of the local driving cycles developed in the world are presented in the Figure 1.2

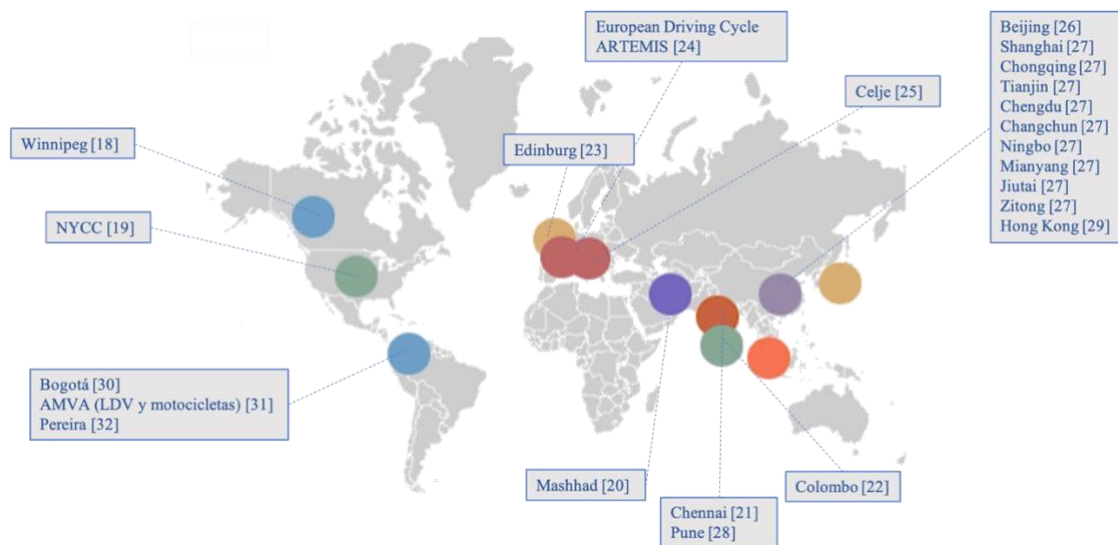


Figure 1.2 Local driving cycles developed in cities or regions around the world. Figure built based on [18], [19], [28]–[32], [20]–[27]

The local driving cycles are considered as a signature of the driving patterns of a city or region. The driving pattern varies from city to city and from region to region [23]. Local factor influencing the driving patterns, and its driving cycles, are the size of the studied city or region, the composition of the fleet, the infrastructure and morphology of the local road network, and driving habits [22]. Variations on the driving patterns also generate variations in the emissions and energy consumption of the vehicles when they are tested under their representative driving cycle.

Representativeness is the main issue for building a local driving cycle. The author of reference [33] indicates that the representativeness of a local driving cycle depends mainly on three factors:

- i) availability of a considerable amount of vehicle operation data
- ii) appropriate selection of the method of construction of the driving cycles
- iii) appropriate selection of parameters for the evaluation of the representativeness of the cycles

The vehicle operation variables via OBD (On-board diagnosis system), and geolocation data are currently available through the information and telecommunication technologies with high quality. Regarding the selection of the method for the construction of the driving cycles, two stochastic methods have been used historically: Micro-trips (MT), Markov Chain Monte Carlo (MCMC) and a deterministic method named trip-based method (TBM) [1]–[3]. To evaluate the representativeness of a driving cycle with respect to the driving patterns of a region, the aforementioned methods use criteria such as: average speed, maximum speed, average accelerations, number of accelerations per kilometer, among others, which are called characteristic parameters (CPs). Although current methods for constructing local driving cycles assures the representativeness in terms of driving patterns, they do not guarantee representativeness in terms of energy consumption and tailpipe emissions. This work proposes to move from measuring representativeness only in terms of driving patterns to measure it along with energy consumption and emissions.

The research questions established for this thesis are:

1. How to develop driving cycles that reproduce the driving patterns, energy consumption and emissions of a region?
2. How to reduce the gap between the energy consumption and the vehicle emissions results from the dynamometer test respect to the values perceived by the vehicle users?

1.2 Thesis objectives

To address these research questions the proposed general objective of this research project is

- Redesign the Micro-trips method for the construction of driving cycles, incorporating driving patterns, energy consumption and vehicle emissions, measured under real driving conditions, as representative criteria.

To achieve the general objective, the following specific objectives are established:

1. Incorporate the specific fuel consumption (SFC) as an evaluation criterion of the degree of representativeness of the driving cycles obtained under the Trip-based method (TBM).
2. Compare the representativeness of the driving patterns obtained with the driving cycles built using the methods: i) Micro-trips (MT), ii) Markov Chain Monte Carlo (MCMC) with respect to the method developed in objective 1.
3. Incorporate the specific fuel consumption (SFC) and vehicle emissions to the MT method, and evaluate the representativeness of the driving patterns that are obtained with the driving cycles built with this new method.

4. Identify the set of characteristic parameters, that together with fuel consumption, best describe the driving patterns of a region.
5. Analyze the relationship between the time duration of the driving cycle and the representative results of the driving patterns.

1.3 Structure of this document

The activities and results of each specific objective are presented by chapters. Chapters 1, 2, 3, and 4 correspond to articles published in scientific journals, while chapters 5 and 6 correspond to articles that are finished and in the process of being submitted to evaluation and publication process. Chapter 7 shows the technical characteristics and validation tests of a vehicle monitoring equipment developed from this project. Chapter 8 presents a general discussion of the thesis results. The thesis structure is explained below and the chapters corresponding to each specific objective are specified. Likewise, the information of the scientific journals where the articles have been published, the authors and the own contribution to each of the articles are presented.

Chapter 1. Introduction

Chapter 2 (Objective 1)

Huertas, J.; Giraldo, M.; Quirama, L.; Díaz, J. **Driving Cycles Based on Fuel Consumption**. *Energies* 2018, 11(11), 3064; <https://doi.org/10.3390/en11113064>.
<https://www.mdpi.com/1996-1073/11/11/3064>

Quirama, L.: supported the design of the methodology, supported the development of the algorithm and software management, state of art review, data analysis, supported the writing of the original draft and visualization of the results.

Chapter 3 (Objective 2)

Huertas, J.; Quirama, L.; Giraldo, M.; Díaz, J. **Comparison of Three Methods for Constructing Real Driving Cycles**. *Energies* 2019, 12(4), 665.
<https://doi.org/10.3390/en12040665>.
<https://www.mdpi.com/1996-1073/12/4/665>

Quirama, L.: supported the conceptualization of the project, supported the design of the methodology, supported the development of the algorithm and software management, supported the development of the research, state of art review, data analysis, supported the writing of the original document and analysis of the results.

Chapter 4 (Objective 3)

Quirama, L.; Giraldo, M.; Huertas, J.; Jaller, M.

Driving cycles that reproduce driving patterns, energy consumptions and tailpipe emissions, *Transportation Research Part D: Transport and Environment*, Volume 82, 2020, 102294, ISSN 1361-9209,
<https://doi.org/10.1016/j.trd.2020.102294>.
<https://www.sciencedirect.com/science/article/pii/S1361920919312507>

Quirama, L.: development of research, analysis and data filtering, support for the writing of the original draft and visualization of the results

Chapter 5 (Objective 4)

Quirama, L.; Giraldo, M.; Huertas, J.; Tibaquirá, J; Cordero, D.

Main characteristic parameters to describe driving patterns

Quirama, L.: supported the conceptualization of the project, supported the design of the methodology, supported the development of the algorithm and software management, supported the development of the research, state of art review, data analysis, supported the writing of the original document and analysis of the results.

Chapter 6 (Objective 5)

Quirama, L.; Giraldo, M.; Huertas, J.; Tibaquirá, J.

Relationship between the time duration of a driving cycle and its representativeness result

Quirama, L.: supported the conceptualization of the project, supported the design of the methodology, supported the development of the algorithm and software management, supported the development of the research, state of art review, data analysis, supported the writing of the original document and analysis of the results.

Chapter 7

Quirama, L.; Tibaquirá, J.; Huertas, J.; Castillo, J.; Mejia, J.; Valencia, M.

Development of telemetry equipment for monitoring fuel consumption and vehicle operating variables

Quirama, L.: supported for the conceptualization of the project, supported for the design of the methodology, supported for the development of the algorithm and software, analysis and filtering of data, supported for the writing of the original draft and visualization of the results.

Chapter 8

General discussion of the thesis results

2 Driving Cycles Based on Fuel Consumption

Abstract: Type-approval driving cycles currently available, such as Federal Test Procedure (FTP) and Worldwide harmonized Light vehicles Test Cycles (WLTC), cannot be used to estimate real fuel consumption nor emissions from vehicles in a region of interest because they do not describe the local driving patterns. We defined a driving cycle (DC) as the time series of speeds that when reproduced by a vehicle, the resulting fuel consumption and emissions are similar to the average fuel consumption and emissions of all vehicles of the same technology driven in that region. We also declared that the driving pattern can be described by a set of characteristic parameters (CPs) such as mean speed, positive kinetic energy and percentage of idling time. Then, we proposed a method to construct those local DC that use fuel consumption as criterion. We hypothesized that by using this criterion, the resulting DC describes, implicitly, the driving pattern in that region. Aiming to demonstrate this hypothesis, we monitored the location, speed, altitude, and fuel consumption of a fleet of 15 vehicles of similar technology, during 8 months of normal operation, in four regions with diverse topography, traveling on roads with diverse level of service. In every region, we considered 1000 instances of samples made of m trips, where m varied from 4 to 40. We found that the CPs of the local driving cycle constructed using the fuel-based method exhibit small relative differences ($<15\%$) with respect to the CPs that describe the driving patterns in that region. This result demonstrates the hypothesis that using the fuel-based method the resulting local DC exhibits CPs similar to the CPs that describe the driving pattern of the region under study.

Keywords: driving patterns; characteristic parameters; fuel consumption

Frequent symbols and acronyms

Symbol	Description	Unit
<i>ARD</i>	Average Relative Difference	%
<i>R²</i>	Coefficient of determination	-
<i>CP</i>	Characteristic Parameter	-
<i>DC</i>	Driving Cycle	-
<i>ECU</i>	Engine Computer Unit	-
<i>FC</i>	Fuel Consumption	L/km
<i>GPS</i>	Global position system	-
<i>LoS</i>	Level of Service	-
<i>m.a.s.l.</i>	Meters above sea level	m
<i>OBD</i>	On board diagnosis system	-

<i>PKE</i>	Positive kinetic energy per distance traveled	m/s ²
<i>QoF</i>	<i>Quality of Fit</i>	-
<i>SAPD</i>	Speed acceleration probability distribution	-

2.1 Introduction

Currently, there is a need for local driving cycles. Existing type-approval driving cycles do not describe correctly the driving patterns of a region of interests causing large differences between the fuel consumption (FC) observed during every day normal use of the vehicle in that region and the FC reported by the manufactures [9].

At present, there is not a clear definition for driving patterns. This term is used vaguely to describe the way drivers drive. Authors describe driving patterns in terms of a set of characteristic parameters (CPs), also known as performance values (PVs). They are speed-time based variables such as average speed, percentage of idling time, average positive acceleration, positive kinetic energy, etc. It remains unclear which set of CPs properly describes a driving pattern but there is an agreement among authors that driving patterns influence vehicle fuel consumption [34], [35].

Driving cycles (DC) are time series of speeds that represent driving patterns [2], [34]. They have been constructed in the way that the values of the CPs of the DC are approximately equal to the values of the CPs that describe the driving patterns. DCs describe the workloads imposed on the vehicles and therefore have been used for assessing the environmental impact of traffic [36], and for optimizing new vehicles' powertrain configurations and engine control strategies to reduce fuel consumption (FC) [18]. In this manuscript, we distinguish two types of DC: local and type-approval DC.

Presently, the Worldwide harmonized Light vehicles Test Cycles (WLTC) and Federal Test Procedure (FTP), are some of the most well-known type-approval DCs [19], [37], [38]. These two DCs, as all type-approval DCs, are mainly used for the determination of vehicles' fuel consumption and the mass emission of air pollutants, for comparative and certification processes [33], [39], [40]. Manufactures report the measured fuel consumption when the vehicle follows a type-approval DCs as part of the introduction process of a new technology in the vehicles market [17], [41]. However, these existing type-approval DCs do not describe correctly the real-world driving patterns of any particular region.

The key issue relative to local DCs is their representativeness of the real-world local driving patterns. Authors look for DCs that provide a synthesized representation of the local driving patterns [36], [42], [43].

Two main approaches have been used to construct DCs. The first one is the micro-trips-based approach in which a large sample of time series of speeds (trips) are divided into micro-segments (known as micro-trips) which are speed vs. time sections with initial and final speeds equal to zero. Then, a set of micro-trips are selected "quasi-randomly" and spliced

together to form a candidate representative DC. A clustering step is occasionally applied for gathering micro-trips with similar speed-acceleration values. The selected DC is the one with CPs values similar to the respective average values of CPs of the trips collected. LA92, Singapore, Hong Kong and Bangkok DCs were obtained with this micro-trips approach [24], [40], [43].

The second approach to construct DCs is based on Markov theory and uses the Monte Carlo technique. Some examples are found in [1], [44], [45]. In this second approach, speed and acceleration ranges are discretized into n and m sections, respectively. They configure a matrix of $n \times m$ states. The measured values of speed and acceleration from all the sampled trips are grouped into those states, forming the speed acceleration frequency distribution (SAFD) or the speed acceleration probability distribution (SAPD) when the SAFD is normalized. Next, an $[(n \times m) \times (n \times m)]$ probability transition matrix is computed. Similar to the SAPD, those probabilities are computed by counting the number the times that vehicles moved from one state to another and then normalizing with respect to the total number of transitions. Then, the Monte Carlo simulation technique is used to produce a candidate DC. The process consists of using a random number to select the next state in a manner in which transitions with the highest probabilities are the most likely to be chosen. The process is repeated until a given distance is covered or a given trip time has been completed. Finally, as in the micro-trips' method, the representativeness of the candidate Monte Carlo simulated DC is evaluated with respect to a set of CPs whose average values are obtained from the entire set of sampled trips. Usually, an arbitrarily established threshold of ~15% defines the degree of similarity or maximum allowed differences [12], [45], [46]. Some authors use the SAPD with the same role of a CP and use a threshold of 10^{-3} as criteria of similitude between the SAPD of the driving patterns and the SAPD of the candidate local DC. The LA01 driving cycle was constructed using this approach [45]. The major drawback of these two approaches to construct DC is that they are based on stochastic processes and therefore, although the methods are reproducible, they are not repeatable. That is, the resulting DC is different every time the methods are applied.

Some authors have suggested to express the representativeness of the DC in terms of vehicle FC, where FC is expressed as the volume of fuel consumed over the distance traveled (L/km) [2], [47], [48]. However, none of them has evaluated this alternative due to the lack of simultaneous measurements of FC and vehicle speed.

To advance in this alternative, in this study we propose to redefine a representative DC as the time series of speeds that when reproduced by a vehicle, the resulting FC is similar to the average FC of all vehicles of the same technology driven in the same region. In this line of thought, several alternatives can be used to construct a representative DC. As first approach, we propose to sample a large set of time series of speeds (trips), simultaneously with vehicle FC. Then, the trip with the FC closest to the average value of FC of the entire population of trips sampled is selected as the representative DC. This approach is repeatable and reproducible. This work aims to demonstrate that by using this fuel-based method to construct DCs, the representativeness of driving patterns is also implicitly achieved.

2.2 Material and Methods

As stated before a driving pattern is the way drivers drive their vehicles in a given region. A local DC is a time series of speeds that represent that pattern. Both, driving patterns and local DCs are described by a set of CPs, such as average speed and average positive acceleration. Therefore, a local DC represent a driven pattern when for each CP, the value of that CP for the local DC is similar to the value of that CP for the driving pattern. For example, when the average speed of the local DC is equal to the average speed of the drivers in the region of interest. Aiming to demonstrate that by defining representativeness of the DC in terms of fuel consumption, representativeness in terms of driving patterns is also achieved:

- We monitored, for long periods of time, FC and vehicle speed of a fleet of vehicles of the same technology, running on regions with diverse characteristics.
- We evaluated the relative differences of the CPs of the selected fuel-based-DC with respect to the average CPs of the trips sampled. We repeated the process for a large number of subsets of sampled trips.

Next, we describe the details of each of these tasks.

2.2.1 Regions of Study

With the goal of providing generality to our work, we looked for regions with different topographies, located at high altitudes, featuring well-maintained roads and with different level of services (LoS).

Table 2.1 Characteristics of the roads considered in this work.

Parameter	Unit	Urban 1	Urban 2	Uphill	Mountain	General
Location	-	Mexico City	TOL	-	-	TOL-MEX
Facility	-	Local roadway	Arterial	Freeway	Freeway	Combined
Level of traffic	-	High	Medium	Medium	Low-Medium	Low-High
<i>LoS*</i>	-	F	E	C	C-B	B-F
Speed limit	km/h	60	60	80	110	60-110
Number of lanes	-	3	3	4	4	3-4
Length	km	11.5	18.8	16.1	41.3	71.6
Ave road grade	%	1.4	1.8	6.1	5.6	4.0
Max road grade	%	5.2	9.0	15.0	15.0	15.0
Min altitude	m.a.s.l.	2255	2611	2255	2233	2233
Max altitude	m.a.s.l.	2258	2637	3313	3313	3313

TOL: Toluca, MEX: Mexico. *LoS: Level of service. LoS is the level of quality of a traffic facility and represents a range of operating conditions, generally in terms of service measures such as speed and travel time, freedom to maneuver, traffic interruptions, and comfort and convenience. Classification was done according to the US Highway capacity manual [49].

The US Capacity Manual defines six levels of services (LoS). The letters designate each level, from A to F, where A represents the best operating conditions and F the worst. Each level of service represents a variety of operating conditions and the driver's perception of those conditions. A description for each LoS is presented below:

LoS A: describes primarily free-flow operations at average travel speeds, usually about 90 percent of the Free Flow Speed (FFS) for the given street class. Vehicles are completely unimpeded in their ability to maneuver within the traffic stream. Control delay at signalized intersections is minimal.

LoS B: describes reasonably unimpeded operations at average travel speeds, usually about 70 percent of the FFS for the street class. The ability to maneuver within the traffic stream is only slightly restricted, and control delays at signalized intersections are not significant.

LoS C: describes stable operations; however, ability to maneuver and change lanes in midblock locations may be more restricted than at LoS B, and longer queues, adverse signal coordination, or both may contribute to lower average travel speeds of about 50 percent of the FFS for the street class.

LoS D: borders on a range in which small increases in flow may cause substantial increases in delay and decreases in travel speed. LoS D may be due to adverse signal progression, inappropriate signal timing, high volumes, or a combination of these factors. Average travel speeds are about 40 percent of FFS.

LoS E: is characterized by significant delays and average travel speeds of 33 percent or less of the FFS. Such operations are caused by a combination of adverse progression, high signal density, high volumes, extensive delays at critical intersections, and inappropriate signal timing.

LoS F: is characterized by urban street flow at extremely low speeds, typically one- third to one-fourth of the FFS. Intersection congestion is likely at critical signalized locations, with high delays, high volumes, and extensive queuing.

We selected regions open to private companies offering regular passenger and cargo transit services. We considered four cases (Table 2.1).

- Urban 1, which corresponds to a flat, densely populated region. We arbitrarily selected a set of roads covering 11.5 km inside Mexico City (2255 m above sea level (m.a.s.l.)). These roads are characterized by highly congested traffic (i.e., *LoS E* or *F*).
- Urban 2, which corresponds to a flat region located on the outskirts of an urban region. We selected an 18.8 km-long road located on the outskirts of Toluca City (2611 m.a.s.l.), which has four lanes with a medium traffic flow (i.e., *LoS E*).
- Mountain, whose topography includes significant altitude changes (>500 m). We selected a 41.3 km-long highway connecting the cities of Toluca and Mexico. This region starts

at 2255 m.a.s.l., ascends to 3313 m.a.s.l., and then it descends to 2611 m.a.s.l. with a maximum road grade of approximately 15%. It has four lanes with high traffic (~33,632 daily vehicles, i.e., *LoS C*).

- General, which is a combination of the previous cases. The selected set of regions spans 71.6 km, with altitude variations from 2233 and 3313 m.a.s.l. and a maximum road grade of approximately 15%. This set of regions has both urban and suburban sections.

A comparison with the Real Driving Emissions (RDE) requirement conditions is provided in Annex A.

2.2.2 Vehicles

We looked for vehicles of the same technology with similar maintenance conditions, aiming to eliminate their effects on our study. Our collaborating company has a fleet of 680 passenger buses, with 28 express buses that operate in the regions described previously, making no intermediate stops to pick up or drop off passengers. The fleet of buses used in this study were made between 2012 and 2014. They use diesel-fueled engines (Cummins ISM 425) that deliver 425 HP and 2102 Nm. These busses have a capacity of 49 passengers and their gross vehicle weight is 13,850 kg. They are 3.6 m tall, 12.85 m long and 2.6 m wide. They exhibit an aerodynamic drag coefficient of 0.64 and a rolling resistance coefficient of 0.006 [50].

2.2.3 Instrumentation

The measurement of instantaneous FC is essential to our work. Automotive diesel technology controls the amount of fuel injected into the engine combustion chamber by controlling the fuel injection time. This variable is available in the engine control unit (ECU) and can be read via the on-board diagnosis (OBD) system. We used the OBD interface provided by the engine manufacturer to read, report and store the instantaneous engine FC at a 1 Hz sampling period. We verified the accuracy of the data obtained using this interface by comparing the FC obtained via OBD with results obtained using an external graduated tank, which is the standard procedure to determine vehicle FC [51], [52]. Based on the determination coefficient ($R^2 > 0.9$) and calibration slopes ($m = 1.06$) obtained in a correlation analysis between the results obtained by these two methods, we concluded that the determination of fuel consumption via OBD produces results comparable to the ones obtained using the calibrated tank.

High precision GPSs (Table 2.2) were used to monitor position, altitude and speed of the vehicles as functions of time. Algorithms were developed to identify events where data were missing or had atypical values. Trips with less than 90% of data availability were disregarded. It was observed that the speed values reported by GPS were equivalent to those reported by the OBD system. The GPS altitude was compared with manual measurements of altimetry. An additional algorithm was developed to correct frequent errors in the GPS-reported altitude.

Table 2.2 Technical characteristics of the instruments used in this study.

Variable	Instrument/ Trademark	Technical Characteristics
Position: latitude, longitude and altitude	GPS/Garmin 16x	Position: 3–5 m, 95% typical Frequency: 1 Hz Speed: 0.05 m/s RMS steady state PPS time: 1 microsecond at rising edge of PPS pulse
Speed and time		
Instantaneous fuel consumption	-	Estimated through the injection time Reported by ECU through OBD2

GPS: global position system; OBD2: on-board diagnostic system, second generation; ECU: engine control unit.

2.2.4 Data Collection

Four monitoring campaigns were carried out to obtain real on-road driving data. One monitoring campaign was performed per region as described in Table 2.1 (Urban 1, Urban 2, Mountain and General). Each region was measured in both directions using the instrumented buses described in the previous section. Buses were driven by the company's regular drivers, and the buses were in service while we monitored the driving variables (speed and time) along with altitude and instantaneous FC at a frequency of 1 Hz, minimizing any disruption to regular vehicle operation. The monitoring campaigns included trips during different hours of the day, different days of the week, including weekends, and different seasons of the year. The data quality was verified. Trips with less than 90% of data availability were disregarded. After QA/QC analyses, 46 trips per region were left with simultaneous measurements of position, altitude, speed, FC, and mass emission of pollutants.

2.2.5 Assessment Methodology

To gain generality in our conclusions, we studied the effects of the number of trips sampled on our results by randomly selecting sub-samples of trips out of the 46 trips sampled per region. The size of the sub-samples varied between 4 and 40. For each sample size, we repeated the sub-sampling process 1000 times.

At each instance, we applied the fuel-based method. This is, we selected the trip j with the FC closest to the mean value for the FC of the sub-sample (\overline{FC} in Equation (2.1)):

$$DC = Arg\{min_j |FC_j - (\overline{FC})|\} \quad (2.1)$$

Statistically speaking, the average FC calculated from the sub-sample is an estimation of the true mean FC of the whole population of busses monitored in each region. As we will show

later, the FC in every region followed a normal distribution (Figure 2.1) and therefore, the average value of the sub-sample is a good descriptor the true mean FC.

We hypothesized that by using the fuel-based method, implicitly, the obtained DC represents the driving patterns. i.e., the characteristic parameter i of the obtained local DC (CP_i^*) will be close to the average value obtained for that parameter from the sampled trips (\overline{CP}_i). To test this hypothesis, we calculated the relative difference of CP_i^* with respect to \overline{CP}_i at each iteration of the analysis described previously. Then, for each of the CP_i listed in Table 3, we reported the average relative differences (ARD_i) obtained for each sample size from $j=1$ to $j=n$. In this case the value of n was set on 1000 iterations (Equation (2.2)):

$$ARD_i = \sum_{j=1}^n \frac{(CP_{i,j}^* - \overline{CP}_i)}{n\overline{CP}_i} \quad (2.2)$$

Additionally, we used the quality of fit (QoF) metric (Equation (2.3)), [53] to evaluate the degree of similarity of the speed-acceleration probability distribution (SAPD) of the selected fuel-based DC to the SAPD of the subset of sampled trips. In Equation (2.3), $P_{i,j}^*$ is the probability that the vehicle travels within the bin i, j of speeds and accelerations, in the states matrix obtained for the selected DC. \overline{P}_{ij} is the corresponding average probability obtained for the sub-sample of trips. This metric is independent of the number of bins used in the discretization of the speed and acceleration ranges and has a maximum value of 2:

$$QoF = \sum_{i=1}^n \sum_{j=1}^m (P_{i,j}^* - \overline{P}_{ij})^2 \quad (2.3)$$

2.3 Results and Discussion

2.3.1 Description of Driving Patterns

As stated before, driving patterns are described by CPs but currently it is unknown which set of CPs fully describe them. It is feasible that some CPs could be no good descriptors of the driving pattern and that some CPs could be redundant (linearly dependent of others). Furthermore, it is also feasible that additional CPs or metrics are needed to fully describe those patterns. This could be the case of driving patterns in mountain regions where metrics that directly influence FC, such as average road grade, should be added to the set of CPs.

As the primary objective of this work is not to determinate the CPs or metrics required to fully describe a driving pattern, we selected the CPs most used in the literature. Table 2.3 lists those CPs. It also includes their average values obtained from the 46 trips sampled during the monitoring campaign and their confidence intervals with confidence level of 95%.

Additionally, for comparison purposes, we included the values of these CPs for the heavy-duty urban dynamometer driving schedule (HD UDDS). As expected, the resulting values depend on the local conditions and therefore their inter-comparison is meaningless.

Table 2.3 Characteristic parameters (CPs) that describe the driving patterns followed by drivers during the monitoring campaigns at every region considered in this study

			Regions												
CP		Unit	General			Urban 1			Urban 2			Mountain			HD UDDS
Dynamics	RMS	m/s ²	0.39	±	0.01	0.41	±	0.02	0.43	±	0.02	0.35	±	0.02	0.47
	PKE	m/s ²	0.25	±	0.01	0.34	±	0.02	0.34	±	0.02	0.19	±	0.01	0.27
	Accelerations per kilometre	km ⁻¹	7.9	±	0.8	11.8	±	2.5	8.5	±	0.8	6.6	±	0.8	10.7
Operation modes	Percentage idling	%	14.7	±	1.7	21.9	±	3.9	20.3	±	2.7	2.6	±	0.9	33.3
	Percentage acceleration	%	27.6	±	1.0	27.6	±	1.9	28.8	±	1.7	27.3	±	1.4	22.2
	Percentage deceleration	%	24.6	±	0.8	25.9	±	1.5	25.0	±	1.7	24.3	±	1.2	20.2
	Percentage cruising	%	33.1	±	1.5	24.6	±	1.8	25.9	±	1.8	45.7	±	2.6	24.3
Speed	Average speed	m/s	10.5	±	0.7	6.8	±	0.9	7.9	±	0.7	16.6	±	1.2	8.4
	SD speed	m/s	9.0	±	0.2	6.2	±	0.5	7.3	±	0.2	8.6	±	0.6	8.9
	Maximum speed	m/s	28.6	±	0.5	21.9	±	1.0	26.5	±	0.6	28.5	±	0.5	25.9
Acceleration	Average acceleration	m/s ²	0.43	±	0.01	0.46	±	0.01	0.46	±	0.02	0.37	±	0.01	0.57
	Average deceleration	m/s ²	-0.48	±	0.01	-0.49	±	0.02	-0.52	±	0.02	-0.43	±	0.02	-0.64
	SD acceleration	m/s ²	0.24	±	0.01	0.25	±	0.01	0.25	±	0.01	0.21	±	0.01	0.37
	SD deceleration	m/s ²	0.35	±	0.02	0.35	±	0.01	0.39	±	0.02	0.31	±	0.02	0.40
	Maximum acceleration	m/s ²	1.51	±	0.07	1.37	±	0.08	1.41	±	0.06	1.31	±	0.08	1.96
	Maximum deceleration	m/s ²	-2.29	±	0.15	-1.96	±	0.10	-2.13	±	0.14	-2.05	±	0.16	-2.07

SD: standard deviation, RMS: root mean square, HD UDDS: heavy duty urban dynamometer driving schedule, PKE: positive kinetic energy. $PKE = \frac{1}{L} \sum_{i=2}^n v_i^2 - v_{i-1}^2$, for $v_i > v_{i-1}$, otherwise $PKE = 0$. L is the distance traveled and v_i is vehicle speed at second i.

2.3.2 The SFC Distribution

As described in Section 2.2.5, we first needed a criterion to describe the mean FC of the subset of sampled trips. Classical statistics recommends the use of average values for this purpose, but this parameter is limited to cases in which the data exhibit a normal frequency distribution.

Figure 2.1 shows the FC frequency distribution obtained for all the buses in the regions considered in this study. We performed Anderson-Darling goodness-of-fit tests to evaluate if the FC of the vehicles were normally distributed and found p -values greater than 0.12 for all regions. This result indicates that, with a probability of 95%, those distributions fit a normal distribution. The 16 t buses monitored in this study showed a FC of 0.41 ± 0.04 L/km

in the region with high traffic (Urban 1), and of 0.37 ± 0.02 L/km in the region with medium level of vehicular traffic (Urban 2), which represent an FC with relative differences of less than 11% with respect to the combined region (0.37 ± 0.03 L/km). Unexpectedly, the minimum FC was obtained in mountainous regions with an average of 0.36 ± 0.04 L/km. For the purposes of possible future comparisons, these vehicles showed an SFC of 0.62 ± 0.03 L/km when they were travelling uphill on an average road grade of 6.1% and at an average speed of 66.6 km/h.

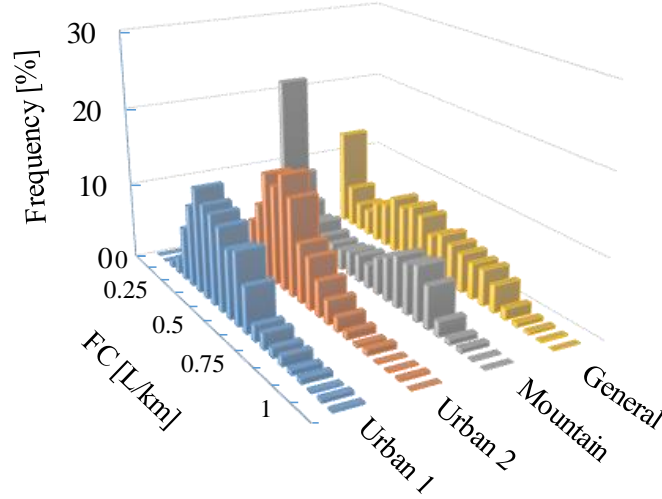


Figure 2.1 Frequency distribution of the FCs measured of all trips considered in this study.

2.3.3 Similitude of CPs and SAFDs

As stated before, we aimed to demonstrate that the fuel-based DC exhibit CPs (CP_i^*) close to the respective average CPs of the sampled trips (\overline{CP}_i). Figure 2.2 shows the average relative differences (ARD_i), as function of sample size, for some common CPs used to describe driving patterns.

Figure 2.2a shows the ARDs for the case of positive kinetic energy (PKE), which is a CP that directly influences FC. It shows that for all the regions, these differences are on average $<10\%$ after considering 1000 potential cases. These ARDs tend to decrease with the number of trips sampled, reaching a value of approximately 1.0% for a sample size of 40.

The same behavior was observed for the case of average speed (Figure 2.2b) and average acceleration (Figure 2.2c) but the ARDs were $<20\%$. These percentage of relative differences continue being small, especially considering they could range from zero to infinity and that they were obtained after considering 1000 possible cases.

Figure 2.2d shows the results of the ARDs for case of the percentage of idling time. It shows that the ARDs exhibit the same behavior as in previous cases but these differences on average are smaller than 40%, except for the mountain region. In this last region, the obtained ARD can be high ($<80\%$), and it does not always decrease with an increase in the number of trips sampled. Table 2.3 shows that in this region, the percentage of idling time is small (2.6%)

and therefore small absolute variations on idling time make the relative difference (ARDs) high. Idling time is a CP that weakly influence FC. It could be considered as an external factor or a non-related-human-factor, in consideration that when travelling, drivers naturally do not stop unless external factors force them to stop.

Other CPs are shown in Appendix A. For all CPs, the ARDs obtained are smaller than 20% except for the mountain region that in some cases reach ARDs of up to 40%.

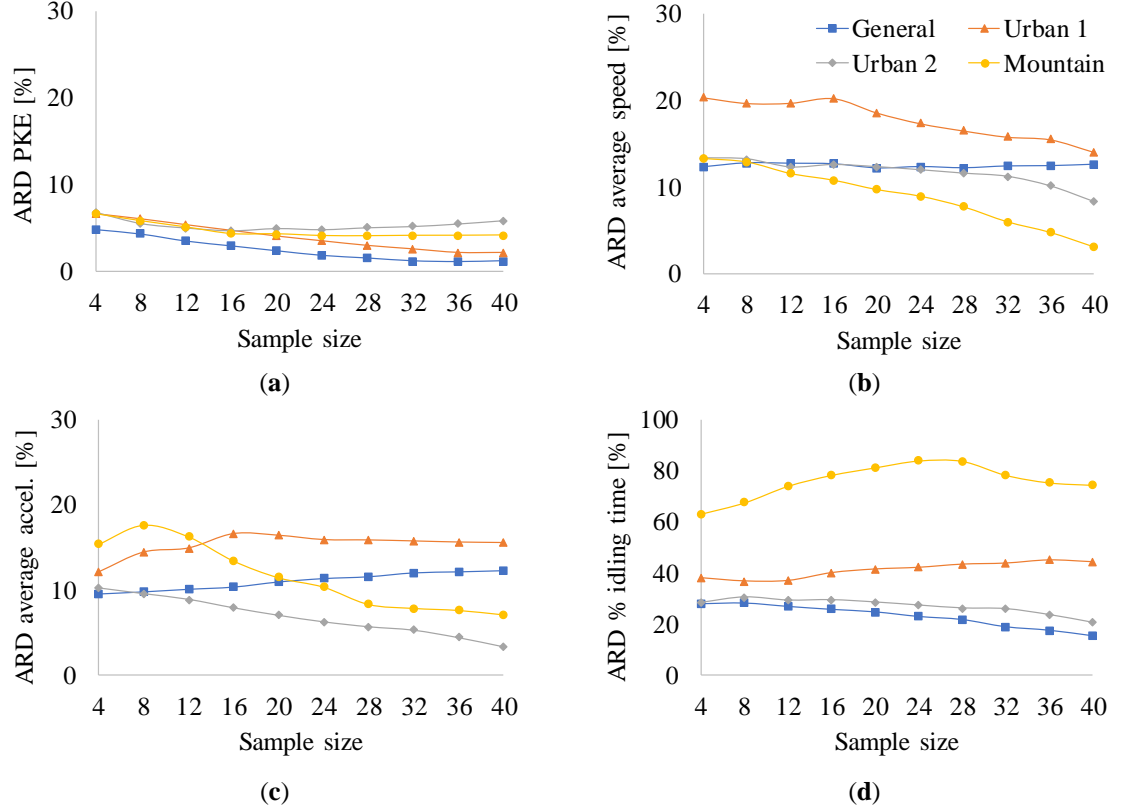


Figure 2.2 Average relative differences (ARD) of common characteristic parameters (CPs) used to describe driving cycles (DC) as a function of the number of trips sampled and the type of regions used in this study. (a) positive kinetic energy (PKE); (b) average speed; (c) percentage of time with positive acceleration; (d) percentage of idling time.

Several authors also use the speed-acceleration probability distribution (SAPD) as an alternative to describe DCs [2], [24], [33]. The SAPD can be thought of as a two-dimensional CP. We evaluated the level of closeness of the obtained SAPD for the selected fuel-based DC and the SAPD for the trips sampled, following the methodology described in Section 2.2.5.

Figure 2.3 shows (as an example) the SAPD obtained for a sample of 10 trips in the Urban 1 region (Figure 2.3a) and the corresponding SAPD obtained for the obtained fuel-based DC (Figure 2.3b). Qualitatively, they look similar. We used the quality of fit metric (QoF , Equation (2.3)) to quantify the level of similarity. Figure 2.3c shows the QoF metric as a function of the numbers of trips sampled. It shows that the QoF in all cases is smaller than

0.05, and those differences in probabilities expressed by the QoF tend to decrease with sample size, except for the case of the Mountain region. These values are negligible compared with the maximum value that this metric can assume ($QoF = 2$). Additionally, these values are also comparable to the ones found by Günther et al. [53] for the case of two similar DCs ($QoF \sim 10^{-3}$). These observations confirm that the SAPD of the DC with the FC closest to the average measured FC of the sample is similar to the SAPD of the sampled trips.

These results confirm that by using FC as the criterion of representativeness for a DC, the fuel consumption, CPs and SAPD of the fuel-based DCs are close to the measured fuel consumption, CPs and SAPD in flat regions.

Our experimental result for ARDs and $QoFs$ also suggest that samples of 10 to 20 trips are sufficient to describe the driving patterns in flat regions. However, we highlight that this result is valid for a single vehicle technology used with a single purpose, which is the scope of our work reported in this manuscript.

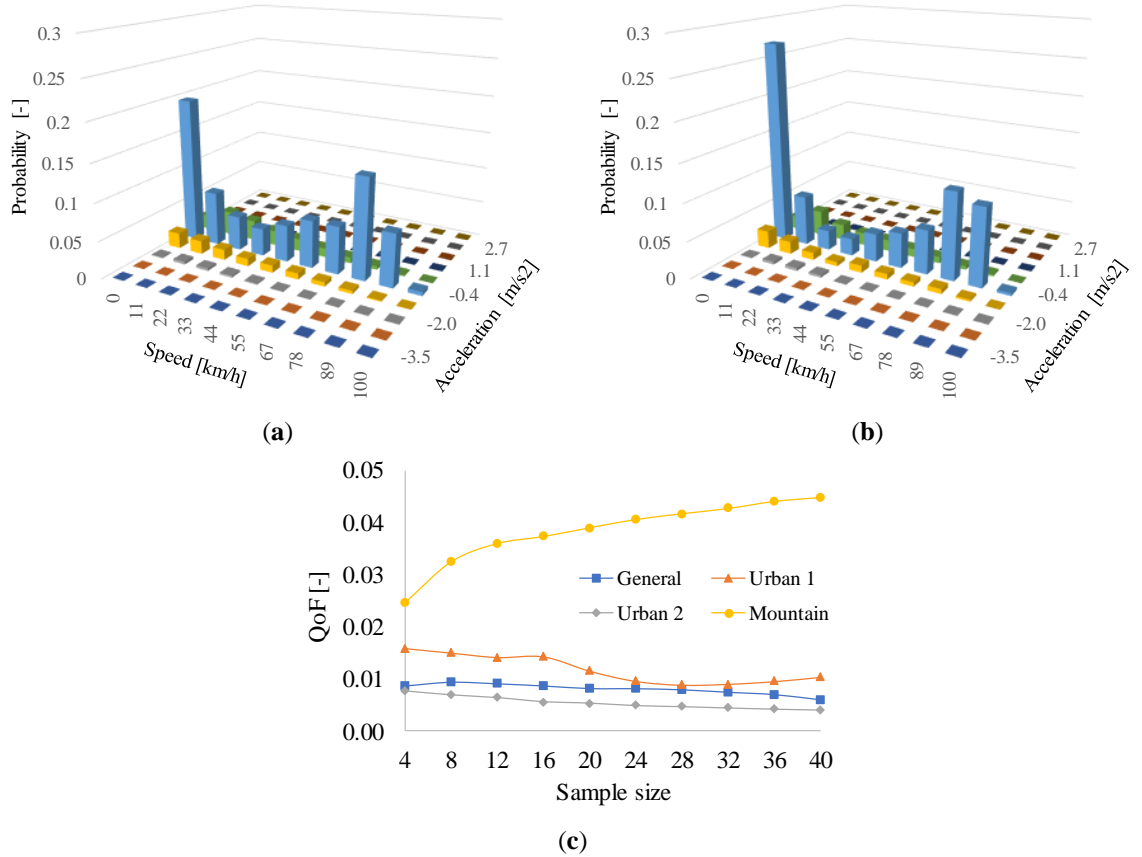


Figure 2.3 Comparison of the speed-acceleration probability distribution (SAPD) obtained for: (a) The sampled trips and, (b) The SFC closest to the average measured SFC of the sampled trips; (c) QoF as a function of the number of sampled trips.

2.4 Conclusions

Large differences currently observed in fuel consumption (FC) with respect to the FC reported by manufactures are mainly due to the lack of representativeness of the local driven conditions contained in the type-approval driving cycles used by manufactures during the introduction process of new vehicle technologies in the market.

A driving cycle (DC) represents the typical driving pattern of a given region when its characteristic parameters (CPs) exhibit similar values to the average CPs that describe the driving pattern in that region. Current alternatives to construct DC are repeatable but no reproducible, and there is no evidence that the resulting DC reproduce real vehicle fuel consumption (FC).

To address these two issues, we followed the suggestion of several authors of using FC as criteria to construct those DCs. We hypothesized that by re-defining a DC as the time series of speeds that when followed by a vehicle, its FC is similar to the average FC of all vehicles of similar technology operating in the same region, implicitly, the resulting DC describes the driving patterns in that region. Thus, we proposed to sample a large set of time series of speeds (trips), simultaneously with vehicle FC. Then, the trip with the FC closest to the average value of FC of the entire population of trips sampled is selected as the representative DC.

To demonstrate this hypothesis, we simultaneously monitored at a frequency of 1 Hz, for 8 months, the location, speed, altitude, and FC of a fleet of 15 vehicles of similar technology operating under normal conditions of use, in four regions of diverse topography and on roads of diverse level of service (LoS). We observed the average relative difference (ARD) between the CPs of the selected fuel-based DC and the CPs of the monitored driving pattern.

For the flat regions considered in this study, we obtained differences smaller than 15% for the CPs related to speed and acceleration that are directly influenced by the driver's decisions, such as average speed, positive kinetic energy, and average positive acceleration. We also observed that the speed-acceleration probability distribution (SAPD) of the selected fuel-based DC is similar to the SAPD of the sampled trips ($QoF \leq 0.05$). Furthermore, the level of similarity between CPs and SAPDs increased with the number of trips sampled.

These results confirmed our hypothesis. However, the percentage of idling time that could be considered an external factor (not a descriptor of driver patterns) showed the highest relative differences (up to 80% for the case of mountain regions). These differences could still be considered acceptable taking into consideration that: (1) this variable range from 0 to infinity; (2) we obtained those results after considering 1000 possible cases and (3) for the case of the mountain region the time spent by vehicles idling was short and therefore any small absolute difference has a large value when expressed as relative difference. Nevertheless, additional work is required to confirm the results described in this manuscript for several other vehicles technologies, and to establish the methodology to implement the resulting DC in a chassis dynamometer, specially, for the case of mountain regions.

2.5 Appendix A

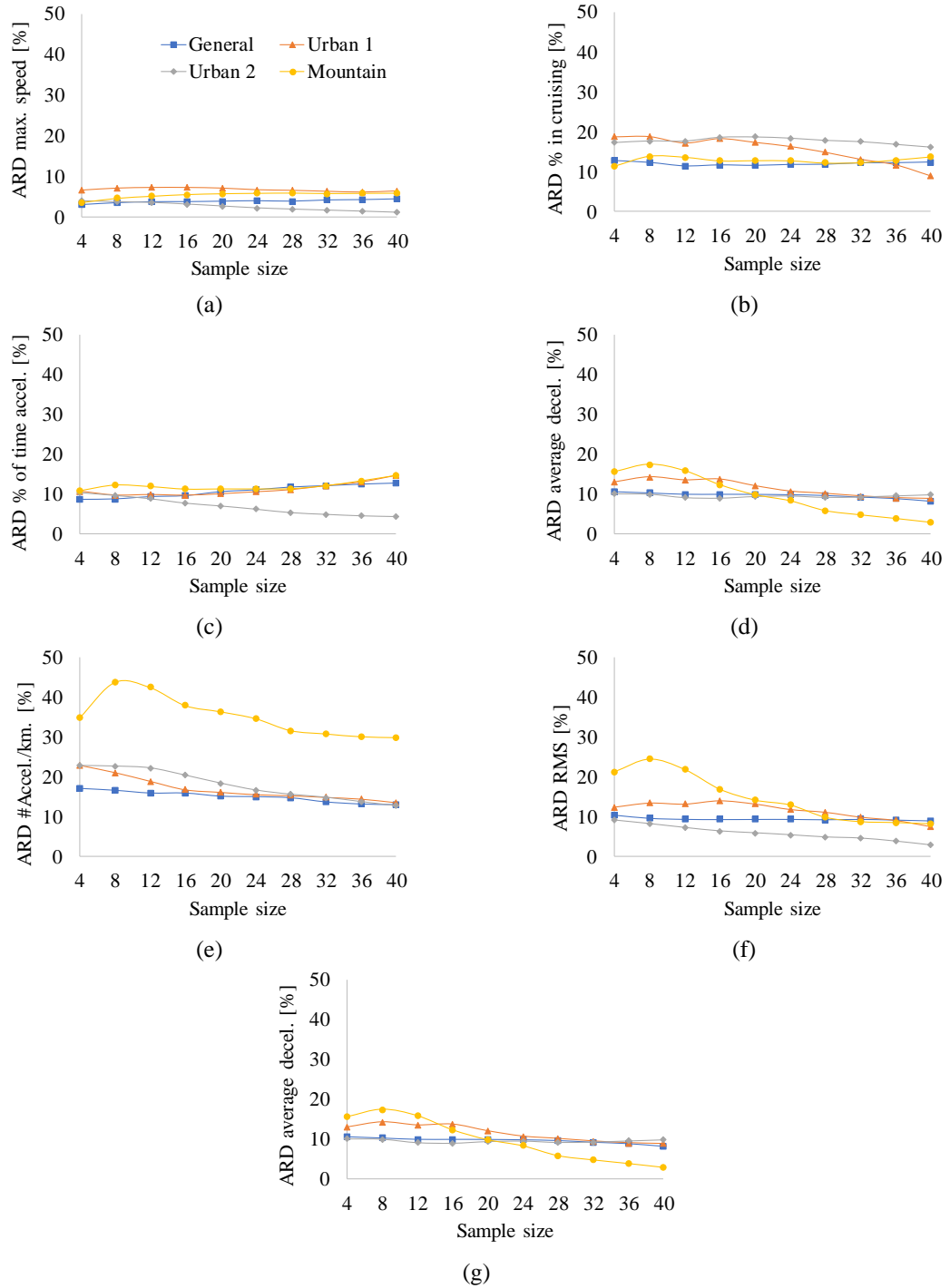


Figure 2.4 Average relative differences (ARD) of characteristic parameters (CPs) commonly used to describe driving cycles (DC) as a function of the number of trips sampled and the type of regions used in this study. (a) maximum speed; (b) percentage of time in cruising; (c) percentage of time with positive acceleration; (d) average deceleration; (e) number of accelerations per kilometer; (f) root mean square and (g) percentage of time in deceleration.

2.6 Appendix A

	General characteristics of the RDE test	Characteristics of the studied regions
Regions	34% in urban zone (ZU), 33% in rural zone (ZR) y 33% in highway (H). $ZU \geq 29\%$	Urban zone: 42% (Urban 1:16%, Urban 2: 26%) Mountain zone: 58%
Speed	Below 60 km/h in ZU. Between 60 km/h and 90 km/h in ZR. Above 90 km/h in H. The average speed in ZU must be between 15 km/h – 30 km/h	Average speed Urban 1: 24.48 km/h Urban 2: 28.44 km/h Mountain: 59.76 km/h Maximum speed Urban 1: 78.84 km/h Urban 2: 95.4 km/h Mountain: 102 km/h
Time	The time duration of the trip must be between 90 min and 120 min	Average time Urban 1: 1474 s Urban 2: 1986 s Mountain: 1305 s
Distance	Minimum 16 km / h in each of the regions.	Urban zone: 30,3 km Mountain zone: 41,3 km
Altitude	Moderate: less than or equal to 700 meters above sea level (m.a.s.l) Extended: between 700 m.a.s.l -1300 m.a.s.l The difference in height between the starting point and the end point must not exceed 100 m	Urban 1 Minimum: 2225 m.a.s.l. Maximum: 2258 m.a.s.l. Urban 2: Minimum: 2611 m.a.s.l. Maximum: 2637 m.a.s.l. Mountain Minimum: 2233 m.a.s.l. Maximum: 3313 m.a.s.l.
Temperature	Moderate: 273 K (0 °C) less than or equal to 303 K (30 °C) Extended: above or equal to 266 K (– 7 °C) less than or equal to 308 K (35 °C)	The temperature of the monitored trips is on average between 16°C and 22°C
Devices	Normal use of air conditioning and other auxiliary devices under road conditions	Vehicles monitored under normal operating conditions

3 Comparison of three methods for constructing real driving cycles

Abstract: This work compares the Micro-trips (MT), Markov chains–Monte Carlo (MCMC) and Fuel-based (FB) methods in their ability of constructing driving cycles (DC) that: (i) describe the real driving patterns of a given region and (ii) reproduce the real fuel consumption and emissions exhibited by the vehicles in that region. To that end, we selected four regions and monitored simultaneously the speed, fuel consumption and emissions of CO₂, CO and NO_x from a fleet of 15 buses of the same technology during eight months of normal operation. The driving patterns exhibited by drivers in each region were described in terms of 23 characteristic parameters (CPs) such as average speed and average positive kinetic energy. Then, for each region, we constructed their DC using the MT method and evaluated how close it describes the observed driving pattern in each region. We repeated the process using the MCMC and FB methods. Given the stochastic nature of MT and MCMC methods, the DCs obtained changed every time the methods were applied. Hence, we repeated the process of constructing the DCs up to 1000 times and reported their average relative differences and dispersion. We observed that the FB method exhibited the best performance producing DCs that describe the observed driving patterns. In all the regions considered in this study, the DCs produced by this method showed average relative differences smaller than 20% for all the CPs considered. A similar performance was observed for the case of fuel consumption and emission of pollutants.

Keywords: Fuel-based method; Micro-trips method; Markov Chains and Monte Carlo method; Driving patterns; Fuel consumption; Vehicle emissions.

List of symbols and acronyms

Symbol	Description	Unit
$ARDi$	Average relative difference of the characteristic parameter i	%
CP	Characteristic parameter	-
DC	Driving cycle	-
ECU	Engine control unit	-
FB	Fuel based	-
$IQRi$	Inter-quartile range of RD_i	%
MCMC	Markov Chain – Monte Carlo	-
MT	Micro – trips	-
RD_i	Relative difference of the characteristic parameter i	%
SAPD	Speed acceleration probability distribution	-
SFC	Specific fuel consumption	L/100 km

3.1 Introduction

As summarized in Figure 3.1, recent studies have shown that both fuel consumption and emissions in the real world are between 8% and 60% larger than those reported by manufacturers. Those differences cause inaccuracies in the vehicle emission inventories and mislead the efforts of the government authorities oriented towards the vehicles' fuel consumption and pollutants emission reductions. They also twist the fair evaluation of the energy and environmental performance of the vehicles and interfere with the healthy competition among automotive companies for producing greener vehicles. We hypothesize that the incorrect representation of the local driving patterns of the type-approval DC is the major source of the differences observed. Thus, there is a need for DCs that truly represent the local driving patterns.

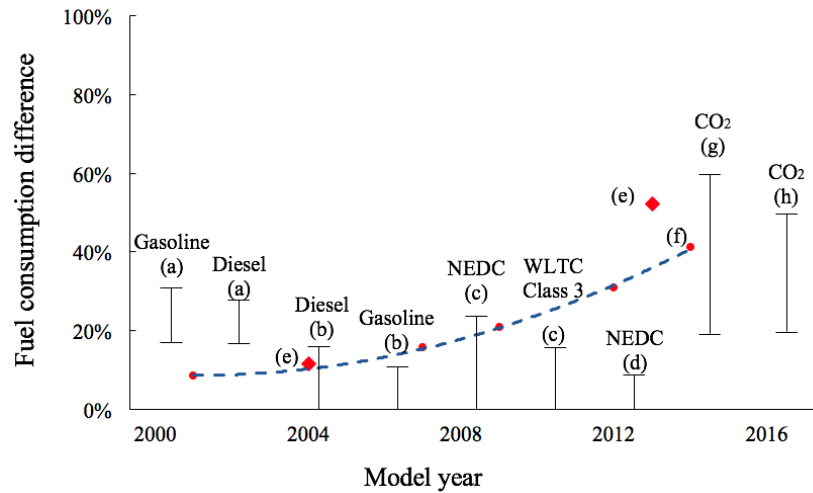


Figure 3.1 Relative differences of the values reported by manufacturers with respect to the real fuel consumption or real CO₂ emissions as function of the vehicles' model year.

Sources: (a) [9], (b) [10], (c) [11], (d) [12], (e) [13], (f) [14], (g) [15], and (h) [16]. Dotted line shows the tendency obtained from data of reference (f) which are shown as red dots.

References e-h include diesel and gasoline.

A driving cycle (DC) is a speed vs. time series that describe or represent the driving pattern in a given region of interest [2]. DCs are mainly used by manufactures and environmental authorities to evaluate the fuel consumption and pollutant emissions from vehicles as part of the regulatory process to introduce new vehicle technologies into the market [9], [10]. When the DC is used for regulatory purposes, we refer to it as a type-approval DC. Currently, the Federal Test Procedure (FTP) 75, Urban Dynamometer Driving Schedule (UDDS), New European Driving Cycle (NEDC), and Worldwide harmonized Light vehicles Test Cycles (WLTC) are some of the most widely type-approval DCs used by manufactures to report fuel consumption and emissions from their vehicles [17], [19], [37], [46].

Driving pattern is a term used to refer to the way drivers drive in a given region [54]. Although it is not explicitly stated, authors describe the driving patterns in terms of a set of

Characteristic Parameters (CPs) also known as Performance Values (PV) [2], [24]. They are parameters or variables that result from any combination of speed and time, such as mean speed, mean positive acceleration. DCs are also described by characteristic parameters. In this manuscript we use CP for the characteristic parameters that describe driving patterns and CP* for the characteristic parameters that describe DCs. There is a tacit agreement that a DC correctly describes a driving pattern when its CP*s are equal or close to the CPs that describe the driving pattern. The level of similitude is usually measured through the relative difference between them. Previous studies have proposed values between 5% and 15% as acceptable differences [24], [29]. However, the selection of the CPs and their thresholds values of similitude depend on the researcher's criteria or on empirical results.

The correct representation of the local driving pattern through a DC depends mainly on three factors: a) the quantity and quality of the vehicles' operation data used to describe the driving pattern, b) the CPs used as criteria during the construction process of the DC, and c) the DC construction method [33]. Next, we explore each one of them.

Currently, advances in information and vehicles technologies allow the monitoring of large samples of vehicles at high frequency (~ 1 Hz) with high quality and without interfering with their normal use. The preferred alternative is the direct reading of the Engine Control Unit (ECU). The ECU takes decisions on the engine operation based on the values reported by the sensors included by the manufacturer in the vehicle to monitor the instantaneous operational variables such as engine speed (in revolutions per minute), fuel consumption, engine load, etc. Thus, vehicle operation data collected from a large sample of vehicles operating in the region of interest, during long periods and different seasons can be used to correctly describe the driving patterns on that region.

There is not an agreement on the set of CPs that fully describe a driving pattern [55]. The mean speed, the idling time percentage and the Speed-Acceleration Frequency Distribution (SAFD) are the CPs most frequently used [2], [24]. Those CPs are not necessarily the CPs that most influence the vehicle's fuel consumption [54].

Finally, there is not a standard or unified method to construct DCs. Presently, the Micro-trips (MT) and the Markov chains - Monte Carlo (MCMC) methods are the most common approaches [45]. These methods are stochastic in nature and therefore they are repeatable but not reproducible, which means that they produce a different DC every time they are applied.

Even though fuel consumption is not a CP, as it does not describe a driving pattern, Huertas et al. [47] theorized that by guaranteeing similitude in terms of fuel consumption, similitude in pollutants emissions and representativeness of the driving patterns are implicitly achieved. Thanks to the advance in vehicle technology, nowadays it is possible to monitor, at low cost, in a large sample of vehicles, the instant vehicle fuel consumption rate through the ECU. This feature enables the possibility of constructing driving cycles based on the fuel consumption criterion [47]. We will refer to it as the fuel-based method (FB method).

Thus, this work aims to evaluate how well the DCs produced by the MT, MCMC and the FB methods represent local driving patterns. It also aims to evaluate the level of accuracy and precision that can be expected when they are used to measure real fuel consumption and pollutant emissions from vehicles. As an intermediate step, we developed a methodology to

assess the representativeness of the DC produced by each method of constructing DC and a procedure to ensure the correct implementation of those methods. We highlight the novelty and the relevance to our work of using fuel consumption and the emissions of pollutants linked to the assessment of the representativeness of the DCs.

3.2 Materials and Methods

Aiming to compare the MT, MCMC and FB methods, we implemented them in the same region and compared the DCs obtained by each method in relation to their ability i.) to describe the driving patterns of that region and ii.) to reproduce the fuel consumption and emissions exhibited by the vehicles in that region. To that end, we followed the activities described in Figure 3.2. To gain generality in our conclusions we repeated the process in four regions of different characteristics. The monitoring campaigns were described in a companion paper [54]. For the reader's convenience, next, we will summarize each of those activities.

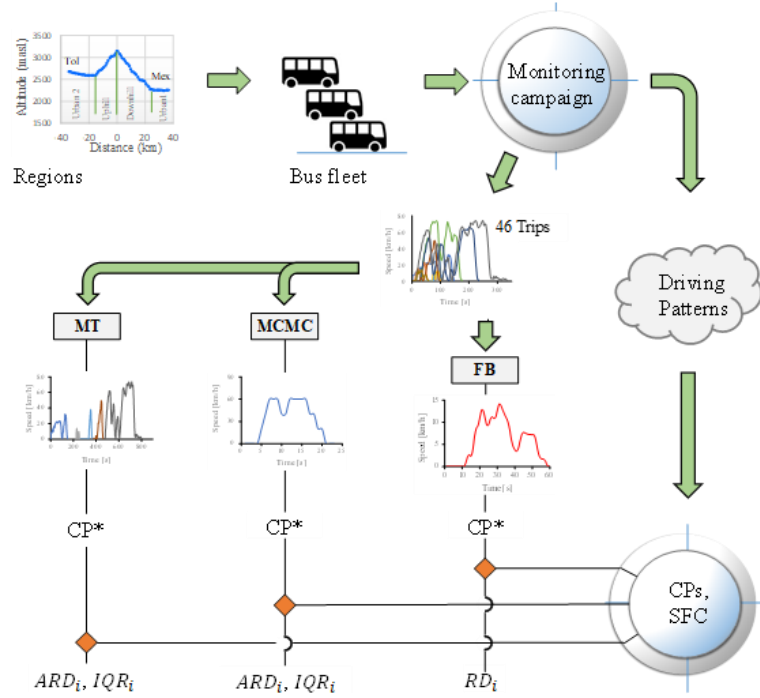


Figure 3.2 Illustration of the methodology followed to compare three alternatives to construct representative driving cycles

3.2.1 Selected regions

We considered four regions located at different altitudes and with different levels of traffic flow. Table 3.1 describe the characteristics of those regions.

Table 3.1 Description of the regions considered in this work. Taken from Huertas et al. [54]

	Units	General	Urban1	Urban2	Mountain
Location	-	TOL-MEX	Mexico City	TOL	-
Description		Combination of the Urban1, Urban2 and Mountain.	Flat, densely populated region inside Mexico City	Flat region located in the outskirts of the Toluca City	Topography includes significant altitude changes (>500 m)
Number of lanes	-	3-4	3	3	4
Facility	-	Combined	Local roadway	Arterial	Freeway
LoS*	-	B-F	F	E	C-B
Level of traffic	-	Low-High	High	Medium	Low-Medium
Length	km	71.6	11.5	18.8	41.3
Speed limit	km/h	60-110	60	60	110
Ave road grade	%	4.0	1.4	1.8	5.6
Max road grade	%	15.0	5.2	9.0	15.0
Max altitude	masl	3313	2258	2637	3313
Min altitude	masl	2200	2255	2611	2200

* LoS: Level of service. LoS is “the level of quality of a traffic facility and represents a range of operating conditions, generally in terms of service measures such as speed and travel time, freedom to maneuver, traffic interruptions, and comfort and convenience.” Number of passenger cars per mile per lane: A: 0–11, B: 12–18, C: 19–26, D: 27–35, E: 36–45 and F: >45, [49]

3.2.2 Monitored vehicles and instrumentation

We looked for a fleet of buses with the same emission control technology and with similar maintenance conditions in order to eliminate the effects of their variations in our results. The fleet of transit buses selected for this study was provided by the passengers’ transportation company Flecha Roja. Buses were manufactured between 2012 and 2014. They use diesel-fueled engines (Cummins ISM 425, 6 cylinders, and 10.8 liters) that comply with USEPA 1998 regulation for buses newer than 2004. Engines include EGR but they do not include catalytic converters (Selective Catalytic Reduction-SCR nor Diesel Oxidation Catalysts-DOC). They neither include particulate matter filters (DPF). These engines deliver 2102 Nm and 425 HP. Each bus has a capacity of 49 passengers and 13850 kg of gross vehicle weight. The buses are 12.85 m long, 3.6 m tall and 2.6 m wide

Table 3.2 shows the technical characteristics of the instruments used in this work. We obtained fuel consumption measurements, at a frequency of 1 Hz, using the engine manufacturer interface to read these data directly from the Engine Computer Unit (ECU).

The ECU controls the fuel injected into each engine's combustion chamber by controlling the time the fuel injector remains open at each engine stroke. We confirmed the accuracy of these data by comparing them with results obtained following the standard procedure to determine the vehicle's fuel consumption [51], [52]. The corresponding correlation analysis showed a determination coefficient (R^2) greater than 0.9 and calibration slope of 1.06

We used a high-precision GPS to monitor vehicle's position (latitude, longitude and altitude) as a function of time. Current technology in GPS is inaccurate measuring altitude. Hence, we took actual altimetry measurements and developed an algorithm to correct frequent errors in the GPS reported altitude [47].

Emissions measurements of CO, CO₂, NO, and NO₂ were carried out using a Sensors Inc. (Saline, MI, USA) PEMS, SEMTECH ECOSTAR model, with two modules, the SEMTECH-FEM and SEMTECH-NOx. The SEMTECH-FEM module measures CO and CO₂ emissions using a non-dispersive infrared gas analyzer with a resolution of 10 ppm and a range of 0-8% for CO, and a resolution of 0.01% and range of 0-20% for CO₂. The SEMTECH-NOx module measures NO and NO₂ using a non-dispersive ultraviolet gas analyzer with a range of 0-3000 ppm and 0-500 ppm, respectively, and a resolution of 0.3 ppm for both gases. Mentioned measurement methods are recommended by the USEPA [56].

Table 3.2 Technical characteristics of the instruments used in this work.

Variable	Instrument	Technical characteristics		
Instantaneous fuel consumption	Engine manufacturer	Reported by ECU based on fuel injection time Frequency: 1 Hz		
Position: latitude, longitude and altitude	GPS/Garmin 16x	Position: 3-5 m, 95% typical Frequency: 1 Hz Speed: 0.05 m/s RMS steady state		
		Technique	Range	Resolution
CO ₂	PEMS/ SEMTECH ECOSTAR	Non-Dispersive Infrared	0 - 20% v/v	0.01% v/v
CO		Non-Dispersive Infrared	0 - 8% v/v	10 ppm v/v
NO		Non-Dispersive Ultra Violet	0 - 3000 ppm v/v	0.3 ppm v/v
NO ₂		Non-Dispersive Ultra Violet	0 - 500 ppm v/v	0.3 ppm v/v
Flow Measurement		Exhaust Flow Meter	-	0.1 kg/h

Following manufacturer's instructions, we conducted leak checks and did zero and span calibrations prior to each test using NIST traceable calibration gases. We also used the automatic self-calibration option that this PEMS technology provides to control possible zeroing issues with the CO and NO_x PEMS's sensors. Self-calibrations occurred after every hour of continuous operation.

3.2.3 Vehicle monitoring campaign

We monitored 15 buses that were in service and were driven by the company's regular drivers while we obtained real on-road driving data at a frequency of 1 Hz, minimizing any disruption to regular vehicle operation. We carried out one monitoring campaign per region. Each campaign included trips carried out during different seasons of the year, different days of the week, and at different hours of the day.

Data quality was checked in three phases. During the first phase, trips with more than 5% of missing data were disregarded. The second phase identified outlier data for each trip. In this phase, we also checked for potential drifting problems of the CO and NO_x sensors by observing the evolution of CO and NO_x data. Additionally, we checked that, measurements of CO and NO_x concentrations came back to zero. We also plotted the 1-s CO and NO_x concentration frequency distribution and checked for potential positive or negative offsets. Finally, we plotted 1-s fuel rate vs. CO+CO₂ mass emission rate and checked for negligible offsets.

The last phase consisted of synchronizing the data from the vehicle's ECU with the emissions data reported by the PEMS. Data synchronization was obtained by dephasing each data set until maximum correlation was observed between variables that according to physics should be correlated, such as fuel consumption, engine speed, and emissions. After data quality analyses, we kept 138 trips with simultaneous measurements of position, altitude, speed, fuel consumption, and mass emission of pollutants.

3.2.4 Implementation of the MT, MCMC and FB Methods

We followed the most common approaches to implement the MT and MCMC methods. In the MT method, the trips sampled are partitioned into segments of trips bounded by vehicle speed equal to 0 km/h. These segments are called "micro-trips". Micro-trips are often clustered as function of their average speed and average positive acceleration. Then, a set of micro trips are quasi-randomly selected based on the frequency distribution of the clusters, and later spliced together producing a candidate DC [1], [3], [48].

In the case of MCMC method, the speed vs. time data of the trips sampled are encoded into operational states of speed-acceleration dyads [12], [46]. The occurrence frequency of the operational states is recorded in a state matrix. Using the same speed vs. time data a probability transition matrix is built by computing the frequency of moving from state X_i to state X_{i+1} . Then, the Monte Carlo technique is used to quasi-randomly select a collection of consecutive states that conform a state's vector. Subsequently, this vector is decoded in terms of speed vs time producing a candidate DC [24], [46] .

In both methods, the similarity between the candidate DCs and the observed driving pattern is evaluated using the relative differences between some selected CPs (Table 3.3). The CPs and the number of CPs selected depend on the researcher criteria. If the level of similarity is within the pre-established thresholds (relative difference <5%), the candidate DC is selected

as the representative DC. Otherwise, the process is repeated. The resulting DCs change each time any of these methods is applied, due to their stochastic nature. This means that these methods are repeatable but not reproducible.

We also implemented the FB method. In this approach, the average specific fuel consumption (SFC) of the trips sampled is computed. Then, the trip with the SFC closest to the average SFC is selected as the representative DC. The duration of the selected DC cannot be controlled, but the trip-based method is repeatable and reproducible.

3.2.5 Test to Verify the Correct Implementation of the DC Construction Method

Before comparing the results of the three methods to construct DCs, a verification step was performed to identify potential errors in the implementation of each method.

The implementation of the FB method was verified by comparing the results of the method implemented in this work with the results obtained by Huertas et al. [47]. In the case of the MT and MCMC methods, we started by specifying the values for the following input parameters: cycle duration, list of CPs used as criteria for the construction of the local DC, and the threshold used for the relative differences between the CPs. Table 3.3 shows the input parameters used.

To verify the correct implementation of the MT and MCMC methods, we designed the following test: use a unique and simple trip as input to the method for constructing DC and verify that the resulting DC is the same as the input trip. A different result will indicate that the method or the implementation of the method is unable of capturing the known driving pattern. Initially, we designed the artificial trip shown in Figure 3.3a Then we used it as substitute for the set of monitored trips that each method uses as input data. As all the input trips were exactly the same, the MT and the MCMC methods must produce the expected input trip as the resulting DC. As an example, Figure 3a shows the result reported by the MCMC method. These results confirmed our correct implementation of these two methods.

Table 3.3 Input parameters used in the three methods of constructing DC.

Criteria		MT	MCMC	FB
Cycle time (min)	General	105±2		~105*
	Urban 1	25±2		~25*
	Urban 2	29±2		~29*
	Mountain	35±2		~35*
CP_i or criteria used to construct the local DC		Average speed, % idling	Average speed, % idling	SFC
Acceptable relative difference between CP_i * and \overline{CP}		5 %	5%	$Min SFC_c - \overline{SFC} $
Other considerations		Categorization of micro-trips based on average speed	Speed and acceleration discretization	-

As a second phase of the test, we created the artificial trip shown in Figure 3b, and repeated the process. In this case, the trip consisted of three micro-trips, each with different acceleration ramps and cruise speeds. As an example, this figure displays the result reported by the MT method. It shows the ability of the methods to capture driving patterns and our correct implementation of the methods. For the description of the driving patterns, it is acceptable that the resulting DC exhibits changes in the sequence that the consecutive micro trips show up.

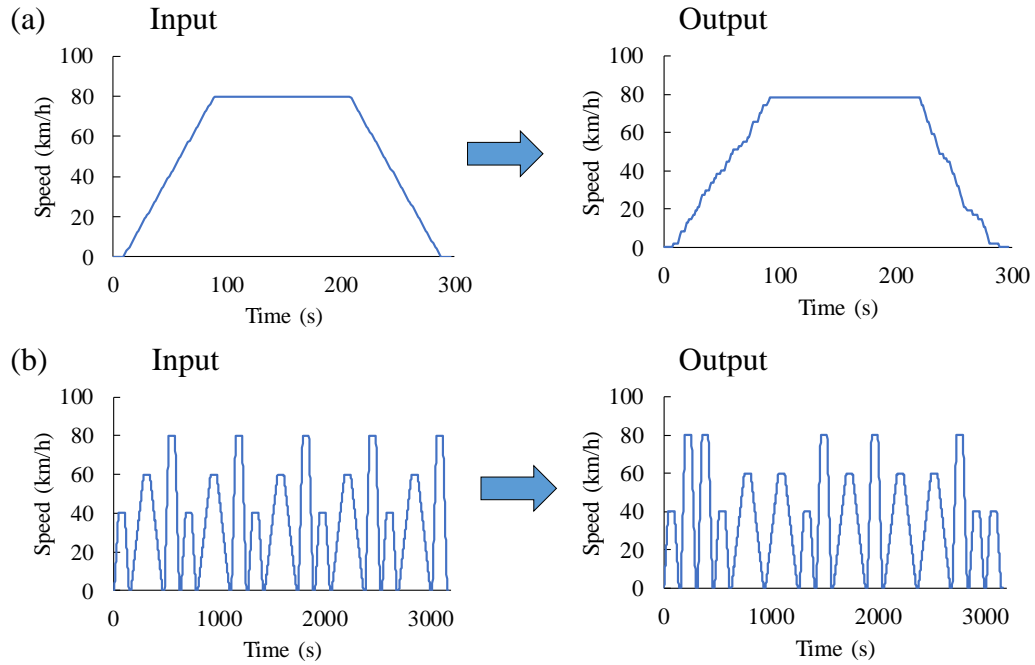


Figure 3.3 Illustration of the test used to verify the correct implementation of the methods to construct DCs. Artificial trips used (left side) and DCs (right side) obtained by (a) the MCMC and (b) the MT methods.

3.2.6 Methodology used to compare the MT, MCMC and FB methods

As stated before, the objective of this work is to compare the MT, MCMC and FB methods in their ability of producing DCs that (i) describe the driving patterns of a given region and (ii) represent the fuel consumption and emissions exhibited by the vehicles in that region. The introduction section explained that driving patterns and DC are described by a set of CPs, and that a DC represents a driving pattern when its CP_i^* match the CP_i of the driving pattern. Therefore, for each CP considered in this study we computed the relative difference (RDi) among CPs according to Equation 3.1. Table 3.4 shows the CPs considered in this study.

$$RD_i = \left| \frac{CP_i^* - CP_i}{CP_i} \right| \quad (3.1)$$

Equation 3.1 was also used to evaluate the relative differences of the vehicle's fuel consumption and its NOx, CO and CO2 emissions. For the case of the MCMC method, the fuel consumption and emissions associated to the resulting DC cannot be computed because each speed-acceleration operational state exhibited excessively large variations of fuel consumptions and emissions.

Equation 3.2 was used to calculate the relative differences between SAPDs. As stated before, the SAPD is an alternative way of describing driving patterns:

$$RD_{SAPD} = \frac{\sum_{i=1}^m \sum_{j=1}^r |P_{ij}^* - P_{ij}|}{2} \quad (3.2)$$

where P_{ij}^* is the probability that the vehicle travels at speed i and acceleration j according to the DC selected by any of the methods, and P_{ij} is the same variable for the driving pattern. r and m are the number of bins used for the discretization of the speed and acceleration, respectively. The maximum value that can reach the absolute difference between P_{ij}^* and P_{ij} is 2.

Table 3.4 CPs that describe the driving patterns, fuel consumption and emission of pollutants, observed in regions G (General), U1 (Urban 1), U2 (Urban 2) and M (Mountain). Average relative differences (in percentage) observed between CPs of driving pattern and driving cycle, after 500 iterations. Boxes highlighted in green correspond to CPs with average relative differences below 10%. The numbers highlighted in italic and blue, indicates that the corresponding CP was used by the specified method as the assessment criteria for the construction of the DC. N/A: Not applicable.

Characteristic parameters (CPs)			Observed driving pattern				Average relative differences after 500 iterations											
							FB				MT				MCMC			
Name		Symbol	G	U1	U2	M	G	U1	U2	M	G	U1	U2	M	G	U1	U2	M
Speed	Maximum speed	Max S	28.4	22.3	26.2	27.9	2.0	1.4	3.1	1.7	3.7	3.4	5.1	2.3	4.0	6.0	8.7	3.7
	Average speed	Ave S	11.9	7.3	10.0	17.0	20.6	0.0	0.0	0.0	2.4	2.5	2.5	3.8	2.6	2.5	2.4	2.5
	Standard deviation of speed	SD S	8.9	6.9	7.7	9.1	4.1	0.0	3.2	3.1	3.1	11.2	5.5	8.7	5.5	12.3	8.0	17.1
Acceleration	Maximum acceleration	Max a+	1.3	1.3	1.3	1.3	0.0	0.0	0.0	0.0	32.3	32.4	27.8	7.1	24.8	45.6	34.8	26.2
	Maximum deceleration	Max a-	-2.1	-2.1	-2.1	-2.1	0.0	0.0	0.0	0.0	19.8	20.0	19.1	36.1	22.5	18.6	19.4	11.2
	Average acceleration	Ave a+	0.4	0.5	0.4	0.4	0.7	1.7	4.0	0.0	2.6	3.4	4.9	3.1	77.1	42.4	59.6	141.3
	Average deceleration	Ave a-	-0.5	-0.5	-0.5	-0.4	1.4	0.0	10.7	6.9	3.1	6.0	7.2	10.3	69.7	46.5	60.8	121.5
	Standard deviation of acceleration	SD a+	0.2	0.2	0.2	0.2	0.0	5.0	6.5	1.2	3.0	7.9	20.3	25.0	35.1	17.5	32.1	47.3
	Standard deviation of deceleration	SD a-	0.4	0.4	0.4	0.4	1.9	5.1	3.4	4.5	3.7	12.3	12.8	28.3	17.3	13.8	14.3	19.3
Operational modes (% of time)	Idling	% idl	9.3	15.1	13.6	0.7	7.7	61.3	6.9	0.6	2.4	2.5	2.5	3.0	2.5	2.5	2.6	3.3
	Acceleration	% a+	30.2	32.9	33.8	25.4	7.9	9.1	6.3	9.9	3.2	3.3	5.0	5.2	36.7	23.5	34.5	49.8
	Deceleration	% a-	25.6	29.3	29.1	24.1	4.9	13.8	2.0	2.3	4.1	3.1	6.0	5.4	33.7	26.4	34.9	49.9
	Cruising	% cru	34.7	22.7	25.9	46.2	12.9	10.2	23.5	3.4	5.4	3.9	10.1	12.9	57.1	67.2	74.6	61.2
Dynamics	Number of accelerations per km	Accel/km	7.3	8.6	6.1	7.1	17.9	0.0	4.1	4.8	6.3	19.0	9.6	7.2	26.8	71.9	163.8	13.6
	Root mean square of acceleration	RMS	0.4	0.5	0.5	0.3	3.1	5.1	6.9	8.0	3.5	5.4	5.8	5.4	21.3	12.1	12.6	34.4
	Positive kinetic energy	PKE	0.2	0.4	0.3	0.2	10.6	9.0	11.6	0.0	4.7	5.2	6.4	6.6	5.0	5.8	6.1	7.5
	Speed-acceleration prob distribut	SAPD	0.0	0.0	0.0	0.0	7.5	2.3	2.2	9.8	3.6	6.2	5.6	9.3	7.2	27.1	8.7	35.9
	Vehicle specific power	VSP	8.3	4.8	7.0	11.9	29.8	0.0	0.0	12.9	8.8	3.2	7.3	18.0	N/A	N/A	N/A	N/A
	Kinetic intensity	KI	0.6	0.8	0.7	0.5	0.0	2.7	14.6	5.2	9.3	38.1	10.1	21.2	N/A	N/A	N/A	N/A
Fuel consumption and emissions	Specific fuel consumption	SFC	0.4	0.4	0.4	0.4	0.0	0.0	11.3	9.8	7.6	5.5	8.1	23.0	N/A	N/A	N/A	N/A
	Emission index of CO ₂	EF CO2	792.0	839.0	749.2	775.9	10.3	10.6	0.8	5.9	7.0	6.4	6.9	17.3	N/A	N/A	N/A	N/A
	Emission index of CO	EF CO	25.7	37.2	39.4	14.2	6.6	0.0	20.5	16.0	8.8	8.3	14.2	8.8	N/A	N/A	N/A	N/A
	Emission index of NOx	EF NOx	4.5	5.0	3.9	4.7	12.5	0.0	4.2	12.1	6.8	7.8	8.5	14.9	N/A	N/A	N/A	N/A

A major complication of this evaluation process is that the MT and MCMC methods produce different results every time they are used. To overcome this complication, we repeated the DC construction process several times and observed the average of the RDi obtained ($ARDi$). Figure 3.4a shows, as an example, the $ARDi$ obtained for the speed related CPs after 100, 500, and 1000 iterations of applying the MT method. Similarly, Figure 3.4b shows the $ARDi$ obtained for the CPs related to the of applying the MCMC method. Both figures also show the confidence interval of variation of the $ARDi$.

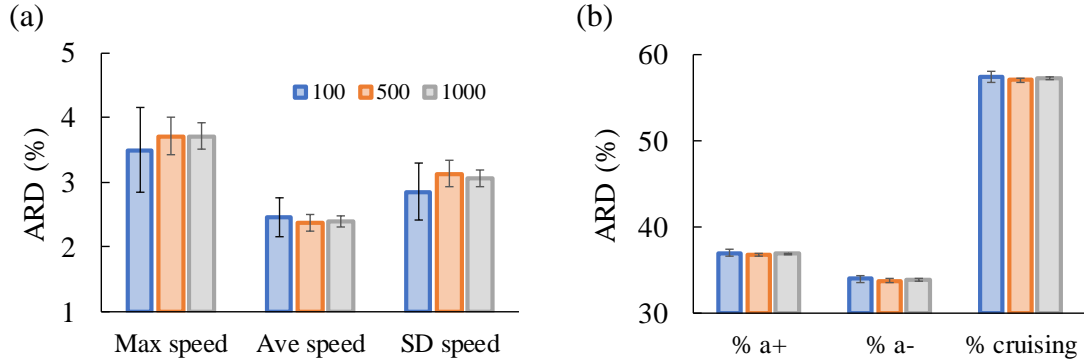


Figure 3.4 $ARDi$ and their confidence intervals for some CPs with different number of runs. (a) Speed related CPs when applied MT. (b) Operation mode related CPs when applied MCMC.

Figures 3.4a-b show that after 500 iterations the $ARDi$ and their confidence intervals remain constant. Pairwise hypothesis tests on the difference of means and the difference of variances confirmed this observation with a significance value of $\alpha=0.05$ for all $ARDi$. Thus, from this point on we will only report $ARDi$ after 500 iterations. The comparison of the FB, MT and MCMC methods of constructing DCs was complemented with a dispersion analysis of the RDi . We observed the variation of the RDi during the first 500 iterations. Some of the RDi exhibited an asymmetric distribution. Thus, we decided to use the inter-quartile range (IQR) as a metric for dispersion and to present the results in terms of whiskers and boxes plots.

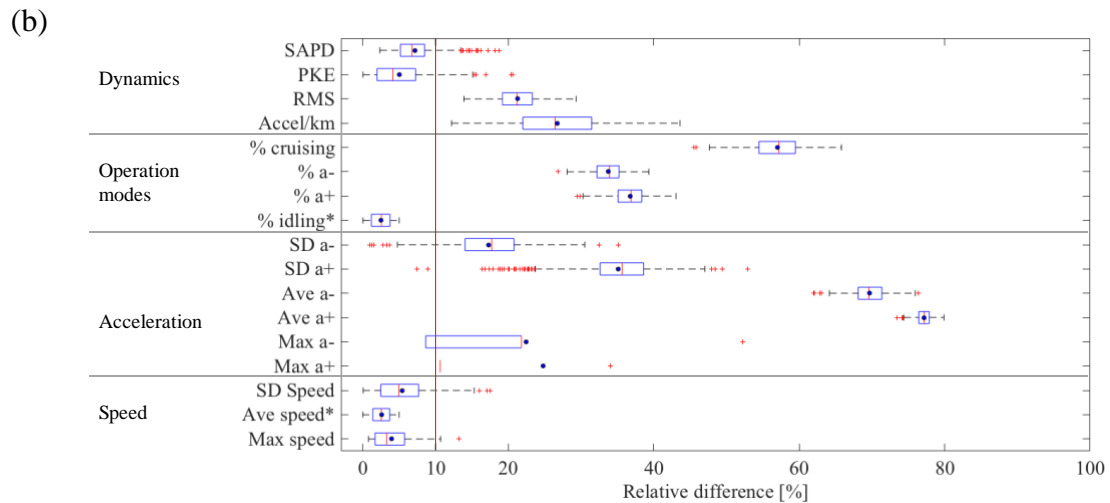
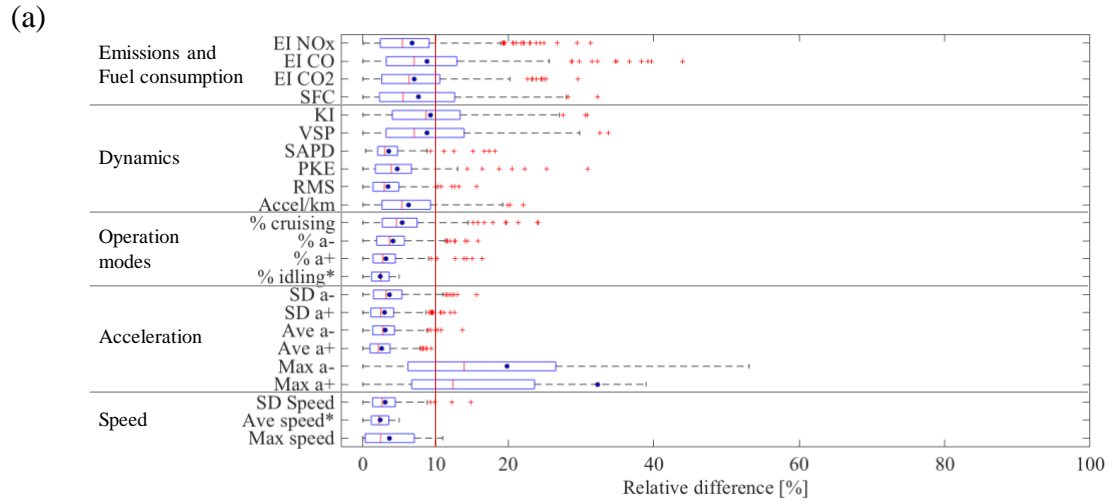
3.3 Results and discussion

Initially, we used the data from the 46 trips sampled in each region and obtained the average values for the 23 CPs that describe the respective driving pattern, fuel consumption and emission of pollutants. Table 3.4 shows the results obtained.

Then, we evaluated the ability of the three methods of producing DCs that represent the observed driving patterns. For the case of the general region, Figures 3.5a-b show the $ARDi$ and the interquartile range of the RDi exhibited by the DCs obtained by the MT and MCMC methods, respectively, after repeating the application of each method 500 times. Figure 3.5c shows the same information for the case of the FB method. As mentioned before in this last

case, results are the same every time the method is applied and therefore $ARDi = RDi$ for all CPs. In Figures 3.5a-b, the $ARDi$ are shown as blue dots, the $IQRi$ by boxes, and the outliers by red “+” signs. The CPs used by each method as criteria for the construction of the DC are marked with (*).

A low $ARDi$ (<10%) indicates that the method produced DCs that represent the driving pattern. The potential range of variation of the $ARDi$ is from zero to infinity and therefore $ARDi < 10\%$ indicates a high level of similitude. Table 3.4 presents the values of $ARDi$ obtained for the 23 CPs. In this table, the $ARDi$ below 10% are highlighted in green.



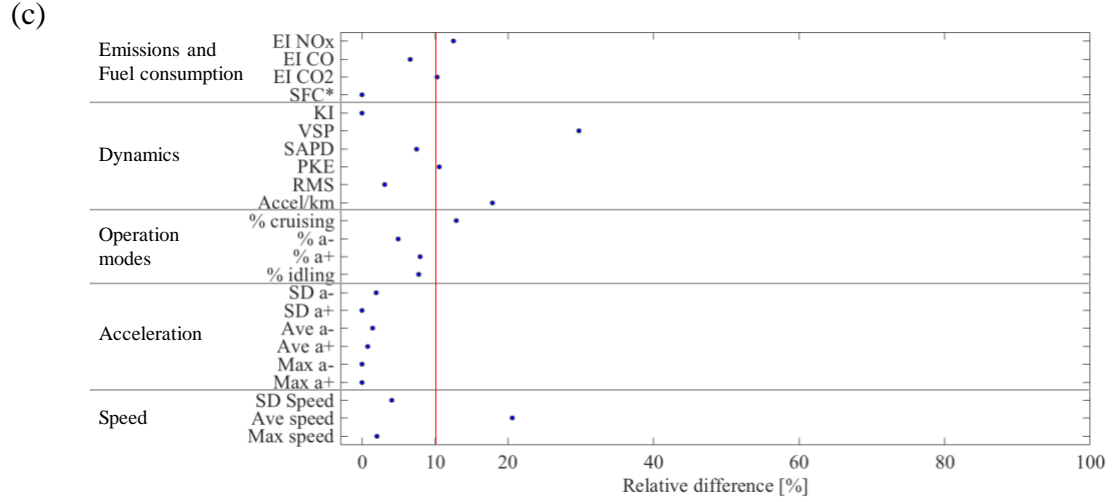


Figure 3.5 Boxplots of the relative differences (RDi) of the CPs that describe the DCs obtained by the (a) MT, (b) MCMC, and (c) FB methods in the general region after 500 iterations. The ARDi are shown as blue dots, the IQRi by boxes, and the outliers by red “+” signs. The CPs used by each method as criteria for the construction of the DC are marked with (*).

Since the set of CPs that describes a driving pattern is still undefined, the method’s ability of producing DCs that capture the local driving pattern is judged as the number of CPs where the $ARDi < 10\%$. However, in this evaluation it is important to:

- Do not include the CPs used as the assessment criteria by the method under consideration to construct the DC because those CPs by design should be smaller than 5%.
- Consider as an independent case the SAPD due to the high relevance of this metric for some researchers and because its range of variations is from 0 to 200%.

For the general region, Table 3.4 and Figure 3.5.a show that the FB method had 14 out of 19 CPs with $ARDi < 10\%$, while the MT had 15 out of 17, and the MCMC only had 4 out of 15 CPs under this threshold.

The same analysis was repeated for the case of the Mountain, Urban 1 and Urban 2 regions. Figure 3.6 shows that the results obtained for these three regions are similar to the results observed for the general region. Table 3.4 quantifies, in terms of $ARDi$, the performance of each method in the four regions considered in this study. Considering all the regions, the FB method showed 83% of the $ARDi$ under 10%, while the MT showed 69% and the MCMC 20%, excluding the CPs used as assessment criteria. The average of the $ARDi$ of the 19 CPs in the four regions was 5.8%, 10.1% and 34.9% in the FB, MT and MCMC methods, respectively.

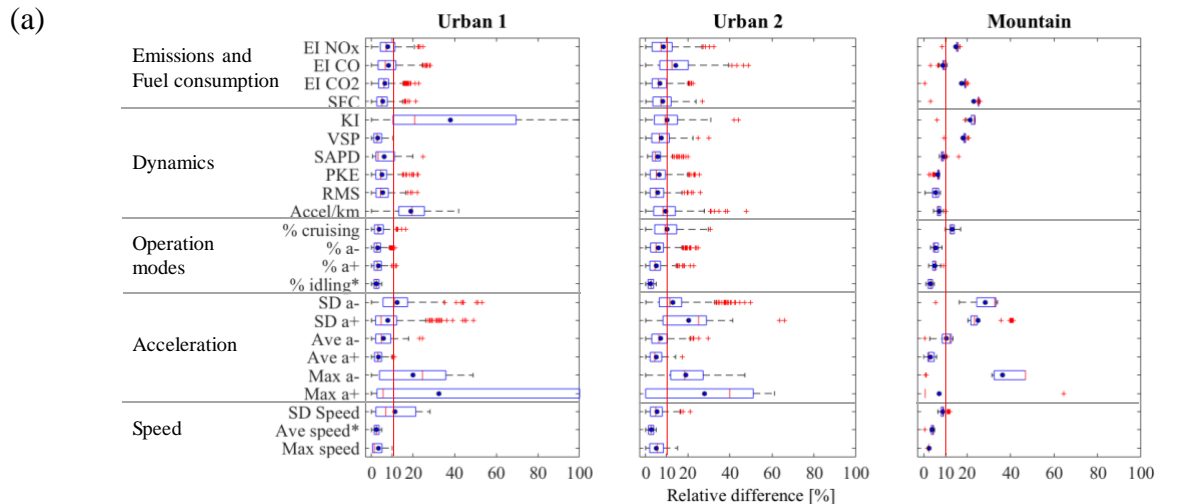
On average over the four regions, the FB method constructed DCs with RDi smaller than 19.1%. The maximum RDi were observed for the percentage of idling time in the Urban 1 region and VSP in the General region that reached a RDi of 61.3% and 29.8%, respectively. The best performance of the FB method was observed in the mountain region where all RDi

were below 16%. The FB method showed the most stable performance among the three methods in the four regions considered in this study.

The MT method (Figure 3.5a) produced DCs that represent well all CPs. Kinetic energy intensity and max des-acceleration were the CPs that showed the smallest agreement with *ARDi* of up to 38.1% and 36.1%, respectively. Compared to the general region, the MT method deteriorated its performance for the case of the region with highly congested traffic (Urban 1), where the CP associated to the kinetic energy intensity showed an *ARDi* of 38.1% with a large dispersion (*RDi* of up to 59%). Its performance worsens for the case of the mountain region where only 10 out of 17 CPs were below the 10% threshold for the *ARDi*.

The MCMC method showed the worst performance in producing DCs that represent local DC. It showed the smallest numbers of *ARDi* below the 10% threshold and the maximum range of variation of the *RDi*. The CPs with the largest *ARDi* were the number of accelerations per kilometer and the average positive acceleration reached *ARDi* of 163.8% (in the Urban 1 region) and 141.3% (in the mountain region), respectively, and with outliers for the corresponding *RDi* larger than 100% (not shown in Figure 3.5b). We also expected that this method produced DCs with the SAPD close to the SAPD of the driving pattern observed in each region, in consideration to its approach of constructing DCs. However, its performance was worse than the other two methods in this metric. On average over the four regions, it showed an *ARDi* of 19.7% vs an *ARDi* of 5.5% for the FB method and 6.2 for the MT method.

Previous results demonstrate the outstanding performance of the FB and MT methods producing DCs that represent the observed local driving patterns. Next, we will describe their performance reproducing fuel consumption and emissions of pollutants. By design, the FB method reproduced fuel consumption in all regions (*RDi* < 11% and on average 5.3%). Figures 3.5.c, 3.6.c and Table 3.4 show that this method reproduced the CO, CO₂ and NO_x emissions with an *RDi* < 20%. The average *RDi* was 8.3%. This performance was followed closely by the MT method. On average, the MT method produced DCs that reproduced fuel consumption with an average *ARDi* of 11.1% and an average *ARDi* of 9.6% for the CO, CO₂ and NO_x emissions, in the four regions considered in this study.



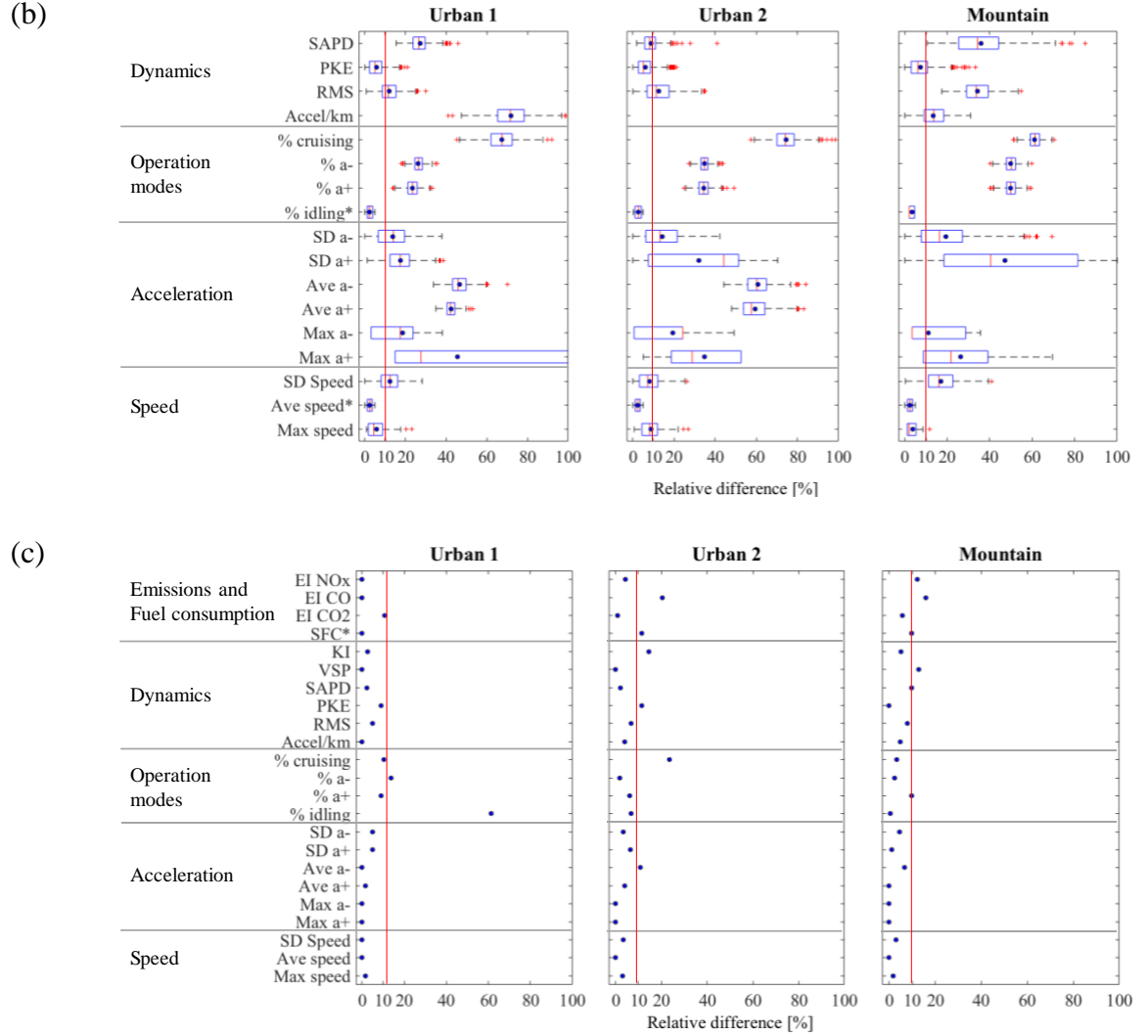


Figure 3.6 Boxplots of the relative differences (RD_i) of the CPs that describe the DCs obtained by the (a) MT, (b) MCMC, and (c) FB methods in the Urban 1, Urban 2 and Mountain regions after 500 iterations. The ARD_i are shown as blue dots, the IQR_i by boxes, and the outliers by red “+” signs. The CPs used by each method as the criteria for the construction of the DC are marked with (*).

As described before, the methodology used in this work does not allow to evaluate the performance of the MCMC method reproducing fuel consumption nor emission from the vehicles.

Previous results demonstrate that the FB method showed the best performance obtaining DCs that represent the driving patterns, the fuel consumption and emissions from the vehicles in the four regions considered in this study. Previous results also confirm that by using local DC instead of the type-approval DC, the differences between the fuel consumption and emissions from vehicles reported by manufactures and those observed in the normal use of the vehicles can be reduced substantially (<11% depending on the method used for constructing the local DC).

3.4 Conclusions

We hypothesized that the incorrect representation of the local driving patterns contained in the type-approval driving cycles used by manufacturers to report fuel consumption and emissions from vehicles, is one of the major sources of the differences observed between those values and the observed in the normal use of the vehicles. Thus, there is a need for local driving cycles (DCs) that truly represent local driving patterns and that could be used during the type-approval tests. However, there is not a unified method to construct those local DC. As an intermediate step, this work compared three common methods of constructing local DCs in their ability of producing DCs that i.) represent the local driving patterns and ii.) reproduce the fuel consumption and emissions exhibited by the vehicles in that region. The methods studied were the Micro-Trips (MT), the Markov Chains - Monte Carlo (MCMC) and the Fuel-Based (FB).

To that end, we implemented those methods in four regions with different topographies, different altitudes, and featuring well-maintained roads with different Level of Services (LoS). We monitored during a prolonged period of time (~8 months) the operation of a fleet of 15 busses with the same emission control technology and with similar maintenance conditions in order to eliminate the effects of their variations in our results. We measured simultaneously fuel consumption, CO, CO₂ and NO_x emissions, speed, and location at 1 Hz.

Driving patterns and DCs can be described by characteristic parameters (CPs) such as mean speed, mean positive acceleration, among others. Hence, a DC represents a local driving pattern of a given region when its CPs are equal to the CPs that describe the driving pattern in that region. The level of similarity is measured by the relative differences among them. Since the MT and the MCMC are repeatable but no reproducible, we repeated the implementation of those methods up to 1000 times and reported the average relative differences (*ARDi*) of the obtained CPs.

Results demonstrated that the FB method showed the best performance obtaining DC that represent the driving patterns, the fuel consumption and emissions from the vehicles in the four regions considered in this study, followed closely by the MT method. The MCMC method has difficulties producing representative DCs. In all regions, the FB method exhibited 83% of the CPs with *ARDi* under 10%, while the MT and MCMC presented 69% and 20%, respectively. By design, the FB method reproduced fuel consumption in all regions (*ARDi* ~ 5.3%). Furthermore, this method also reproduced the CO, CO₂ and NO_x emissions with *ARDi* of 8.3%. This performance was followed closely by the MT method. On average, the MT method produced DCs that reproduced fuel consumption with an *ARDi* of 11.1% and of 9.6% for the CO, CO₂ and NO_x emissions.

Previous results also confirm that by using local DC instead of the type-approval DC, the differences between the fuel consumption and emissions from vehicles reported by manufactures and the observed in the normal use of the vehicles can be reduced substantially (<11% depending on the method used for constructing the local DC).

Besides providing a methodology to assess the representativeness of driving cycles and the performance of the methods to construct them, this work contributes suggesting alternatives to strengthen the MT method and a procedure to test the correct implementation of any method to construct driving cycles. Our work can also be used to identify the minimum set

of CPs that fully describe driving patterns, and the design of a method to construct driving cycles for mountain regions. However further work is required to extend the scope of our conclusions to several vehicle technologies and to identify alternatives of implementing the resulting DC in chassis dynamometers.

3.5 Appendix A - Analysis of variation of the characteristic parameters in stochastic methods

Micro-trips (MT) and Markov Chain Monte Carlo (MCMC) are two of the most widely used stochastic methods in the construction of local driving cycles. In these methods, a synthetic driving cycle is generated from the random junction of micro-trips or operating states.

In MT method, the speed-time data, collected during the vehicle monitoring campaign, is divided into trip segments bounded by a vehicle speed equal to 0 km/h. These segments are called "micro-trips". The micro-trips are gathered according to their speed and acceleration. Then a set of micro-trips is randomly selected based on their probability of occurrence. The number of micro trips selected depends on the desired duration of the driving cycle.

In MCMC method, the speed-acceleration data is encoded in operating states. The frequency of occurrence of the states is recorded in a state matrix. From the same speed and time database, and from the state matrix, the probability of moving from state X_i to state $X_i + 1$ is calculated. The results are recorded in a probability transition matrix. This matrix is used to make a quasi-random selection of states that form a vector of states. Finally, the driving cycle is calculated by decoding this vector of states in terms of speed and time.

These two methods are stochastic in nature, in this sense the speed profile changes each time when a method is applied, which makes the method repeatable but not reproducible. The change in the speed profile also generates changes in the characteristic parameters (CP*) used to describe the driving cycle. In this sense, it is not possible to associate a single value to each CP* analyzed. This phenomenon is explained in the following example:

1. Using the same set of trips data, the MT method was applied five times, obtaining five driving cycles with different speed and time profiles. Figure 3.7 shows the driving cycles.
2. Different characteristic parameters were calculated to describe the driving patterns of the study region, and each one of the five driving cycles generated. In this particular case, the average speed and the percentage of idle time were used as selection criteria for the construction of the cycles. Table 3.5 shows the values of the calculated CPs.
3. The relative difference between the characteristic parameters of driving patterns (CPs) and the characteristic parameters of driving cycles (CPs*) was calculated. Table 3.6 shows relative differences, mean and inter-quartile range.

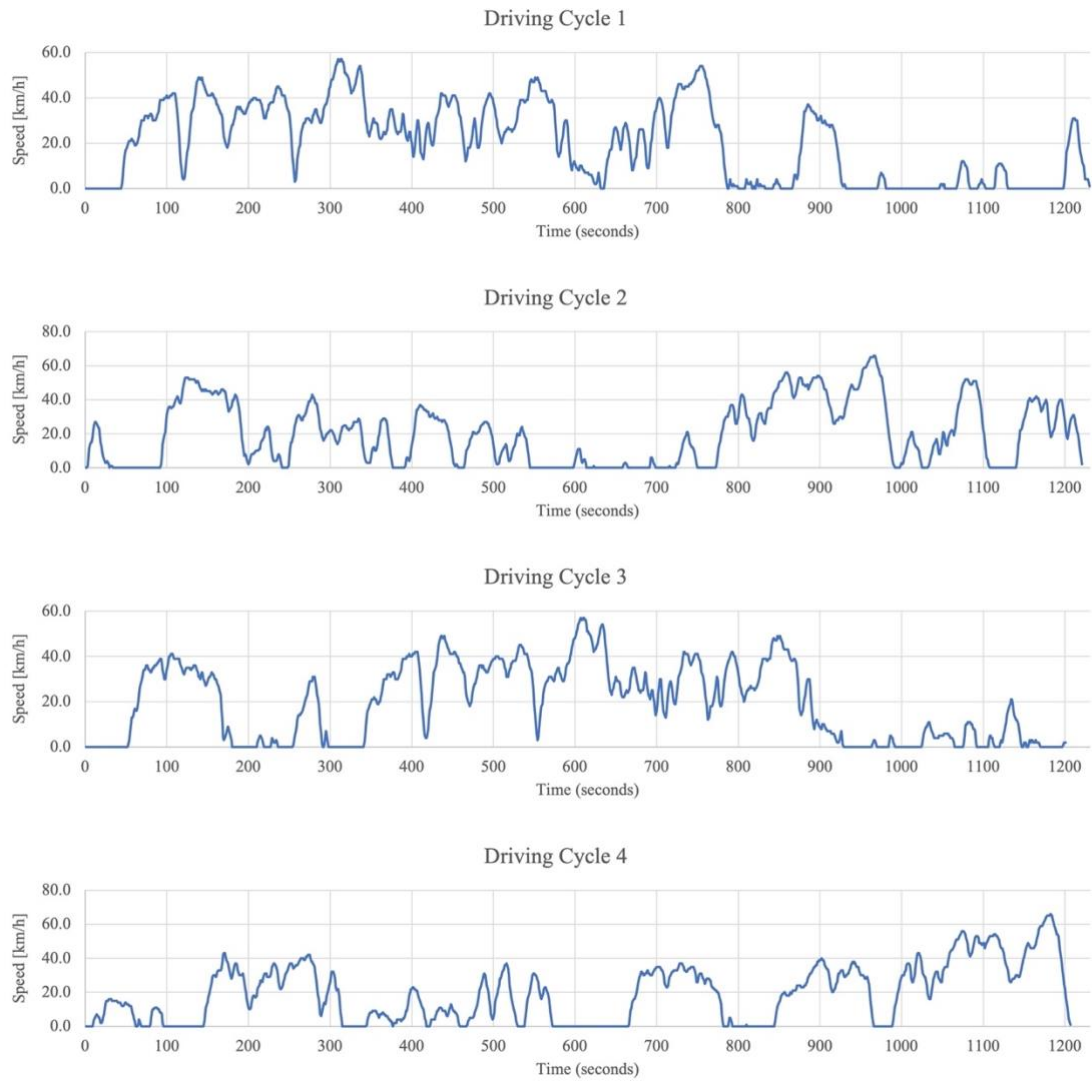


Figure 3.7 Driving cycles calculated from the same set of trips data and using a stochastic method.

Table 3.5 Characteristics parameters (CPs) that describe the driving patterns and the five driving cycles

CPs		Driving Patterns	Driving Cycles				
			1	2	3	4	5
Max Speed	m/s	16.81	15.83	18.33	15.83	18.33	18.33
Ave Speed*	m/s	5.57	5.64	5.55	5.36	5.38	5.61
SD Speed	m/s	4.69	4.71	5.06	4.64	4.69	4.82
Max Accel	m/s ²	1.90	1.48	1.83	1.37	1.39	1.81
Max Decel	m/s ²	0.50	-1.78	-1.76	-1.94	-1.69	-1.60

Ave Accel	m/s ²	0.31	0.50	0.52	0.46	0.48	0.50
Ave Decel	m/s ²	-1.93	-0.53	-0.58	-0.51	-0.56	-0.56
SD Accel	m/s ²	-0.54	0.30	0.31	0.27	0.26	0.30
SD Decel	m/s ²	0.34	0.35	0.35	0.37	0.34	0.33
% Idling*	%	24.71	24.23	25.63	25.56	24.86	25.06
% Accel	%	27.01	28.70	30.88	28.73	29.00	30.65
% Decel	%	25.37	27.24	27.85	25.90	25.35	27.86
% Cruise	%	17.40	19.84	15.64	19.82	20.80	16.43
Accel / km		16.80	17.00	15.21	18.16	17.42	15.52
RMS	m ² /s ²	0.45	0.46	0.49	0.43	0.44	0.47
PKE	m/s ²	0.38	0.36	0.39	0.34	0.35	0.38
VSP	kW/ton	1.04	1.05	1.07	0.98	1.00	1.06
KI	1/m	1.90	1.77	1.64	1.76	1.70	1.75

*: CPs used as assessment criteria for the proposed driving cycles

Table 3.6 Relative difference, average relative, and inter-quartile range of characteristics parameters (CPs)

CPs	Relative difference [%]					Average Relative difference ARD [%]	Inter- quartile range IQR [%]
	1	2	3	4	5		
Max Speed	5.8	9.1	5.8	9.1	9.1	7.8	3.3
Ave Speed*	1.3	0.4	3.7	3.5	0.8	2.0	2.9
SD Speed	0.4	7.8	1.2	0.0	2.6	2.4	3.6
Max Accel	22.0	3.7	28.0	26.8	4.9	17.1	22.6
Max Decel	7.8	9.0	0.6	12.6	17.4	9.5	7.8
Ave Accel	0.1	2.4	8.4	4.8	0.0	3.1	5.6
Ave Decel	0.9	8.0	4.8	3.5	4.6	4.4	2.7
SD Accel	3.4	1.0	14.0	16.7	3.4	7.7	11.9
SD Decel	2.8	0.6	6.5	2.3	5.1	3.5	3.6
% Idling*	1.9	3.8	3.5	0.6	1.4	2.2	2.3
% Accel	6.3	14.3	6.4	7.4	13.5	9.6	7.4
% Decel	7.4	9.8	2.1	0.1	9.8	5.8	8.2
% Cruise	14.0	10.1	13.9	19.5	5.6	12.6	6.4
Accel / km	1.2	9.4	8.2	3.7	7.6	6.0	5.4
RMS	2.7	9.4	3.7	1.3	5.8	4.6	4.3
PKE	4.7	2.9	9.6	6.3	0.2	4.7	5.0

VSP	0.9	3.2	5.2	3.4	1.9	2.9	2.2
KI	6.5	13.7	7.2	10.1	7.9	9.1	4.0

*: CPs used as assessment criteria for the proposed driving cycles

From this example it is possible to observe the variations on the profile of the cycles and their characteristic parameters generated by the stochastic nature of the MT and MCMC methods. The only characteristic parameters that maintained relative differences below 5% were the average speed and the percentage of time in idle, since they were selected as evaluation criteria of the proposed cycles.

Additionally, these variations in the driving profiles generate changes in fuel consumption and emissions of the vehicles that run under these specific driving cycles, this is due to the fact that both consumption and emissions are variables that depend on behaviors and changes of the cycle at the local level (short time intervals) and not of its global performance.

To overcome this issue, we repeat the process of constructing the driving cycles multiple times and observe the trends in the average relative differences and dispersion in the interquartile ranges. Analyzes were carried out for 100, 500 and 1000 repetitions in order to verify the minimum number of iterations to perform. From these results, an analysis of variance was performed where the null hypothesis raises average relative differences (ARD) for each equal CPs for 100, 500, and 100 iterations, while the alternative hypothesis establishes that at least one of the ARDs is different. If the p-value is less than the significance level, which was adjusted to 0.05, then it is concluded that at least one average relative difference (ARD) is different.

The following table presents the p-values for the general region, urban 1 and urban 2. In it, the p-values less than 0.05 are highlighted in red.

Table 3.7 P-values for different CPs in three study regions.

CPs		MT - General		MT - Urban 1		MT - Urban 2	
		100-500	500-1000	100-500	500-1000	100-500	500-1000
Speed	Max speed	0.56	1.00	0.11	0.26	0.73	0.44
	Ave speed*	0.58	0.81	0.96	0.24	0.67	0.57
	SD speed	0.27	0.57	0.11	0.12	0.95	0.09
Acceleration	Max a+	0.62	0.51	0.65	0.49	0.96	0.75
	Max a-	0.72	0.05	1.00	0.09	0.59	0.84
	Ave a+	0.10	0.67	0.97	0.81	0.84	0.51
	Ave a-	0.42	0.83	0.41	0.25	0.39	0.27
	SD a+	0.37	0.52	0.25	0.13	0.68	0.95
	SD a-	0.77	0.14	0.92	0.67	0.99	0.46

Operation modes (% of time)	% idling*	0.57	0.62	0.33	0.34	0.48	0.57
	% a+	0.87	0.45	0.07	0.47	0.63	0.52
	% a-	0.78	0.40	0.85	0.81	0.21	0.60
	% cruising	0.86	0.40	0.92	0.86	0.43	0.68
Dynamics	Accel / km	0.41	0.29	0.03	0.12	0.67	0.42
	RMS	0.14	0.29	0.58	0.17	0.54	0.18
	PKE	0.79	0.15	0.23	0.24	0.03	0.76
	SAPD	0.40	0.97	0.15	0.18	0.59	0.21

*: CPs used as assessment criteria for the proposed driving cycles

An analysis with the same characteristics was performed for the MCMC method, obtaining similar results. Based on the results of the previous table, it is recommended that for the driving cycles constructed with stochastic methods an iterative process of at least 500 repetitions be carried out, which allows establishing the trend of the CPs and reducing their dispersion.

4 Driving cycles that reproduce driving patterns, energy consumptions and tailpipe emissions

Abstract: This study presents the Energy Based Micro-trip (EBMT) method, which is a new method to construct driving cycles that represent local driving patterns and reproduce the real energy consumption and tailpipe emissions from vehicles in a given region. It uses data of specific energy consumption, speed, and percentage of idling time as criteria of acceptable representativeness. To study the performance of the EBMT, we used a database of speed, fuel consumption, and tailpipe emissions (CO_2 , CO, and NO_x), which was obtained monitoring at 1 Hz, the operation of 15 heavy-duty vehicles when they operated within different traffic conditions, during eight months. The speed vs. time data contained in this database defined the local driving pattern, which was described by 19 characteristic parameters (CPs). Using this database, we ran the EBMT and described the resulting driving cycle by 19 characteristics parameters (CPs*). The relative differences between CPs and CPs* quantified how close the obtained driving cycle represented the driving pattern. To observe tendencies of our results, we repeated the process 1000 times and reported the average relative difference (ARD) and the interquartile range (IQR) of those differences for each CP. We repeated the process for the case of a traditional Micro-trip method and compared to previous results. The driving cycles constructed by the EBMT method showed the lowest values of ARDs and IQRs, meaning that it produces driving cycles with the highest representativeness of the driving patterns, and the best reproduction of energy consumption, and tailpipe emissions.

Keywords: Micro-trips method; Specific fuel consumption; Emission indexes; Heavy-duty vehicles; Driving patterns; Characteristic parameters.

Frequent symbols and acronyms

Symbol	Description	Units
ARD_i	Average relative difference of the i^{th} characteristic parameter	%
CP_i	Values of the i^{th} characteristic parameter that describe the driving pattern	-
CP_i^*	Values of the i^{th} characteristic parameter that describe the driving cycle	-
IQR_i	Interquartile range of the i^{th} characteristic parameter	-
KI	Kinetic intensity. Ratio of characteristic acceleration to aerodynamic speed.	1/m
SFC	Specific Fuel Consumption	L/km
RD_i	Relative difference of the i^{th} characteristic parameter	%

EBMT	Energy based micro-trip
GPS	Global Positioning system
LoS	Level of Service
MT	Micro-trip

4.1 Introduction

Currently, there is an increasing interest in driving cycles that truly represent local driving patterns, and that could be used to reproduce energy consumption in electric vehicles, and fuel consumption and tailpipe emissions in engine-powered vehicles.

A driving pattern expresses the manner that drivers, on average, drive in a given region [54]. A driving cycle is a time series of speeds that describes this driving pattern [2], and that when it is followed by a vehicle, its energy consumption and tailpipe emissions are similar to the average energy consumption and tailpipe emissions of all vehicles of similar technology operating in the same region [47], [57]. They are used for the design of vehicles' power train and of strategies to reduce energy consumption in the transport sector [58], [59]. Driving cycles are mainly used to measure and compare the vehicles' energy consumption and tailpipe emissions [44], [48]. Therefore, the representativeness of the local driving pattern is the key issue of a driving cycle. Both, the driving patterns and the driving cycles can be described by characteristic parameters [2], [24], which are metrics based on speed and time, like average speed, average positive acceleration. We use CP to denote the characteristic parameters that describe driving patterns, while CP* indicates the characteristic parameters that describe the driving cycles. Then a driving cycle represents the driving patterns of a given region accurately if $CP^*s \approx CPs$ [60]. The relative difference (*RD*) between corresponding CPs and CP*s assesses the level of representativeness of a driving cycle.

The driving cycle representativeness depends mainly on three factors: (a) the quality and quantity of vehicle operation data, (b) the driving cycle construction method, and (c) the CPs used to assess the driving cycle representativeness [33]. Currently, state of the art in information and communication technologies allows monitoring the operating variables (speed, time, fuel consumption) of a large sample of vehicles with a sample rate of 1 Hz at a low cost. Nonetheless, there is not a unified methodology to construct driving cycles and assess their representativeness. Therefore, the interest in driving cycles has been focused on the study of factors (b) and (c).

Table 1 lists examples of driving cycles developed for different countries and regions. Some of them are type-approval driving cycles, i.e., they are used to verify the compliance of maximum levels of energy consumption and vehicle emissions established by local authorities as requirements for new vehicle technologies before they are approved to enter into the local automotive market. However, the existing driving cycles used as type approval driving cycles frequently do not represent the local driving patterns.

Table 4.1 Some relevant driving cycles and the methods used for their construction.

Driving Cycle	Method	Parameters used as driving cycle's assessment criteria
FTP 72, FTP 75	ST	Average speed, average acceleration and maximum speed. [61]
LA92, Unified Cycle	MT	SAPD. [45]
LA01	MCMC	Average speed, SAPD, maximum and minimum speed. [45]
Heavy-Duty Diesel Truck Cycle (HHDDT)	MT	Average speed, percentage of idling time, creeping, acceleration, cruising and deceleration. Maximum speed. [2]
IEC	ST	Average speed, average running speed, average acceleration, average deceleration, mean length of micro-trips, average number of acceleration / deceleration changes, average number of stops and percentage of idling time, acceleration, cruising and deceleration. [24]
ARTEMIS Cycle	MT	Average speed, average running speed, average acceleration, average deceleration, average number of stops, percentage of idling time, SAPD and maximum speed. [32]
TRL Cycle	MT	Average speed, average acceleration, mean length of micro-trips, maximum and minimum speed. [2]
Sydney Cycle	MT	Average speed, percentage of idling time, RMS acceleration and SAPD. [24]
Melbourne Peak Cycle	MT	Average speed, percentage of idling time, RMS speed, RMS acceleration, KE and SAPD. [24]
Perth Cycle	KT	Average speed, average number of stops, percentage of idling time, RMS acceleration, KE, rate of change of acceleration and SAPD. [24]
Taipei Motorcycle Driving Cycle (TMDRIVING CYCLE)	ST	Average running speed, average acceleration, average deceleration, mean length of micro-trips, percentage of idling time, and acceleration SAPD. [55]
Kaohsiung Driving Cycle (KHM)	MT	Average speed, average running speed, average acceleration, average deceleration, mean length of micro-trips, average number of acceleration / deceleration changes, acceleration, cruising and deceleration. RMS acceleration. [2]
China Cycles	MT	Average speed, average running speed, average acceleration, average deceleration, average number of acceleration / deceleration changes, percentage of idling time, acceleration, cruising and deceleration. KE. [22]
Beijing Cycles	MT	Average speed, average running speed, average acceleration, average deceleration, percentage of idling time, acceleration, cruising and deceleration. VSP and maximum speed. [2]
World Harmonized Vehicle Cycle (WHVC)	MT	Average speed, average stop time, number of stop per km, power-time distribution, speed-acceleration distribution, average power during the engine delivers power to drive shaft, relative positive acceleration, % of time the engine delivers power to drive-shaft during operation, relative energy demand. [17]
World Motorcycle Test Cycle (WMTC)	MT	Speed-acceleration matrix. [62]
WLTC (World-wide harmonized Light duty Test Cycle).	MT	SAPD, average speed, average acceleration, acceleration and deceleration ratio. [19]

MT: Micro-trips, MCMC: Markov chain Monte Carlo, ST: select trip, KT: Knight tour, SAPD: speed-acceleration probability distribution, RMS: root mean square, KE: kinetic energy, VSP: vehicle specific power.

Table 1 shows that the most used method to construct driving cycles is the Micro-trips (MT) method. Due to its stochastic nature, this method is repeatable but not reproducible. It means

that the speed-time profile of the resulting driving cycles is different each time the method is applied, despite that it uses the same input data. Table 1 also shows that there is not an agreement about a unique set of CPs that should be used to evaluate the driving cycles representativeness. The average speed and percentage of idling time are the CPs most used as assessment criteria. It could be expected that the driving cycles constructed by the MT method, using these two CPs as assessment criteria, are unable of reproducing energy consumption in the vehicles, since energy consumption depends more on the short time variations of the speed-time profile [46] rather than on the overall values of the CPs used as assessment criteria.

Even though driving cycles are mainly used for the measurement of energy consumption and the emissions of pollutants, these two parameters are rarely used as the assessment criteria to ensure the driving cycles representativeness. Reference [2] suggested recording fuel consumption and vehicle emissions data simultaneously with the speed and time data. Reference [63] developed a methodology for clustering micro-trips using estimated values for fuel consumption and driving parameters as the classification criteria. From a different perspective, reference [64] developed a modal emission model based on driving cycles using CPs. Reference [65] used the model developed by [64] to study how to solve the vehicle routing problem applying the minimization of fuel consumption as an objective function. Reference [48] used the Vehicle Specific Power model to quantify the fuel consumption expected from vehicles using different driving cycles. However, none of these works have used fuel consumption to evaluate the representativeness of the driving cycles.

Until a few years ago (~10), the measurement of instant fuel consumption in vehicles required the use of flow sensors installed in the fuel lines, which makes the process of collecting a fair amount of fuel consumption data from a representative sample of vehicles cumbersome and costly. This fact hampered the use of fuel consumption and emissions as assessment criteria. As an alternative, reference [50] used a fuel consumption estimation function based on CPs to compute the specific fuel consumption (SFC) of the sampled trips. Then, the trip with the closest SFC to the average SFC of the sampled trips was selected as the driving cycle. Later on, reference [54] collected experimental fuel consumption and tail emission data from a fleet of vehicles and proposed the fuel-based method to construct driving cycles. In the fuel-based method, the representative driving cycle is the trip with the measured fuel consumption closest to the average fuel consumption of all the sampled trips. Then, they compared the driving cycles obtained by three different approaches: fuel-based, MT, and the Markov Chain Monte Carlo method, and found that the fuel-based method exhibited the best performance producing driving cycles that describe the region driving patterns and reproduce energy consumption and emission of pollutants [60]. However, they could not control the duration of the driving cycles because it is determined by the duration of the trip selected as the driving cycle. Therefore, the resulting driving cycle could be too long for being used on a chassis dynamometer, or too short to grasp a symbolic value for fuel consumption of the vehicle out of the many uncertainties occurring in the test. On the MT method, the duration of the driving cycle is an input parameter.

As an alternative, this work explores the feasibility of using fuel consumption and emission of tailpipe pollutants as assessment criteria of a traditional MT method. We named this new method as the *Energy Based Micro-Trip (EBMT)* method. We will show that the EBMT method produces driving cycles that genuinely represent the local driving patterns and

reproduce the real energy consumption and emissions from the vehicles in the region of interest. We also propose to add a final step in the MT method to improve its performance, which consists of repeating many times (>1000) the traditional MT method, and select as the representative driving cycle, the one with the minimum average relative difference of all CPs. This step makes the MT method repeatable and reproducible.

4.2 Materials and methods

To compare the representativeness of driving cycles obtained by the EBMT method with respect to those constructed by the traditional MT method, the authors followed the methodology illustrated in Figure 4.1, which consist of the following steps: i) Select regions and routes of general characteristics, ii) Instrument of a large sample of vehicles. iii) Carry on a monitoring campaign to record the vehicle's position, speed, fuel consumption, and tailpipe emissions, during a long time of regular operation. iv) Use the obtained database to construct driving cycles following the EBMT and MT methods. v) Assess the degree of representativeness of the driving cycles obtained by each method. These steps are described in detail below.

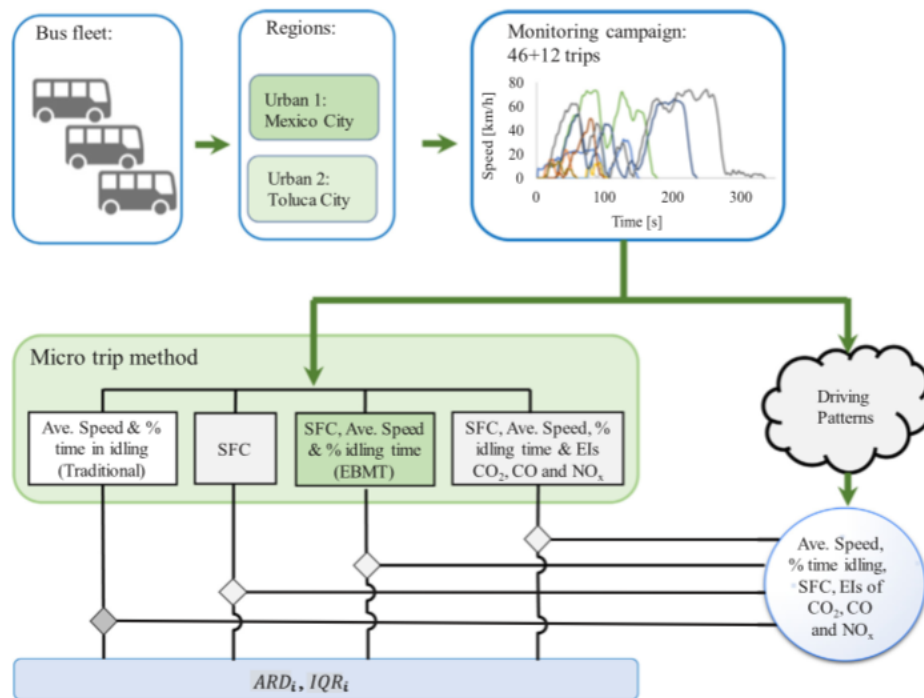


Figure 4.1 Proposed methodology to evaluate the representativeness of the driving cycles constructed following the EBMT method.

4.2.1 Route selection

Aiming to test the performance of the EBMt method, we selected two urban regions: Urban 1 (Mexico City) and Urban 2 (Toluca). The selected regions are flat and have roads with different levels of service (*LoS*). The *LoS* of a road is defined by the [49] as a qualitative measure that describes the operational conditions within a traffic stream, based on service measures such as speed and travel time, freedom to maneuver, traffic interruptions, comfort, and convenience. The route selected in the Urban 1 region corresponds to the 11.5 km of the TOL-MEX route inside Mexico City, which is completely urban. The route in the Urban 2 region corresponds to the 18.8 km of the TOL-MEX route located in the urban and suburban areas of Toluca city. Table 4.2 shows the characteristics of the routes selected.

Table 4.2 Characteristics of routes considered in this work.

Parameter	Unit	Urban 1	Urban 2
Location	-	Mexico City	Toluca City
Facility	-	Local roadway	Arterial
Level of traffic	-	High	Medium
<i>LoS</i>	-	F	E
Speed limit	km/h	60	60
Number of lanes	-	3	3
Length	km	11.5	18.8
Ave road grade	%	1.4	1.8
Max road grade	%	5.2	9.0
Min altitude	m.a.s.l.	2255	2611
Max altitude	m.a.s.l.	2258	2637

4.2.2 Vehicle fleet and instrumentation

The company that cooperated in this study operates around 7000 buses around the country, 10% of that fleet operates in the Mexico City region. 25 buses cover the routes described previously. We monitored 15 of these buses. They have the same powertrain and emission control technology and have gone through a similar maintenance program. Table 4.3 shows the technical characteristics of the vehicles. The frontal area, drag coefficient, and rolling resistance coefficient were calculated following the procedures outlined in [50].

Table 4.3 Technical characteristics of the vehicles used in this study.

Parameter	Unit	Value
Long	m	12.85
Wide	m	2.6
Tall	m	3.6
Capacity	passengers	49
Fuel	-	diesel
Gross vehicle weight	kg	13850
Engine	-	Cummins IMS 425
Number of cylinders	-	6
Engine displacement	L	10.8
Power	HP	425
Torque	Nm	2102
Bus maker	-	Busscar
Model	-	Vissta Buss Elegance 360
Model year	-	2012 - 2014
Traveled kilometers	km	100,000 – 200,000
Control emission technology	-	EURO IV
EGR	-	Yes
DOC	-	No
SCR	-	No
Frontal area	m ²	8.47
Drag coefficient	-	0.64
Rolling resistance coefficient	-	0.006
Applied load	kg	2100

The database consists of simultaneous measurements of position, speed, fuel consumption, and CO₂, CO, and NO_x (NO + NO₂) tailpipe emissions, sampled at a rate of 1 Hz. Fuel consumption was read directly from the ECU (Engine Control Unit) via the OBD II (On-Board Diagnostics System, version II) port. The ECU controls the instantaneous engine fuel consumption by controlling the fuel injection time. The aggregate value of the fuel consumption measurements had a correlation level (R^2) greater than 0.9 when compared against the measurements obtained with a gravimetric tank.

This study used a SEMTECH ECOSTAR PEMS (Portable Emission Measurement System) with a SEMTECH-FEM module to measure the CO and CO₂ concentration using a non-dispersive infrared gas analyzer with a resolution of 10 ppm and a range of 0-8% for CO and a resolution of 0.01% and range of 0-20% for CO₂. It also included a SEMTECH-NO_x module to measure NO and NO₂ using a non-dispersive ultraviolet gas analyzer with a range of 0-3000 ppm and 0-500 ppm, respectively, and a resolution of 0.3 ppm for both gases. Table 4.4 summarizes the equipment characteristics. We followed recommendations from the U.S. Environmental Protection Agency (EPA) for the measurement of vehicle emissions concentration [56]. Additionally, the PEMS was calibrated before and after each trip following the manufacturer recommendations. The study also used a high precision GPS

(Global Positioning System) to measure the position (latitude, longitude, and altitude), and the speed of the vehicles with the required sample rate.

Table 4.4 Technical characteristics of the instruments used in this study

Variable	Instrument/ Trademark	Technical characteristics		
Position: latitude, longitude and altitude	GPS/Garmin 16x	Position: 3-5 m, 95% typical Frequency: 1 Hz Speed: 0.05 m/s RMS steady state PPS time: 1 microsecond at rising edge of PPS pulse		
Speed and time				
Instantaneous fuel consumption	-	Estimated through the injection time Reported by ECU through OBD II		
		Technique	Range	Resolution
CO ₂		Non-Dispersive Infrared	0 - 20% v/v	0.01% v/v
CO		Non-Dispersive Infrared	0 - 8% v/v	10 ppm v/v
NO	PEMS	Non-Dispersive Ultraviolet	0 - 3000 ppm v/v	0.3 ppm v/v
NO ₂	SEMTECH ECOSTAR	Non-Dispersive Ultraviolet	0 - 500 ppm v/v	0.3 ppm v/v
Flow Measurement		Exhaust Flow Meter	-	0.1 kg/hour

GPS: global position system; OBD II: on-board diagnostic system, second generation; ECU: engine control unit.

4.2.3 Monitoring campaign

A monitoring campaign was developed during eight months in different seasons of the year to include the effects of the environmental conditions. The vehicle fleet operated in the selected routes, in both directions, under real-world driving conditions, and under normal conditions of use. Buses were driven by the company's regular drivers, during week and weekend days, at different hours of the day, to obtain representative driving data.

For the measurement of tailpipe emissions, the vehicles were loaded with 2,100 kg of water tanks to simulate the weight and inertia of the passengers. Emissions data were collected over two months following the same routes and under similar conditions.

The data quality was verified in three phases: i) In the first phase, trips with less than 90% of data availability were disregarded. Frequently GPS data is lost when the vehicle cross under a bridge or moves along a tunnel, and PEMS data is lost when the device self-calibrates in the middle of a trip. ii) The second phase identified outlier data for each trip. They were data with values outside ranges physically possible. For example, negative values for vehicle speed, or values of oxygen concentration higher than 21%. They are also data with values outside typical values like vehicle acceleration with values greater than 3 m/s². iii) The last phase consisted of synchronizing the data from the vehicle's ECU with the emissions data reported by the PEMS. The non-synchronization of data is originated by the differences in the instruments' response time. Data synchronization was done manually by dephasing each data set until we obtained the maximum correlation coefficient between variables that,

according to physics, should be correlated, such as fuel consumption, engine speed (RPM), and emissions. We found that data was unsynchronized by 7 to 11 s depending on the trip.

Using the monitoring campaign outcomes, after data quality analysis, the authors built a database made of 12 monitored trips for each region with simultaneous measurements of mass emission of pollutants, fuel consumption, position, altitude, and speed. We also included 46 additional trips with the same information but without emissions.

4.2.4 Driving cycle construction method and assessment criteria

From that database, we obtained the driving pattern of each region and reported them as the average values for the 19 CPs listed in Table 4.5. We also obtained the average values for fuel consumption and emission indexes, which are also reported in Table 5. The emission indexes are the average mass of CO, CO₂ or NO_x emitted by the vehicle per kilometer traveled (g / km).

Aiming to establish a baseline of comparison for the performance of the EBMT method, we implemented the traditional MT method. It constructs driving cycles by splicing together a series of micro-trips [3], which are segments of trips that start and end with a vehicle speed of zero [1], [45]. Using the trips database described above, we divided the sampled trips into micro-segments and elaborated a secondary database of micro-trips for each region.

Then, the micro-trips were clustered based on their average speed and average positive acceleration. This clustering process was implemented in the statistical software *Minitab*, using centroids as the linkage method, Euclidean distances, and a 95% level of similarity. Then, we calculated the probability speed-acceleration probability distribution for each cluster in the Urban 1 and Urban 2 regions.

Then, we selected micro-trips and spliced them together until they assemble a candidate driving cycle with a duration greater than 20 min. The selection of the micro-trips was made under a quasi-random process, which means that it was affected by the computed cluster speed-acceleration probability distribution. Within each cluster, each micro-trip has the same probability of being selected. We chose this time duration because it is nearly the time duration of the existing type approval driving cycles. We observed that the resulting candidate driving cycles exhibited a time duration between 20 and 22 minutes.

The criteria for acceptance of the candidate driving cycle as the representative driving cycle is based on the degree of similarity between the candidate driving cycle and the driving patterns. This degree of representativeness is measured by the relative difference (RD_i) between the CP_i^* of the candidate driving cycle and the CP_i that describe the driving pattern (Equation 4.1). Values smaller than 5% are typically used as an acceptable threshold. Otherwise, the method restarts and selects a new group of micro-trips.

$$RD_i = \left| \frac{CP_i^* - CP_i}{CP_i} \right| \quad (4.1)$$

As stated before, there is not an agreement on the CPs that should be used during this assessment of representativeness. According to Table 4.1, the CPs most used are the average speed and the percentage of idling time. For the purpose of establishing a baseline of comparison, we adopted them, and we refer to these CPs as assessment criteria. In Equation 4.1, i represent any of the assessment criteria. Some authors have used additional CPs during this step. However, increasing the number of CPs reduces the possibility of identifying a candidate driving cycle.

4.2.5 Assessment of representativeness of the driving cycles obtained by each method

In this work, we propose to use fuel consumption as the assessment criteria in the MT method. To evaluate this alternative and other attractive combinations, we tested the following cases of assessment criteria: i) average speed and percentage of idling time (traditional MT method), ii) Specific fuel consumption (SCF), iii) SFC, average speed and percentage of idling time, iv) SFC, average speed, percentage of idling time, and emission indexes.

Aiming to quantify the degree of representativeness of the driving pattern contained in the driving cycles constructed by the MT method using any of the four sets of assessment criteria described above, we observed the resulting relative differences of all possible CPs (Table 4.5). However, the MT method is reproducible but not repeatable due to its stochastic nature. Therefore, the resulting representative driving cycle changes each time the method is applied despite using the same trips data set as input data. This variation in the resulting driving cycles generates differences in the CPs values obtained, hampering the fair comparison in the degree of representativeness of the driving cycles constructed using the four sets of assessment criteria. As an alternative, we applied the MT method multiple times and determined the trend and dispersion of each RD_i . The trend of the RD_i was described through the average relative differences (ARD_i), which is calculated by Equation 4.2. The dispersion of each RD_i was quantified through its interquartile range (IQR_i).

$$ARD_i = \frac{\sum_{j=1}^n |CP_{i,j}^* - CP_i|}{n CP_i} \quad (4.2)$$

In Equation 4.2, n is the total number of iterations performed (1000), j is the iteration number. Both the ARD_i and the IQR_i can vary between 0 and infinity. ARD_i and IQR_i values close to zero indicate high similarity between the constructed driving cycle and the driving pattern. Finally, the total average value of the ARD_i (\overline{ARD}) was calculated (Equation 4.3) and used to compare the four cases of assessment criteria. Similarly, it was done for the IQR_i (\overline{IQR}),

Equation 4.4). In equations 4.3 and 4.4, the subscripts i refers to any of the CPs in Table 4.5, and therefore $w=19$.

$$\overline{ARD} = \frac{\sum_{i=1}^w ARD_i}{w} \quad (4.3)$$

$$\overline{IQR} = \frac{\sum_{i=1}^w IQR_i}{w} \quad (4.4)$$

Table 4.5 Characteristic parameters (CPs) used in this study to describe driving patterns and driving cycles

Type		Name	Symbol
Speed	1	Average speed	Ave Speed
	2	Maximum speed	Max Speed
	3	Standard deviation of speed	SD speed
Acceleration	4	Maximum acceleration	Max a+
	5	Maximum deceleration	Max a-
	6	Average acceleration	Ave a+
	7	Average deceleration	Ave a-
	8	Standard deviation of acceleration	SD a+
	9	Standard deviation of deceleration	SD a-
Operational modes (% of time)	10	Percentage of idling time	% idling
	11	Percentage Acceleration	% a+
	12	Percentage Deceleration	% a-
	13	Percentage Cruising	% cruising
Dynamics	14	No. of acceleration per kilometer	Accel/km
	15	Root mean square of accel.	RMS
	16	Positive kinetic energy	PKE
	17	Speed acceleration probability distribution	SAPD
	18	Vehicle Specific Power	VSP
	19	Kinetic Intensity	KI
Emissions and energy	20	Specific fuel consumption	SFC
	21	Emission index of CO ₂	EI CO ₂
	22	Emission index of CO	EI CO
	23	Emission index of NO _x	EI NO _x

4.2.6 Empirical results

Table 4.6 presents the values of the CPs that describe the driving patterns in the Urban 1 and Urban 2 regions. They are alike, which was expected as they are similar cities in terms of topography, vehicle technologies used, road characteristics, and social culture. The main differences between these two driven patterns are mean speed (7.3 vs. 10.0 m/s) and VSP (4.8 vs 7.0. kW/t).

Figures 4.2a-d are box and whisker plots that show the results of tendencies and dispersions obtained for the RD_i . The red box in each figure highlights the assessment criteria used in each case. In intermediate steps, we obtained these plots and observed stable results after 500 iterations (variations smaller than 1% between iterations). Figures 4.2a-d are the results obtained after 1000 iterations. CPs with $ARD_i < 5\%$ are highlighted in green in Table 4.6.

Aiming to quantify the effectiveness of the different sets of assessment criteria, the average of the ARD_i and of the IQR_i were calculated for the CPs (\overline{ARD}_{CPs} and \overline{IQR}_{CPs}) and emission indexes (\overline{ARD}_{EIS} and \overline{IQR}_{EIS}), while the ARD and IQR were calculated for the energy consumption (ARD_{SFC} and IQR_{SFC}). These results are shown in Table 4.7 for the Urban 1 and Urban 2 regions.

Table 4.6 Characteristic parameters that describe the driving patterns in Urban 1 and Urban 2 regions. ARDi for each CP

CPI		Driving patterns for:		ARDi							
				Urban 1				Urban 2			
		Urban 1	Urban 2	Av. Speed, % idling	SFC	SFC, Av. Speed, % idling	SFC, Av. Speed % idling, EIs	Av. Speed, % idling	SFC	SFC, Av. Speed, % idling	SFC, Av. Speed, % idling, EIs
Speed	Max speed	22.3	26.2	1.1	4.6	1.1	1.0	4.4	4.6	4.7	5.0
	Ave speed	7.3	10.0	2.5	16.8	2.6	2.5	2.5	11.3	2.5	2.5
	SD speed	6.9	7.7	13.5	13.2	11.2	11.9	3.8	4.2	3.8	3.9
Acceleration	Max a+	1.3	1.3	39.7	33.6	29.4	29.3	16.5	17.2	16.9	17.7
	Max a-	-2.1	-2.1	14.6	13.9	15.2	16.9	12.7	12.3	12.8	12.4
	Ave a+	0.5	0.4	4.1	3.2	3.4	3.7	3.6	2.9	3.1	2.3
	Ave a-	-0.5	-0.5	5.8	4.8	4.0	4.6	6.2	5.0	5.2	4.3
	SD a+	0.2	0.2	7.4	6.0	5.0	5.3	3.2	2.8	2.9	2.8
	SD a-	0.4	0.4	7.7	7.1	6.6	7.7	6.1	5.4	5.0	4.4
Operation modes (% of time)	% idling	15.1	13.6	2.4	45.3	2.4	2.4	2.5	29.6	2.4	2.5
	% a+	32.9	33.8	3.0	8.9	2.8	2.8	4.4	7.5	3.7	3.1
	% a-	29.3	29.1	3.0	8.6	2.3	2.2	3.4	7.0	3.2	2.8
	% cruising	22.7	25.9	6.0	10.3	4.2	4.0	8.9	9.7	7.4	6.1
Dynamics	Accel / km	8.6	6.1	10.9	17.2	9.1	8.4	8.5	14.4	8.4	7.3
	RMS	0.5	0.5	5.2	6.2	3.8	4.3	5.9	5.9	4.7	3.5
	PKE	0.4	0.3	10.0	5.3	6.6	7.3	7.3	4.9	5.2	4.1
	SAPD	0.0	0.0	12.2	16.4	11.9	11.9	11.3	13.9	10.7	10.0
	VSP	4.8	7.0	8.7	12.9	8.6	8.3	11.6	15.3	10.5	11.5
	KI	0.8	0.7	10.4	45.6	15.2	13.5	10.2	8.5	6.8	6.7
Fuel consumption and emissions	SFC	0.4	0.4	9.6	2.5	2.8	2.7	7.5	2.6	2.5	2.4
	EI CO ₂	839.0	749.2	9.5	4.8	4.7	1.8	5.5	4.0	3.3	1.7
	EI CO	37.2	39.4	10.1	8.1	6.3	2.4	10.5	5.9	5.4	2.4
	EI NO _x	5.0	3.9	9.8	6.2	5.1	2.1	6.7	9.7	6.3	2.5

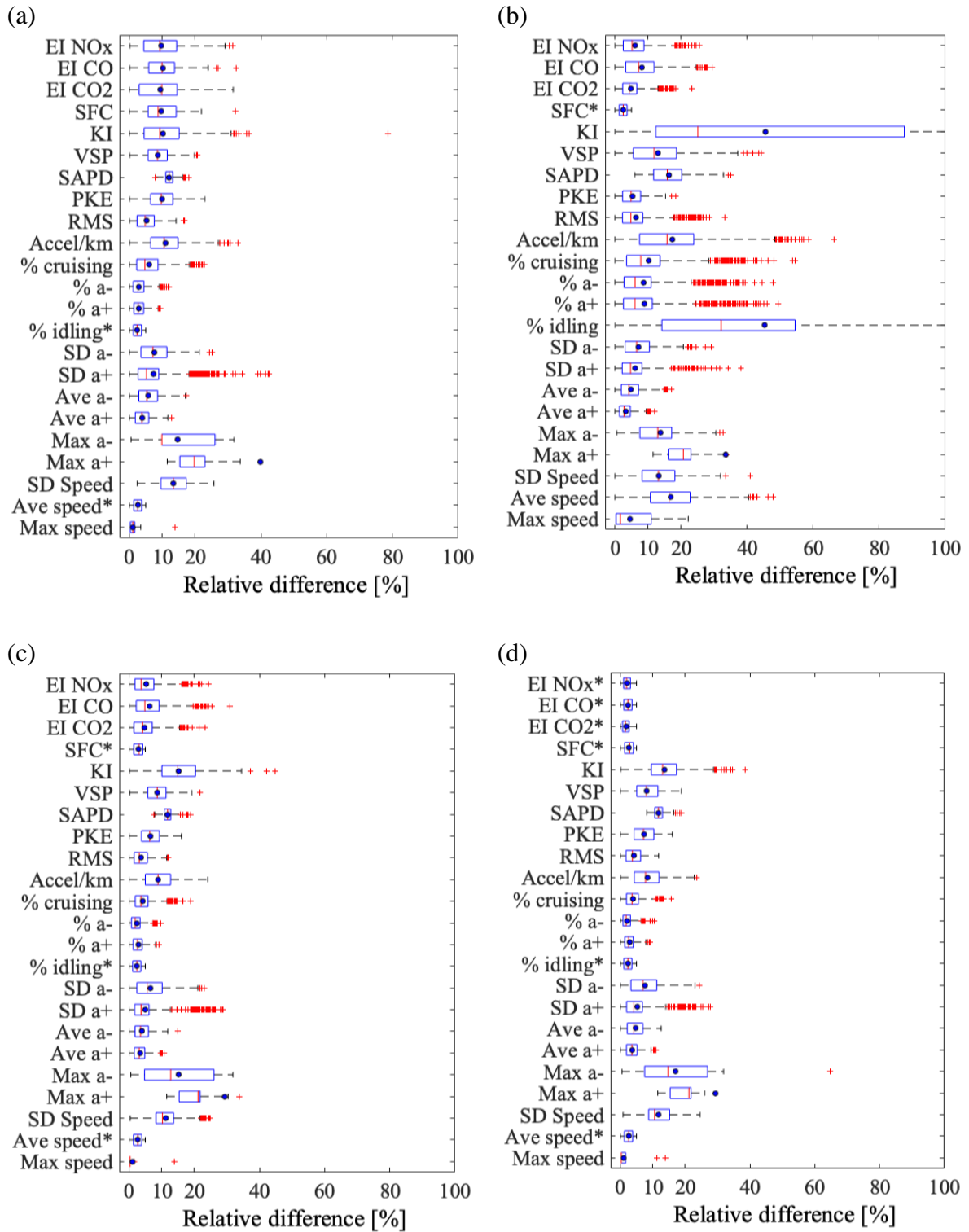


Figure 4.2 Box and whisker plots of the RDi after 1000 iterations obtained by the MT method using as assessment criteria a.) Average speed and % idling, b.) SFC, d.) SFC, Average speed and % idling, and d.) SFC, average speed, % idling and EI of CO₂, CO and NO_x for the case of Urban 1 region.

Table 4.7 \overline{ARD} and \overline{IQR} obtained for the different sets of assessment criteria after replicating the EBMT method 1000 times.

Regions	Urban 1						Urban 2					
	\overline{ARD}			\overline{IQR}			\overline{ARD}			\overline{IQR}		
	CPs	EIs	SFC	CPs	EIs	SFC	CPs	EIs	SFC	CPs	EIs	SFC
a	8.85	9.81	9.64	5.96	9.81	8.53	7.01	7.58	7.50	6.52	7.95	7.26
b	14.74	6.38	2.50	13.84	6.38	2.39	9.61	6.55	2.60	9.11	6.63	2.53
c	7.66	5.36	2.79	5.38	6.14	2.76	6.31	5.04	2.54	5.67	5.09	2.43
d	7.79	2.11	2.69	5.42	2.20	2.71	5.94	2.20	2.39	5.47	2.21	2.35

a: Ave. Speed and % idling; b: SFC; c: SFC, Ave. Speed and % idling; d: SFC, Ave. Speed, % idling and EI of CO₂, CO and NO_x

Table 4.6 and Figure 4.2.a show the tendency and dispersion of the RD_i for the case of the traditional MT method, i.e., when the average speed and the percentage of idling time are used as the assessment criteria (Case a). By design, these CPs (mark with a red box in Figure 4.2.a) have $RD_i < 5\%$. Table 4.6 and Figure 4.2.a show that only 6 and 8 out the 19 CPs have $ARD_i < 5\%$ for the case of Urban 1 and 2 regions, respectively. Table 4.7 shows that $\overline{ARD}_{CPs} = 8.85\%$ and 7.01% for the case of Urban 1 and 2 regions, respectively. However, these RD_i could be as high as 40% (Figure 4.2.a). The same situation occurs with the emission indexes that have $\overline{ARD}_{EIs} = 9.81\%$ and 7.58% , for Urban 1 and 2, respectively, but their RD_i could be as high as 40%. Similarly occurs for the case of SFC ($\overline{ARD}_{SFC} = 9.64\%$ and 7.50% for urban 1 and 2, respectively).

When the SFC is used as the only assessment criterion (Case b, Figure 4.2b), the driving cycles obtained reproduce fuel consumption ($\overline{ARD}_{SFC} < 5\%$) and fairly well emissions ($\overline{ARD}_{EIs} = 6.38\%$ and 6.55% for urban 1 and 2). However, this alternative produces driving cycles that could have problems representing the driving patterns ($\overline{ARD}_{CPs} = 14.74\%$ and 9.61% for Urban 1 and 2, respectively). The kinetic intensity and idling time are de CPs with the most significant problems, especially in the Urban 1 region where the $ARD_i > 45\%$ for these two CPs. When SFC is used as the only assessment criterion, idling time is hard to reproduce because the energy consumption associated with idling is negligible compared to when the vehicle is moving. Thus, driving cycles with long or short idling time exhibit similar fuel consumption. Similarly happens with the kinetic intensity. Even though the vehicle kinetic energy is provided by the fuel, there are other modes of energy that could be more relevant in the operation of the vehicles. For the case of heavy-duty vehicles used for passenger transportation in large urban center, the frequent acceleration-breaking events have a great influence on fuel consumption. In these cases, KI has a low influence on fuel consumption.

Then, we combined both cases to improve the representativeness of the driving cycles produced by the MT method using SFC as assessment criteria, and to improve fuel consumption and emissions reproducibility of the driving cycles produced by the traditional MT method. Table 4.6 and Figure 4.2c show the tendency and dispersion of the RD_i obtained when the SFC, average speed, and percentage of idling time are used as assessment criteria (case c). They show that in the Urban 1 and 2 regions, 9 out of the 19 CPs presented ARD_i values lower than

5%, while 12 of the 19 CPs presented values of IQR_i lower than 5%. They also show that all CPs exhibit ARD_i smaller than 20%, except for the maximum positive acceleration in the urban 1 region, which reached a value of 29%. Furthermore, Table 4.7 shows that this case exhibit the lowest values for \overline{ARD}_{CPs} (7.66% and 6.31% for urban 1 and 2, respectively), and acceptable values for emission indexes \overline{ARD}_{EIs} (5.36% and 5.04% for urban 1 and 2, respectively). These results indicate an appropriate performance of the EBMT method representing the local driving pattern and reproducing fuel consumption and emissions.

We also explored the possibility of adding the emission indexes as assessment criteria (case d). Figure 4.2d and Table 4.6 shows that for this case (SFC, Average speed, percentage of idling time, and emission indexes of CO₂, CO, and NO_x as assessment criteria), the number of CPs with ARD_i and IQR_i , with values lower than 5%, remained the same for the case of Urban 1 region and increased up to 11 CPs for the Urban 2 region. By design, it reduced the \overline{ARD}_{EIs} to values smaller than 5%, while the \overline{ARD}_{CPs} remained approximately constant at values close to 7%. However, the maximum positive acceleration kept being the only CP with ARD_i above 20% for the case of Urban 1 region. Even though this case produces the best performance of the MT method, it requires of measurements of the instant vehicle tailpipe emissions, which is an expensive process that involves the use of Portable Emissions Monitoring Systems (PEMS), making the testing process invasive, i.e., it interferes with the normal use of the vehicle given the large size of this type of instrumentation.

Given the previous results, we recommend adopting the specific energy consumption, average speed, percentage of idling time, and average positive acceleration as the assessment criteria in the MT method to guarantee that the constructed driving cycles represent the local driving pattern and reproduce fuel consumption and emission of tailpipe emission of pollutants. We named this case as the EBMT method.

Aiming to minimize the probability of selecting a driving cycle with high RD_i , which is an inherent problem of the MT method, and to eliminate the lack of reproducibility of this method, we propose to add a final step in the construction of driving cycles. It consists of repeating at least 500 times the method and chose the driving cycle with the smallest ARDs as the best representative driving cycle. This step makes the traditional MT and the EBMT methods reproducible.

This work was conducted using data of a fleet of buses with similar technology. Therefore, it should be extended to different types of vehicle fleets operating in different regions to increase the generality of our conclusions. Additionally, further work is required to identify the appropriate length or duration of the driving cycles. The cost of implementing a driving cycle in a chassis dynamometer increases with its duration, while a minimum duration is required to ensure an appropriate signal to noise ratio of the resulting data of fuel consumption and emission of pollutants.

4.2.7 Summary and conclusions

In this work, we proposed the Energy Based Micro-Trip (EBMT) method for obtaining driving cycles that truly represent local driving patterns, and simultaneously reproduce the energy consumption and tailpipe emissions observed during the normal operation of the vehicles, when a vehicle of similar technology follows the driving cycle in a chassis dynamometer. For the

case of fuel-powered vehicles, the EBMT method consists of the traditional Micro-trips method, where the assessment criteria are the specific fuel consumption (SFC), average speed, and percentage of idling time.

To evaluate the performance of the EBMT method, we implemented it in two urban regions with similar traffic conditions. We used 1 Hz experimental data of speed, fuel consumption, and tailpipe emissions from a fleet of 15 transit buses that operate in these two regions. We established that a driving cycle represents a driving pattern when the CP^*_i that describe it are similar to the CP_i that describe the driving pattern in that region ($CP^*_i = CP_i$). Similarly, we established that a driving cycle reproduces the energy consumption and tailpipe emissions when its SFC^* and emission indexes (EI^*) are similar to the real SFC, and EI observed in the vehicles in their normal operation in the region of interest. We quantified the degree of representativeness of the driving pattern and reproducibility of energy consumption and emissions via their relative differences (RD_i) and established a 5% as the threshold for acceptable performance. As the MT method produces a different driving cycle every time the method is applied, we repeated the process of constructing the driving cycle 1000 times, calculated all RD_i at each iteration, and reported their tendency as the average relative differences (ARD_i) and their dispersion as the interquartile range (IQR_i).

We considered four cases of assessment criteria during the construction process: a.) Average speed and percentage of idling time (traditional MT method); b.) SFC; c.) Average speed and percentage of idling time, and specific energy consumption (EBMT method); d.) Average speed and percentage of idling time, SFC, and emission indexes of CO, CO₂, and NO_x. Best results were produced by the EBMT method (case c). Driving cycles constructed by this method represents the driving patterns with average relative differences $\overline{ARD}_{CPs} < 7.66\%$ and reproduce energy consumptions with $ARD_{SFC} < 2.69\%$ and tailpipe emissions with $\overline{ARD}_{EIs} < 5.36\%$. After 1000 iterations, the ARD_i for all CPs were below 20%, except for the case of the maximum positive acceleration that reached an ARD_i value of 29% in the Urban 1 region. These results mean that the EBMT constructs driving cycles that represent the driving patterns and reproduces the energy and environmental performance of vehicles.

Based on the learnings of this work, we propose to add a final step in the construction methods of driving cycles. It consists of repeating at least 500 times the method and chose the driving cycle with the smallest ARDs as the best representative driving cycle. This step makes the traditional MT method and the EBMT reproducible. The lack of reproducibility of the resulting driving cycle has been the major drawback of the methods based on the MT method. Additional work is required to consider regions with relevant variations in altitude.

5 Main characteristic parameters to describe driving patterns

Abstract: Currently, there is an increasing interest in obtaining driving cycles that truly represent the local driving pattern and reproduce the real energy consumption from electric and engine-powered vehicles use when they are tested on a chassis dynamometer. Both driving patterns and driving cycles are described by a set of characteristic parameters (CP) such as average speed and mean positive acceleration. However, it is unknown which set of CPs to use for these purposes. Aiming to address this issue, we considered two urban regions and sampled their driving pattern by monitoring second by second the regular operation of 15 vehicles for eight months. Then, we hypothesized that 2 or 3 CPs are enough to fully describe driving patterns. Toward that end, we constructed DCs via the Micro-trips method using combinations of 2 or 3 CPs as assessment parameters. We considered 19 CPs widely used, tested 1140 combinations of those CPs, and repeated the process 1000 times for each combination. Finally, we used the methodology proposed by Huertas et al. to evaluate the degree of representativeness of each resulting DCs. We observed the tendency and dispersion of the results. We concluded that, for our cases of study, the average speed, the percentage of idling time, and the standard deviation of the acceleration, are the CPs that properly describe driving patterns, and must be included in the MT method to construct DC that reproduce energy consumption and tailpipe emissions.

Keywords: Driving cycles, Micro-trips method, fuel consumption, tailpipe emissions

Frequent symbols and acronyms

Symbol	Description	Unit
EI_i	Emission Index for pollutant i	g/km
PKE	Positive Kinetic Energy per distance traveled	m/s ²
SFC	Specific Fuel Consumption	L/km
R^2	Coefficient of determination	-
CP	Characteristic Parameter	-
DC	Driving cycle	
GPS	Global Positioning System	
masl	Meters above sea level	
MT	Micro-trip	
OBD	On-Board Diagnostics System	

5.1 Introduction

Currently, there is an increasing interest in establishing the proper way of describing local driving patterns, especially for the design of energy management strategies that minimize the energy use in electric vehicles. Designers use driving patterns for the optimization of electric power trains with smaller electric motors, the design of strategies to maximize vehicle autonomy, and for the design of alternatives of smart mobility.

A driving pattern is related to the human aspects involved in the use of vehicles, representing the way people drive in a specific city or region. Currently, driving patterns are described through characteristic parameters (CPs), which are variables resulting from any combination of speed and time, such as average speed and average positive acceleration. Thus, it is typical to describe how people drive in a specific city specifying the average speed and the average acceleration. However, there are still discrepancies on which set of CPs describes the driving patterns accurately.

Driving patterns are also described by driving cycles (DCs). They are speed-time series that can also be described by their characteristic parameters (CP_i^*). Then a DC represents a driving pattern when its CP_i^* are close to the values of the corresponding CP_i of the driving pattern ($CP_i^* \approx CP_i$). Existing DCs are used by carmakers to evaluate the energy consumption and emissions of their vehicles, as part of the regulatory process established to introduce a new vehicle technology in a market [2], [44], [48]. However, the DCs currently used by carmakers do not represent any local driving pattern. The accurate description of driving patterns through DCs is a pre-requisite to assess the real energy and environmental performance of the vehicles in a given region. Errors in the description of driving patterns have led to significant differences between the fuel consumption reported by manufacturers and the one observed throughout the course of the regular use of the vehicles. Recent studies have shown that both fuel consumption and emissions in the real world are between 8% and 60% larger than those reported by manufacturers [15], [60], [66] .

The DC representativeness depends mainly on four factors: (i) the quality and quantity of vehicle operation data, (ii) the DC construction method, and (iii) the parameters used to evaluate the DC representativeness, and (iv) the duration of the DC [33]. The use of state of the art in Information Technologies (IT) and Global Information Systems (GIS) addresses the first factor. Today, they allow monitoring hundreds of vehicles simultaneously at high frequency (~ 1 Hz).

Regarding the second factor, there are two approaches: stochastic and deterministic methods. The Micro-trips (MT) and the Markov chains - Monte Carlo methods are two conventional stochastic approaches. These methods construct DCs by splicing together trip segments [3] or states [12], [46], which are quasi-randomly selected from the collected trip database [45]. On the other hand, in the deterministic approach, one trip out of a set of monitored trips is selected to be the DC. The MT method is by far the researchers' preferable method (Table 1). The Micro-trip method main drawback is that it produces different results every time the method is replicated (with the same input data). In this work we propose to solve this issue by replicating the method a large number of times (~ 1000 times) and looking at the tendency and dispersion of the results.

Table 5.1 Construction methods and CPs used as assessment parameters in some DCs

Driving cycle	CPs used as assessment parameters																				Method	Reference
	Ave s	Ave s+	Ave a+	Ave a-	Ave l	Accel/km	N	% idl	% Creeping	% a+	% Cruising	% a-	RMS s	RMS a	PKE	RCA	SAPD	VSP	Max s	Min s		
FTP 72, FTP75	*						*												*		TB	[61]
LA92, Unified Cycle																	*				MT	[45]
LA01	*																*		*	*	MCMC	[45]
HHDDT Cycle	*							*	*	*	*	*							*		MT	[2]
Arterial Cycles								*		*	*	*					*	*			MCMC	[2]
Edinburgh Cycle																	*				MT	[2]
IEC	*	*	*	*	*	*	*	*		*	*	*									TB	[24]
ARTEMIS Cycle	*	*	*	*			*	*									*		*		MT	[32]
TRL Cycle	*		*		*														*	*	MT	[2]
Sydney Cycle	*							*					*				*				MT	[24]
Melbourne Peak Cycle	*							*					*	*	*		*				MT	[24]
CUEDC Cycles	*							*		*									*		MT	[2]
Perth Cycle	*						*	*					*	*	*		*				KT	[24]
TMDC		*	*	*	*			*		*							*				TB	[55]
KHM	*	*	*	*	*	*		*		*	*	*		*							MT	[2]
China Cycles	*	*	*	*		*		*		*	*	*			*						MT	[22]
Beijing Cycles	*	*	*	*				*		*	*	*						*	*		MT	[2]
HK and Zhulai Cycles	*	*	*	*	*	*	*	*	*	*	*	*		*	*		*		*		MT	[2]
Pune Cycle	*							*		*	*	*					*				MT	[23]
Metro Manila Cycle	*																*		*	*	MCMC	[2]
BDC Cycle	*	*	*	*			*	*		*	*	*			*						MT	[40]
WLTC	*		*			*											*				MT	[17]
WMTC																	*				MT	[19]

MT: Micro-trips, MCMC: Markov Chain-Monte Carlo, TB: Travel based, KT: Knight Tour

Ave l: Mean length of micro-trips; N: Average number of stops; RCA: Rate of change of acceleration; SAPD: Speed acceleration probability distribution

All these methods evaluate how close the resulting DC represents the driving pattern using as criteria a set of CPs (third factor). Table 1 shows the CPs used in some of the DCs developed around the world. It shows that average vehicle speed and percentage of idling time are the CPs most frequently used. Recently, the specific fuel consumption started to be used as assessment criteria due to the possibility of monitoring fuel rate consumption through the vehicle engine control unit.

Even though the correct description of driving patterns is a pre-requisite to evaluate the energy and environmental performance of the vehicles, Table 5.1 shows that there is not a unique set of CPs used to assess the DC representativeness. Furthermore, work is required to develop a methodology to evaluate if an arbitrary combination of speed-time can be accepted as a CP. Work is also required to establish which variables need to be included as assessment criteria in the construction of DC, regardless if they are CPs.

To address these issues, this study focuses on the identification of the set of CPs that should be used as assessment parameters in the construction of DCs that reproduce the real vehicle energy consumption and tailpipe emissions. The resulting CPs are the ones that best describe the driving patterns in a giving region. In this work we defined metrics to verify and quantify the fulfillment of these 3 requirements. We tested our contributions to new knowledge in a megacity (Mexico City) and a large urban center (Toluca City), using a large data base of simultaneous 1 Hz measurements of speed, fuel consumption and tailpipe emissions, taken from monitoring a large sample of vehicles of the same technology during a long period of time, under normal working conditions.

5.2 Materials and methods

A DC represents a driving pattern when $CP^*_i \approx CP_i$ for all CPs, and when the fuel consumption and tailpipe emissions of the vehicles that follow that DC on a chassis dynamometer are similar to the observed from vehicles of the same technology under normal driving conditions.

Aiming to identify the set of CPs that, when used as assessment parameter, produces DCs that best represent the local driving pattern:

- We obtained the driving patterns of two different urban regions by monitoring second by second the speed of a fleet of busses during eight months of normal operation. We also monitored their fuel consumption and tailpipe emissions for two months. We constructed a common database of trips, vehicle speed, fuel consumption, and tailpipe emissions. In this work, we used the database reported by [57], [67]. However, we will describe briefly the process of constructing that database.
- Using the same database, we tested the level of representatives of the DCs obtained using different combinations of CPs as assessment criteria via the MT method. We hypothesized that 2 or 3 CPs are enough to achieve this objective.
- We identified the combination of CPs that, when used as assessment criteria, systematically produces DCs that best represent the driving pattern in both regions.

Next, we will describe each of these steps.

5.2.1 Selected regions

For this study, we selected two urban regions with different driving conditions. Table 5.2 describes the characteristics of the two studied regions. The first region (Urban 1) corresponds to a flat densely populated region inside Mexico City (2255 meters above the sea level – m.a.s.l.). In this region, we arbitrarily selected a set of roads covering 11.5 km, which are characterized by highly congested traffic (i.e., LoS E or F). The second region (Urban 2) corresponds to a flat region located on the outskirts of Toluca City (2611 m.a.s.l.). In this region, we selected 18.8 km of roads with medium traffic flow (i.e., LoS D).

Table 5.2 Description of the regions considered in this study.

Parameter	Units	Urban 1	Urban 2
Location	-	Mexico City	Toluca
Topography	-	Flat	Flat
Level of traffic	-	High	Medium
Road <i>LoS</i> *	-	E-F	D
Speed limit	km/h	60	60
Number of lanes	-	3	3
Length	km	11.5	18.8
Ave road grade	%	1.4	1.8
Max road grade	%	5.2	9.0
Min altitude	masl	2255	2611
Max altitude	masl	2258	2637

* LoS is the level of quality of a traffic facility. It represents a range of operating conditions, generally in terms of service measures such as speed and travel time, freedom to maneuver, traffic interruptions, and comfort and convenience. The classification was done according to the US Highway capacity manual [49].

5.2.2 Vehicle fleet

Fifteen buses were monitored. They had the same engine technology, similar maintenance conditions, were operated in the same routes, and driven by their regular drivers. The buses were built between 2012 and 2014. With 49-passenger capacity and a curb vehicle weight of 14,435 kg, the buses operate with a diesel engine Cummins ISM 425 with emission control EURO IV, power of 425 HP, and torque of 2,102 Nm. The overall dimensions of the buses are 12.85 m, 3.6 m, and 2.6 m long, wide, and high, respectively. The vehicles were loaded with a weight of 2,100 kg of water tanks to simulate the average passengers' load.

5.2.3 Instrumentation

The vehicle location (Latitude, Longitude and Elevation) and speed were measured by using a global position system (GPS) Garmin 16x. The sampling frequency was 1 Hz. The On-Board Diagnostics (OBD) system was used to acquire fuel consumption through the Engine Control Unit (ECU). Using the electronic fuel injection system of the bus, we determined the instantaneous fuel consumption by reading the opening time of the injector. The collected OBD data were validated using an external graduated tank, which is the standard gravimetric procedure to determine the fuel consumption of vehicles [51], [52]. Based on the correlation coefficient ($R^2 > 0.9$) obtained in a correlation analysis between the results obtained by these two methods, we concluded that the OBD method produces reliable data [57].

Polluting emissions were monitored with a Portable Emission Measurement System (PEMS), SEMTECH ECOSTAR model from Sensors Inc. with the modules for measuring CO, CO₂, NO, and NO₂. With the SEMTECH-FEM module, CO and CO₂ emissions were measured using a non-dispersive infrared analyzer, and the SEMTECH-NOx module for NO and NO₂ emissions using a non-dispersive ultraviolet gas analyzer. Both concentration measurement systems are recommended by the US Environmental Protection Agency (USEPA) for these purposes. At the beginning and at the end of each measurement, the recommended calibration procedure by the manufacturer was carried out using NIST traceable calibration gas tanks. The technical characteristics of the equipment used are presented in Table 5.3.

Table 5.3 Technical characteristics of the instruments used in this study.

Variable	Instrument/ Trademark	Technical characteristics		
Speed, time and position (latitude, longitude and elevation)	GPS / Garmin 16x	Position: 3-5 m, 95% typical Frequency: 1 Hz Speed: 0.05 m/s root mean square steady state Pulse per second (time): 1 microsecond at rising edge of pulse		
Instantaneous fuel consumption	-	Estimated through the injection time Reported by ECU through OBD		
		Technique	Range	Resolution
CO ₂		Non-Dispersive Infrared	0 - 20% v/v	0.01 % v/v
CO		Non-Dispersive Infrared	0 - 8% v/v	10 ppm v/v
NO	PEMS	Non-Dispersive	0 - 3000 ppm v/v	0.3 ppm v/v
	SEMTECH	Ultraviolet		
NO ₂	ECOSTAR	Non-Dispersive	0 - 500 ppm v/v	0.3 ppm v/v
		Ultraviolet		
Flow Measurement		Exhaust Flow Meter	-	0.1 kg/h

5.2.4 Monitoring campaign and data quality analysis

Simultaneous measurements of the variables listed in Table 5.3 were made in the two regions described in Table 5.2. The vehicles described in section 5.2.2 were operated by their usual drivers, at different times of the day and different days of the week, during eight months in different seasons of the year. Data quality analysis was carried out to identify atypical data. Data with values outside physically possible values, like O₂ concentrations higher than 21%, were disregarded. Trips with less than 95% of data availability were disregarded. Then a data

synchronization process was carried out to couple speed, fuel consumption, and emissions using correlation analysis of variables that should be correlated, like CO₂ emissions and fuel consumption. After data quality analysis, we kept 46 trips in each region with simultaneous measurements of speed, fuel consumption, and emissions.

5.2.5 Method to identify the set of CPs that best describes driving patterns

The driving patterns of the Urban 1 and 2 regions were described by means of the 19 CP_i listed in Table 5.4. The values of those CP_i were calculated from the speed-time data of the 46 monitored trips.

Afterwards, we selected a well-accepted method to construct DCs. As described in the introduction section, the MT method is by far the most frequently used method for this purpose. However, there are many variations of this method. We selected the basic or traditional version which we describe next.

Using the trips database described above, we divided the sampled trips into micro-segments and elaborated a secondary database of micro-trips for each region. Then, the micro-trips were clustered based on their average speed and average positive acceleration. This clustering process was implemented in a commercial statistical software, using centroids as the linkage method, Euclidean distances, and a 95% level of similarity. Then, we selected micro-trips and spliced them together until they assemble a candidate driving cycle with a duration greater than 20 min. We chose this time duration because it is nearly the time duration of the existing type approval driving cycles. We observed that the resulting candidate driving cycles exhibited a time duration between 20 and 22 minutes. The selection of the micro-trips was made under a quasi-random process, which means that it was affected by the computed cluster speed-acceleration probability distribution. Within each cluster, each micro-trip has the same probability of being selected.

The criteria for acceptance of the candidate driving cycle as the representative driving cycle is based on the degree of similarity between the candidate driving cycle and the corresponding driving pattern. This method uses a set of 2 or 3 CPs for this purpose and we will refer to them as assessment parameters. The degree of representativeness is measured by the relative difference (RD_i) between the CP_i^* of the candidate driving cycle y and the CP_i that describe the driving pattern (Equation 5.1). In Equation 5.1, i represent any of CPs used as the assessment criteria. Values smaller than 5% are typically used as an acceptable threshold. Otherwise, the method restarts and selects a new group of micro-trips. The selection of the threshold value depends on the researcher's criterion or even on the empirical results. Previous studies have used values between 5% and 15% [24], [29].

$$RD_i = \frac{\sum |CP_i^* - CP_i|}{CP_i} \quad (5.1)$$

The selection of those CPs used as assessment parameters determines the representativeness of the DCs and the reproducibility of the fuel consumption and tailpipe emissions. As stated before, there is not an agreement on the CPs that should be used during this assessment of representativeness. Some authors have increased the numbers of assessment parameters during

this step. Few authors have attempted to use all CPs as assessment parameters. However, increasing the number of CPs reduces the possibility of identifying a candidate driving cycle, make the MT method computationally expensive and in some instances, it could make the MT method to diverge since two CPs may possibly lead to contradictory results.

Aiming to identify the set of 2 or 3 CPs that must be used as assessment parameters we propose to use as assessment parameters all possible combinations of 2 or 3 CPs out of the 19 CPs listed in Table 5.4, and then select the combination that produces the most representative DCs. The resulting combination will be the set of CPs that must be used in the MT method and the ones that fully describe driving patterns. Following this alternative, we tested 171 combinations of 2 CPs and 969 combinations of 3 CPs.

Then, aiming to evaluate how close the resulting DCs represent the driving pattern, we extended the applicability of Equation 5.1 and observed the relative differences of the CPs not included as assessment parameters and expected that they were under a less strict but still acceptable threshold (~20%). Equation 5.1 was also used to establish the relative difference for the specific fuel consumption (SFC) and the CO₂, CO, and NO_x emission indexes.

However, the stochastic nature of the MT method makes that each time the method is applied, the resulting DC changes generating variations in the RD_i . To overcome this situation, for each combination of CPs, we observed the tendency and dispersion of each RD_i after repeating the DC construction method many times ($N=1000$). We used the average relative difference (ARD_i , Equation 5.2) as a metric of tendency and the inter-quartile range (IQR_i) as a measure of dispersion for each RD_i .

$$ARD_i = \frac{\sum_1^N RD_i}{N} \quad (5.2)$$

Then, for each combination of CPs, we averaged the 19 values for the ARD_i and IQR_i and reported them as the \overline{ARD} and the \overline{IQR} , respectively. Finally, we selected the set of CPs that when used as assessment parameters produced DCs with the lowest values of \overline{ARD} and \overline{IQR} i.e., the set of CPs that with the highest probability produces DCs with the best representation of the driving pattern of the two regions under study. Therefore, they, by themselves, are the CPs that best describe the driving patterns in those regions.

Table 5.4 Characteristic parameters used to describe driving patterns.

Type of parameter	Characteristic Parameters (CPs)		Region		Units
	Name	Symbol	Urban 1	Urban 2	
Speed	Maximum speed	Max s	22.3	26.2	m/s
	Average speed	Ave s	7.3	10.0	m/s
	Standard deviation of speed	SD s	6.9	7.7	m/s
Acceleration	Maximum acceleration	Max a+	1.3	1.3	m/s ²
	Maximum deceleration	Max a-	-2.1	-2.1	m/s ²
	Average acceleration	Ave a+	0.5	0.4	m/s ²
	Average deceleration	Ave a-	-0.5	-0.5	m/s ²
	Standard deviation of acceleration	SD a+	0.2	0.2	m/s ²
	Standard deviation of deceleration	SD a-	0.4	0.4	m/s ²
Operational modes (% of time)	Idling	% idl	15.1	13.6	%
	Acceleration	% a+	32.9	33.8	%
	Deceleration	% a-	29.3	29.1	%
	Cruising	% cru	22.7	25.9	%
Dynamics	Number of accelerations per km	Accel/km	8.6	6.1	km ⁻¹
	Root mean square of acceleration	RMS a	0.5	0.5	m ² /s ²
	Positive kinetic energy	PKE	0.4	0.3	m/s ²
	Speed-acceleration probability distribution	SAPD	N/A	N/A	-
	Vehicle specific power	VSP	4.8	7.0	kW/ton
	Kinetic intensity	KI	0.8	0.7	1/m
Other parameters					
Fuel consumption and emissions	Specific fuel consumption	SFC	0.4	0.4	l/km
	Emission index of CO ₂	EI CO ₂	839.0	749.2	g/km
	Emission index of CO	EI CO	37.2	39.4	g/km
	Emission index of NO _x	EI NO _x	5.0	3.9	g/km

5.3 Results

We obtained the driving patterns of Urban 1 and 2 regions by monitoring the second-by-second speed of a fleet of 15 buses during eight months. Table 5.4 shows the values of the 19 CPs that describe those driving patterns. It shows that the average speed in the Urban 1 and 2 regions were 7.3 and 10.0 km/h, respectively, which are typical of regions with highly congested traffic. Additional work is required to confirm that the values of those CPs remain unaltered when monitoring a large sample of vehicles (~100) of different technologies under normal conditions of use. It also shows that in these two regions, 14.6 t diesel buses, equipped with 2004 USEPA technology, consume 0.4 l/km. Furthermore, it shows that they emit 839.0 and 749.2 g/km de

CO₂ in Urban 1 and Urban 2 region, respectively. Similarly, they emit 5.0 and 3.9 g/km de NO_x in Urban 1 and Urban 2 region, respectively.

Using the database of the 1-Hz simultaneous measurements of speed, fuel consumption and tailpipe emissions of the 46 trips monitored, we obtained the ARD_i and IQR_i after constructing 1000 times DCs by the MT method and using different combinations of assessment parameters (Figure 5.1). Then, for each combination, we obtained the \overline{ARD} and \overline{IQR} reported in Table 5.5 for both urban regions. We also obtained the ARD_i for SFC and emission indexes shown in Table 5.5. We highlight that those values were obtained after 1000 repetitions of constructing DCs via the MT method and using the set of CPs shown in Table 5.5 as assessment parameters. Table 5.5 was sorted by the overall average of relative differences (last column). We only show the top 15 out of 1140 of the two or three combinations, with the minimum \overline{ARD} and \overline{IQR} for the 19 CPs, and minimum ARD_i for SFC and emission indexes, for each region.

Table 5.5 shows that, as expected, using combinations of 3 CPs tends to produce smaller \overline{ARD} and \overline{IQR} than with 2 CPs. Only four cases of combinations of two CPs reached the top 15 cases with overall minimum relative differences.

This table also shows that in all cases, the values obtained for these average relative differences are smaller than 14%, which is within the threshold values specified as acceptable (15%). Therefore, any of the combinations of CPs shown in Table 5.5 produce DCs with a high representation of the driving pattern and high reproducibility of SFC and emission indexes.

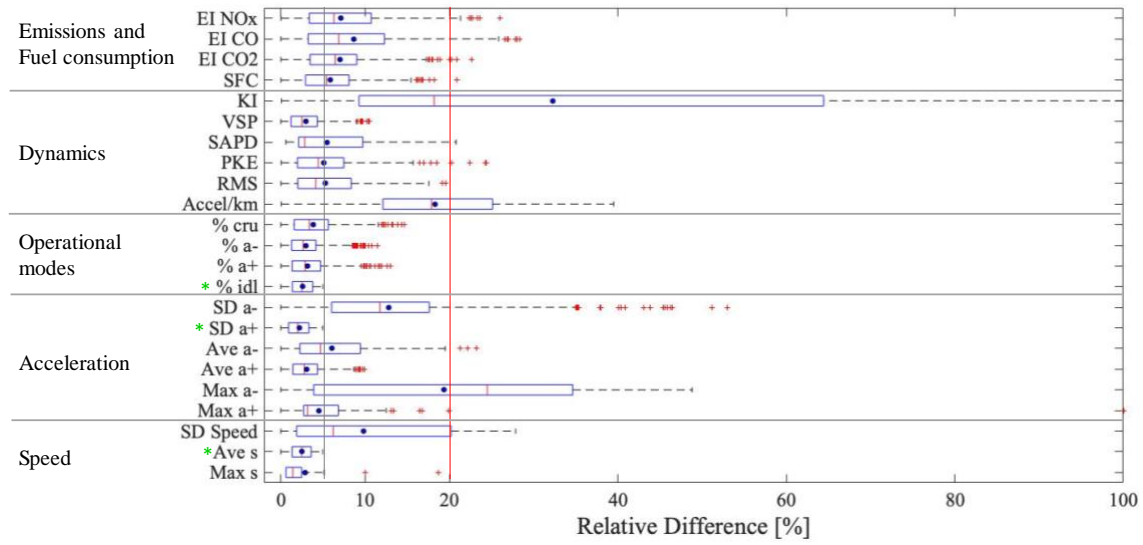
In this table, the highlighted numbers indicate the combination with the minimum values for each variable in each region. It shows that the combination of *KI*, *% idl*, and *VSP* produce, with the highest probability ($\overline{IQR} = 5.3\%$), the best representation ($\overline{ARD} = 7.4\%$) of the driving pattern in the Urban 1 region. For the case of the Urban 2 region, it is produced by the combination of *SD a+*, *% idl* and *Max a-* ($\overline{ARD} = 6.0\%$ and $\overline{IQR} = 5.4\%$).

However, those combinations do not necessarily produce DCs that best reproduce fuel consumption. Table 5.5 shows that *Max a-*, *% cru* and *Acce/km* are the CPs that best reproduce SFC in the Urban 1 region and in the Urban 2 region *SD a+*, *% idl*, and *KI* with an ARD_{SFC} of 3.9 and 3.7, respectively.

Again, *SD a+*, *% idl* and *Ave S*, is the combination of CPs that produce DCs that best reproduce NO_x emissions ($ARD_{NOx} = 7.0\%$) for the case of the Urban 1 region. For the instance of the Urban 2 region, *SDa+* and *Ave S* again was the best combination, but this time along with the *Accel/km* ($ARD_{NOx} = 5.7\%$).

The combination of CPs that best reproduce CO emissions is the same that for SFC with ARD_{CO} of 5.7% and 8.2% for the Urban 1 and 2 regions, respectively. However, we did not obtain an agreement in the combination that best reproduce CO₂ emissions. *SD a+*, *% idl*, and *Acce/km* is the best combination ($ARD_{CO2} = 5.7\%$) for the Urban 1 region while *SD a+*, *SD a-*, and *Ave S* is the best combination ($ARD_{CO2} = 3.5\%$) for the Urban 2 region. We expected that those combinations were the same as the combinations for the best reproduction of SFC. However, it was not the case.

(a)



(b)

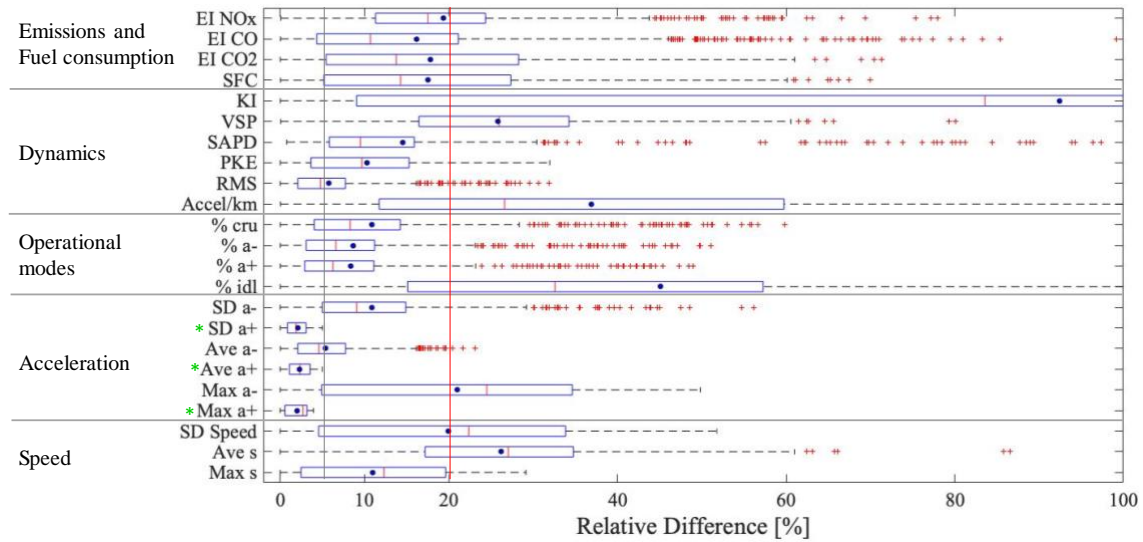


Figure 5.1 Illustrative results for ARDi (blue dots), IQRi (boxes) and outliers (red “+”) obtained after constructing 1000 times DCs by the MT method and using as assessment parameters a.) SD a+, % idl, and the Ave s which is one of the best combination, and b.) SD a+, Ave a+ and Max a+, which is an arbitrary selected combination. The CPs used by each method as criteria for the construction of the DC are marked with (green “*”).

Table 5.5 Top 15 out 1140 combinations of CPs that, when used as assessment parameters in the MT method, produce DCs that best represent driving patterns and best reproduce fuel consumption and tailpipe emissions in 2 urban regions in Mexico.

Region	Combination of CPs used as Assessment parameters			\overline{ARD} (%)	\overline{IQR} (%)	ARD_i (%)				Overall Average (%)
						SFC	EI CO ₂	EI CO	EI NO _x	
Urban 1	<i>KI</i>	% <i>idl</i>	<i>Ave S</i>	7.5	5.5	4.7	6.0	6.7	11.8	7.0
	<i>KI</i>	% <i>a+</i>	<i>Ave S</i>	7.7	6.7	4.0	6.0	6.4	11.8	7.1
	<i>KI</i>	% <i>a+</i>	<i>VSP</i>	7.5	6.7	4.2	6.4	6.3	12.4	7.2
	<i>SD a+</i>	% <i>idl</i>	<i>VSP</i>	7.9	7.3	6.0	6.9	8.0	7.6	7.3
	<i>KI</i>	% <i>idl</i>	<i>VSP</i>	7.4	5.3	5.0	6.5	7.3	12.6	7.3
	<i>Max a-</i>	% <i>cru</i>	<i>Acce/km</i>	7.9	10.8	3.9	5.8	5.7	10.9	7.5
	<i>Max a+</i>	% <i>idl</i>	<i>VSP</i>	7.9	7.0	6.4	6.6	9.6	7.6	7.5
	<i>SD a+</i>	% <i>idl</i>	<i>Ave S</i>	7.8	9.5	5.8	7.0	8.4	7.0	7.6
	<i>Max a+</i>	-	<i>Ave S</i>	9.4	9.5	4.9	7.0	8.1	7.6	7.7
	<i>SD a+</i>	-	<i>Ave S</i>	9.8	9.7	5.0	7.1	7.2	7.9	7.8
	<i>SD a+</i>	-	<i>VSP</i>	10.0	9.7	5.6	6.9	7.1	7.8	7.9
	<i>SD a+</i>	% <i>idl</i>	<i>Acce/km</i>	7.4	7.6	5.9	5.7	7.4	13.6	7.9
	<i>Max a-</i>	% <i>idl</i>	<i>Acce/km</i>	7.6	9.9	4.8	6.3	7.0	13.1	8.1
	<i>SD S</i>	% <i>idl</i>	<i>Ave S</i>	8.0	11.1	4.9	6.4	9.2	9.3	8.1
	<i>Max a+</i>	-	<i>VSP</i>	9.7	9.7	6.1	7.1	8.4	8.1	8.2
Urban 2	<i>SD a+</i>	<i>SD a-</i>	<i>Ave S</i>	6.9	6.4	4.5	3.5	8.6	6.6	6.1
	<i>SD a+</i>	<i>Max a-</i>	<i>Ave S</i>	6.1	5.9	4.5	3.8	8.3	8.0	6.1
	<i>SD a+</i>	% <i>idl</i>	<i>KI</i>	6.5	5.5	3.7	4.8	8.2	8.9	6.3
	<i>SD a+</i>	% <i>idl</i>	<i>Max a-</i>	6.0	5.4	4.7	4.5	8.3	9.6	6.4
	<i>SD a+</i>	% <i>idl</i>	<i>SD a-</i>	6.2	5.9	4.5	4.7	9.0	8.1	6.4
	<i>SD a+</i>	% <i>idl</i>	% <i>a+</i>	6.6	5.9	4.3	5.5	8.9	7.4	6.4
	<i>SD a+</i>	<i>Accel/km</i>	<i>Ave S</i>	6.7	6.0	5.3	5.0	9.9	5.7	6.4
	<i>Max S</i>	<i>Max a-</i>	<i>Ave S</i>	6.8	6.2	4.4	4.4	9.5	7.6	6.5
	<i>SD a+</i>	% <i>idl</i>	<i>Accel/km</i>	6.3	5.6	5.8	5.7	9.9	6.0	6.5
	<i>Max a-</i>	<i>Max a+</i>	<i>Ave S</i>	6.5	6.1	4.9	4.5	10.1	7.1	6.6
	<i>SD a+</i>	% <i>idl</i>	<i>Ave S</i>	6.3	5.7	5.5	5.4	10.4	6.6	6.6
	<i>SD a+</i>	% <i>idl</i>	<i>VSP</i>	6.4	5.6	4.9	5.8	10.5	6.9	6.7
	<i>SD a+</i>	% <i>idl</i>	<i>PKE</i>	6.9	5.9	4.3	5.5	8.2	10.0	6.8
	<i>SD a+</i>	% <i>idl</i>	% <i>a-</i>	6.7	6.1	5.3	5.5	9.4	9.0	7.0
	<i>SD a+</i>	% <i>idl</i>	<i>RMS</i>	6.6	5.8	5.1	6.0	9.7	10.3	7.2

Nonetheless, it is vital to notice that the range of variations of the values reported for \overline{ARD} , \overline{IQR} , and ARD_i is small (<6.6%) in comparison to the range of possible variations (0-∞). This observation means that any of the 15 combinations reported in Table 5.5 produce similar results in terms of representatives of the driving pattern and reproducibility of fuel consumption and tailpipe emissions. For example, Table 5.5 also shows that the 15 combinations of CPs reported for each region, exhibit similar values of \overline{ARD} ($6.9 < \overline{ARD}$

<10), and therefore any of those combinations produce DCs with an acceptable representation of the driving pattern found for each region. Under the previous consideration, we found that the *% idl* and *SD a+* are the most recurrent CPs (21% each), followed by *Ave S* (14%). They are followed by *VSP* and *Max a-* that showed up in less than 8% of the times. That combination showed up (highlighted in Table 5.5) among the top 15 combinations reported for each region. Therefore, we concluded that the *SD a+*, *% idl*, and the *Ave S* are the CPs that best describe driving patterns, and best reproduce SFC and emission indexes.

5.4 Conclusions

The design of energy management strategies to optimize the operation of electric and engine-powered vehicles requires an accurate description of local driving patterns. It also requires driving cycles (DCs) that reproduce the real energy consumption and tailpipe emissions of the vehicles when they are evaluated on chassis dynamometers. Both driving patterns and DCs are described by characteristic parameters (CPs). However, there is disagreement about which CPs to use. This work focusses on the determination of the set of CPs that accurately describe driving patterns and must be included in the Micro trip (MT) method to construct DCs that reproduce energy consumption and tailpipe emissions.

We hypothesized that 2 or 3 CPs are enough to achieve these objectives. Aiming to validate this hypothesis, we considered two urban regions in Central Mexico and sampled their driving pattern by monitoring second by second the regular operation of 15 vehicles for eight months. After data quality analysis, we constructed a database of 46 trips with 1-Hz simultaneous measurements of speed, fuel consumption, and tailpipe emissions (CO_2 , CO, and NO_x). Then, we constructed DCs via the MT method using combinations of 2 or 3 CPs as assessment parameters. We considered 1140 combinations among 19 CPs frequently reported in the literature. Using the definition that a DC represents a driving pattern when the CPs of the DC and of the driving pattern are similar, we evaluated the degree of representativeness. We repeated this process 1000 times for each combination of CPs and observed the tendency and dispersion of the relative differences for each of the 19 CPs considered and for SFC and emission indexes. We reported the top 15 combinations with the highest probability (smallest interquartile range) that the DCs constructed represents the driving pattern (smallest average relative differences of corresponding CPs) with the highest reproducibility of SFC and emissions (smallest average relative differences of SFC and emission indexes).

We observed that all 15 combinations that we reported were within the criteria of acceptance of representatives ($ARD_i < 15\%$). Furthermore, we also observed that the variation in ARD_i among them was negligible (<10%), and therefore, any of those combinations exhibit a similar degree of representativeness. Then we observed that idling time, the standard deviation of the positive acceleration, and average speed were the most recurrent. Therefore, we concluded that they are the ones that must be included in the MT method as assessment parameters to obtain DCs that represent the driving pattern of the region under consideration and that reproduce the real energy consumption and tailpipe emission of the vehicles. This result agrees with the fact that average speed and the percentage of idling time are the CPs most frequently used by researchers for constructing DC. However, our work shows that a

third CP (the standard deviation of the positive acceleration) should be included. Alternatively, kinetic intensity or vehicle specific power can be used for the same purpose.

Previous conclusions stand for the urban regions considered in this study. Additional work is required to extend the scope of these conclusions to any region and any vehicle technology.

6 Relationship between the time duration of a driving cycle and its representativeness result

Abstract: Nowadays, there is an interest in representing properly the driving patterns, energy consumption and vehicle emissions of a region. Driving pattern is understood as the way that people drive their vehicles. One of the ways to represent the driving patterns is through time series of speed, denominated driving cycles (DC). The duration of the DC is an important factor to represent the driving patterns of a region. Short DCs tend to generate higher fuel consumption and emissions results due to fact that the vehicle operates primarily in its warm-up phase. Longer DCs represent higher costs in the type approval tests. The time duration of DCs is a less studied topic in current research of DCs construction. The time duration of each DC is unique since it represents local and particular operating conditions. However, there is no defined methodology to establish the duration of DCs based on the driving characteristics of a specific region. This study aims to study the effect of different time durations of the DCs on their representativeness. We used data of speed, time, fuel consumption and emissions of travels monitored for eight months from a fleet of 15 buses operating in two flat urban regions with different traffic conditions. Using Micro-trips method, we built DCs with a time length of 5, 10, 15, 20, 25, 30, 45, 60 and 120 minutes for each region. For each time length, we built 500 DCs in order to establish the trend and dispersion of their characteristic parameters. The results indicate that for having DCs with relative difference equal or less than 10% respect to the driving patterns, the DCs must have a duration of more than 25 minutes. This time length also guarantees the representativeness, in terms of energy consumption and tailpipe emissions.

Keywords: Representative driving cycles, Time duration of driving cycle, Driving patterns, Characteristic parameters, Micro-trips methods.

Frequent symbols and acronyms

Symbol	Description	Units
ARD_i	Average relative difference of the i^{th} characteristic parameter	%
CP_i	Values of the i^{th} characteristic parameter that describe the driving pattern	-
CP_i^*	Values of the i^{th} characteristic parameter that describe the driving cycle	-
IQR_i	Interquartile range of the i^{th} characteristic parameter	-
SFC	Specific Fuel Consumption	L/km
RD_i	Relative difference of the i^{th} characteristic parameter	%

6.1 Introduction

Nowadays, there is an increasing interest to study the manner that drivers drive the vehicles in a region, and its impact on the energy consumption for electric vehicles, and fuel consumption and tailpipe emissions for vehicles with internal combustion engine. Conceptually, local driving patterns is the term to define the average driving characteristics of region. The driving pattern can be represented by a speed-time series, denominated as driving cycle (DC) [2], [34].

The DCs are mainly used to evaluate the fuel consumption and emissions compliances of a vehicle model before entering into a country automotive market. Moreover, DCs can be used for the powertrain design, to compare performance of the vehicles and to develop emissions inventories [18], [36]. In the latest years, with the deployment of hybrid and pure electric vehicles, as an alternative to reduce the greenhouse gas (GHG), new DCs have been developed for evaluating the energy management, batteries and energy storage capacity, and the vehicle mileage [68]. The representativeness of the local driving pattern is the key issue of a DC and it depends mainly on three factors: (a) the quality and quantity of vehicle operation data, (b) the DC construction method, and (c) the CPs used to assess the DC representativeness [33].

However, a fourth factor that could affect the local driving cycle representativeness, the energy consumption and the tailpipe emissions is the time duration of the DC. Short DCs tend to generate higher fuel consumption and emissions results due to the fact that the vehicle operates in the warm-up phase and has not reached the normal operating temperature. Longer DCs represent higher costs in type approval test [17]. A time duration for the DC must be defined to allow the vehicle operates under its normal operating temperature and to properly represent the local driving patterns [29], the energy consumption and the vehicle emissions. Although the importance of time duration of the DC, this topic has not been totally developed by the researchers in their driving cycle construction process. Moreover, the researchers defined the duration of the DC based on their experience and knowledge of the driving conditions of the study region. Amirjamshidi [69] suggested that a DC generated by micro-trips method must have a time duration between 10 to 30 minutes. Ho [43] noted down that random approaches to build DCs like micro-trips entails to define a pre-determined time duration of more than 1000 s without rational scientific justification which is a shortcoming in the methodology. Ho [43] performed trip distance and time duration survey. The trip distance result was used to define the DC length according to the percentage of each type of road segment. A driving cycle with time duration of 2344 s was obtained for Singapore. A difference of 2.3% between the trip survey (2400 s) and the proposed DC was established. The process followed in the Singapore DC assures the similarity between the DC and the city trip duration. However, this method does not solve the question of the minimum time duration of a DC for having a representativeness in terms of local driving patterns, fuel consumption and emissions. Knez [20] developed the Celje driving cycle and found a relation between the increase of the average speed, the reduction of the trip time and the traffic conditions. Figure 6.1 presents a summary of the time duration and average speed of different driving cycles used in the type approval test or developed for different regions around the world.

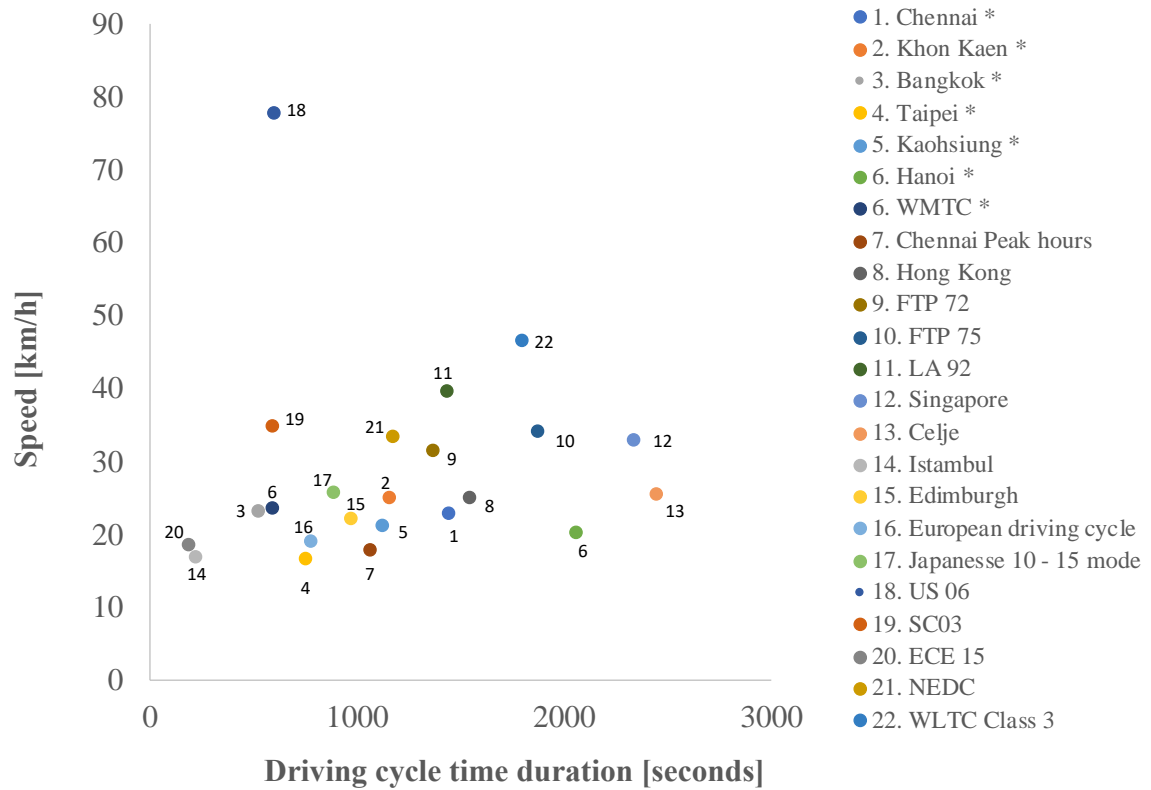


Figure 6.1 Time duration and average speed for driving cycles developed for different regions or cities. * Correspond to driving cycles for motorcycles

The aim of this study is to analyze the effect of different values of time duration of the DCs on the representativeness of local driving patterns, fuel consumption and tailpipe emissions of two urban regions with different traffic characteristics. For this purpose, using the same trips database, we built DCs for each region with a time length of: 5, 10, 15, 20, 25, 30, 45, 60 and 120 minutes. For each time duration, and using the Micro-trip method, we built 500 DCs in order to establish the trend and dispersion of 19 characteristics parameters used to describe both, the local driving patterns and the DCs [19], [30]. The characteristics parameters are metrics, like average speed or average positive acceleration, calculated from the speed and time data collected in the monitored trips. We define CP as the characteristic parameters that describe local driving patterns, while CP* is the characteristic parameter that describe the DCs. Relative differences close to zero, between CP and CP* [60], indicate that the DC represents the local driving patterns of a given region accurately.

The paper is organized as follows. In the materials and method section an overview of the selected region is introduced. Then, the technical aspect of the vehicles and the instrumentation is presented. Next, the details of the monitoring campaign are described. Later, the process of building DCs with different time duration and the method to compare their results in terms of caharacteristic parameters, fuel consumption and emissions is

showed. The next session presents the results obtained for the different time duration. A concluding section outlines the main outcomes of the study.

6.2 Materials and methods

6.2.1 Region selection

We developed this study in two urban road located in high altitude. The selected roads are part of the MEX 15D road, that connects Toluca-Mexico City. The selected road segments have length 11.5 and 18.8 km inside Mexico City (2255 m.a.s.l.) and Toluca City (2611 m.a.s.l.) respectively. The road of Mexico City is characterized by highly congested traffic represented in its Level of Service (LoS) graded F. The road of Toluca City is medium congested traffic with a LoS graded on E. The LoS is the level of quality of a traffic facility and represents a range of operating conditions, generally in terms of service measures such as speed and travel time, freedom to maneuverer, traffic interruptions, and comfort and convenience [49]. The characteristics of the selected roads are presented in Table 6.1.

Table 6.1 Characteristics of the selected region

Parameter	Unit	Urban 1	Urban 2
Location	-	Mexico City	Toluca City
Facility	-	Local roadway	Arterial
Level of traffic	-	High	Medium
<i>LoS</i>	-	F	E
Speed limit	km/h	60	60
Number of lanes	-	3	3
Length	km	11.5	18.8
Ave road grade	%	1.4	1.8
Max road grade	%	5.2	9.0
Min altitude	m.a.s.l.	2255	2611
Max altitude	m.a.s.l.	2258	2637

6.2.2 Instrumented vehicles

Fifteen buses were used during the monitoring campaign. The selected vehicles presented the same maintenance, route of operation, and technology characteristics to reduce noise. They were provided by the passenger transport company *Flecha Roja*. This company offers a non-stop service. The buses were built between 2012 and 2014. They have 49-passenger capacity and a gross vehicle weight of 13850 kg. They operate with a diesel engine Cummins ISM 425 with emission control EURO IV, power of 425 HP, and torque of 2102 Nm. We used the following data: dimensions of 12.85, 3.6, and 2.6 meters long, high and wide

respectively, a frontal area of 8.47 m², a coefficient of rolling resistance of 0.06, and a resistance coefficient aerodynamics of 0.64 [50]. The vehicles were loaded with a weight of 2100 kg of water tanks to simulate the total average weight of passengers.

Vehicle location (Altitude, Latitude, and Longitude) and speed were measured by using a global position system (GPS) Garmin 16x. The data sample frequency was 1 Hz. Regarding fuel consumption, the On-Board Diagnostics (OBD) system was used to read this variable from the Engine Control Unit (ECU). These diesel vehicles have an electronic fuel injection system that, according to the opening time of the injector, the instantaneous fuel consumption is determined. The data obtained in this way were validated by using an external graduated tank, which is the standard procedure to determine the fuel consumption of vehicles [51], [52]. Based on the determination coefficient ($R^2 > 0.9$) obtained in a correlation analysis between the results obtained by these two methods, we concluded that the OBD produces reliable data.

The emissions were monitored with a Portable Emission Measurement System (PEMS), SEMTECH ECOSTAR model from Sensors Inc. with the modules for measuring CO, CO₂, NO and NO₂. With the SEMTECH-FEM module, CO and CO₂ emissions were measured using a non-dispersive infrared analyzer, and the SEMTECH-NO_x module for NO and NO₂ emissions using a non-dispersive ultraviolet gas analyzer. Both concentration measurement systems are recommended by the US Environmental Protection Agency (USEPA) for these purposes. At the beginning and at the end of each measurement, the recommended calibration procedure by the manufacturer was carried out using NIST traceable calibration gas tanks.

6.2.3 Monitoring campaign

Measurements were made in the urban regions described in Table 6.1 during eight months in different seasons of the year. In this time, the vehicles were operated by their usual drivers, at different times of the day and different days of the week. Then, a data verification and synchronization process were carried out to identify atypical data or incomplete trip data (i.e. less than 95%) to be discarded, and to align the data readings from the three different instruments [57]. After analyzing the monitoring campaign results, 46 monitored trips were included on the sample trips data base.

6.2.4 Comparison of the time DCs duration results

The selected method to build the DCs was Micro-trips. In this method, the speed-time data collected in the vehicle monitoring campaign is partitioned in segments of trips bounded by vehicle speed equal to 0 km/h. These segments are called “micro-trips”. Micro-trips are often clustered in function of their average speed and average acceleration. Then, some of them are quasi-randomly selected based on the frequency distribution of the clusters, and later spliced to build a candidate DC [1], [48]. The similarity between the candidate DC and the local driving patterns is calculated through the relative difference (RD_i) of characteristic parameters ($CP_i \approx CP_i^*$). RD_i values equal or smaller than 5% are used as an acceptable threshold for selecting a DC. Otherwise, the method restarts and selects a new

group of micro-trips and proposed a new candidate DC. Equation 1 presents the function to calculate the relative difference.

$$RD_i = \frac{\sum(CP_i^* - CP_i)}{CP_i} \quad 6.1$$

The relative differences were calculated for the 19 characteristic parameters, two of them used as assessment criteria for selecting a DC, the rest of the characteristic parameters were calculated to describe the selected DC representativeness. Moreover, the relative difference between the average specific fuel consumption of the local driving patterns and the specific fuel consumption of the DC was calculated. This analysis was extended to the CO₂, CO and NO_x. Table 6.2 presents the characteristic parameters used in this study.

Due to the stochastic nature of the Micro-trip method, despite the use of same trip database, each time the Micro-trip method is implemented the values of CP_i* change and consequently the RD_i values. For this reason, the process was repeated 500 times and the trend and dispersion of each RD_i were established. The trend was calculated through the Average Relative Difference (ARD_i), presented in Equation 6.2, while the dispersion was calculated through the Inter-quartile range (IQR_i).

$$ARD_i = \frac{\sum_{j=1}^n |CP_{i,j}^* - CP_i|}{n CP_i} \quad 6.2$$

In Equation 6.2, n is the total number of iterations performed (500), and j is the iteration number. ARD_i and IQR_i values close to zero indicate high similarity between the constructed driving cycle and the driving pattern. The aim of this study is to analyze the effect of the time duration on the DC representativeness, then the trend and dispersion analysis was performed for different values of time duration such as 5, 10, 15, 20, 25, 30, 45, 60, and 120 minutes. Tables 6.3 and 6.4 presents the ARD results for region urban 1 and urban 2 respectively. Characteristic parameters with ARD and IQR results below 5% are highlighted in grey.

A set of metrics to compare which time duration of DC best represents the local driving patterns is the average ARD (\overline{ARD}) and the average IQR (\overline{IQR}). Equation 3 and Equation 4 show the manner to calculate the average ARD and the average IQR, respectively.

$$\overline{ARD} = \frac{\sum_{i=1}^k ARD_i}{k} \quad 6.3$$

$$\overline{IQR} = \frac{\sum_{i=1}^k IQR_i}{k} \quad 6.4$$

The subscripts i refer to any of the CPs in Table 6.2, and therefore $k=19$. This analysis is extended to the specific fuel consumption, and emissions presented in the Table 6.2. Low values of average ARD and average IQR indicate that the selected time duration generate driving cycles that well represent the local driving patterns, fuel consumption and emissions. The \overline{ARD} and \overline{IQR} results are presented in a box-plot figure to have an overall view of the time duration impact.

Table 6.2 Characteristics parameters used to describe the driving cycles in this study

Type		Name	Symbol
Speed	1	Average speed*	Ave Speed
	2	Maximum speed	Max Speed
	3	Standard deviation of speed	SD speed
Acceleration	4	Maximum acceleration	Max a+
	5	Maximum deceleration	Max a-
	6	Average acceleration	Ave a+
	7	Average deceleration	Ave a-
	8	Standard deviation of acceleration	SD a+
	9	Standard deviation of deceleration	SD a-
Operational modes (% of time)	10	Percentage of idling time*	% idling
	11	Percentage Acceleration	% a+
	12	Percentage Deceleration	% a-
	13	Percentage Cruising	% cruising
Dynamics	14	No. of acceleration per kilometer	Accel/km
	15	Root mean square of accel.	RMS
	16	Positive kinetic energy	PKE
	17	Speed acceleration probability distribution	SAPD
	18	Vehicle Specific Power	VSP
	19	Kinetic Intensity	KI
Emissions and energy	20	Specific fuel consumption*	SFC
	21	Emission index of CO ₂	EI CO ₂
	22	Emission index of CO	EI CO
	23	Emission index of NO _x	EI NO _x

*: parameters were used as assessment criteria to evaluate the DC representativeness respect to driving patterns.

6.3 Results

Tables 6.3 and 6.4 present the ARD results of the characteristic parameters for regions Urban 1 and Urban 2. We observe that driving cycles with short time length (<10 min) present less number of CPs with an ARD below 5%. For the region Urban 1, DCs with a time length of 5 and 10 min present up to 2 of 17 CPs with ARD values below 5%. For Urban 2, DCs with a time duration of 5, 10 and 15 min present up to 3 of 17 CPs with ARD values below 5%. When the time duration of DCs increase above 15 min, the number of CPs with an ARD

values below 5% increase. It means that DCs with time duration greater than 15 min better represent the driving patterns of the studied region. DCs with a time duration close to 120 min present 13 CPs below 5%, in both regions. However, due to the high cost of dynamometer type approval test and the several amount that are tested before entering in an automotive market, is not feasible to have DCs with 120 min of time length.

In order to establish the suitable time duration of the DCs for both regions, we calculated the \overline{ARD}_{CP} and \overline{IQR}_{CP} . The Figure 6.2a presents the results of the \overline{ARD}_{CP} and \overline{IQR}_{CP} , while Figure 6.2b presents the same analysis (\overline{ARD}_{EI} and \overline{IQR}_{EI}) for the vehicle emissions on region Urban 1. Same analysis is performed for the region Urban 2 in the Figure 6.3.

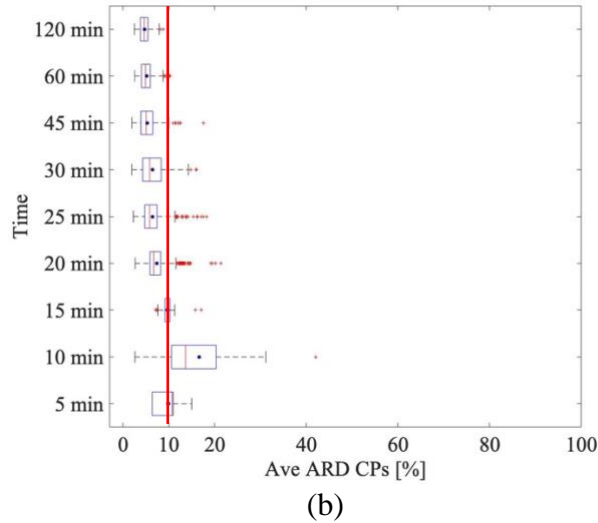
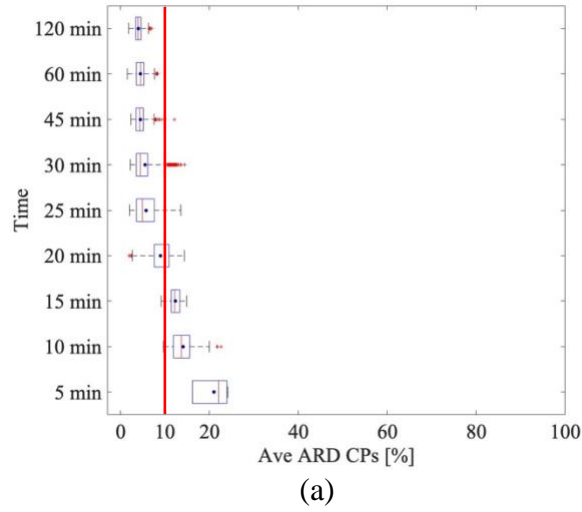


Figure 6.2 (a) Average ARD and average IQR of characteristic parameters for different driving cycle time duration. (b) Average ARD and average IQR of emissions for different driving cycle time duration, for the region Urban 1

Table 6.3 ARD results of the DCs characteristic parameters for the Urban 1 region

ARD of Characteristic Parameters	DC time length (min)								
	5	10	15	20	25	30	45	60	120
Ave Speed*	3.4	2.7	1.9	2.5	2.6	2.5	2.5	2.5	2.5
Max Speed	26.8	17.1	10.0	6.6	2.5	2.2	4.6	5.9	10.8
SD Speed	22.3	25.6	23.3	17.9	8.1	8.1	6.1	6.7	5.4
Max a+	0.2	2.4	6.1	1.8	0.6	0.6	0.0	0.0	0.0
Max a-	4.2	9.7	11.8	9.1	4.9	3.5	1.8	0.7	0.1
Ave a+	8.9	8.0	6.3	3.9	2.9	2.8	2.3	1.9	1.3
Ave a-	22.5	9.5	7.0	4.7	5.5	5.1	3.4	3.7	2.7
SD a+	27.1	9.6	7.5	5.0	3.1	3.2	2.5	2.2	1.5
SD a-	37.1	16.5	8.3	7.6	7.9	6.8	5.1	4.8	3.4
% Idling*	2.2	3.1	2.4	2.5	2.4	2.5	2.5	2.6	2.4
% a+	8.2	6.5	3.6	2.2	2.5	2.4	1.8	1.9	1.4
% a-	5.9	3.0	3.5	2.9	2.5	2.5	2.4	2.0	1.4
% cruising	18.3	11.6	8.6	4.2	3.6	4.1	3.7	3.3	2.4
Accel/km	18.5	5.7	35.8	25.1	17.2	15.8	12.2	13.8	12.9
RMS	25.2	12.4	8.3	4.9	4.4	4.1	3.0	3.0	2.1
PKE	22.6	11.7	8.3	5.3	5.0	4.6	5.1	4.2	2.9
SAPD	17.8	13.0	10.5	7.5	3.7	3.5	2.3	2.2	1.6
VSP	6.0	7.0	2.6	4.0	3.3	3.1	3.7	3.1	2.5
KI	121.6	91.7	67.6	53.4	26.2	26.0	19.0	20.3	18.6
SFC*	3.5	3.4	1.2	2.5	2.6	2.5	2.6	2.5	2.6
EI CO ₂	7.9	15.9	1.8	4.4	4.9	4.1	3.8	3.3	3.4
EI CO	16.7	12.9	17.3	9.0	6.8	6.3	5.2	4.7	4.2
EI NO _x	5.2	21.0	9.9	8.7	7.5	8.8	6.9	7.3	6.5

Table 6.4 ARD results of the DCs characteristic parameters for the Urban 2 region

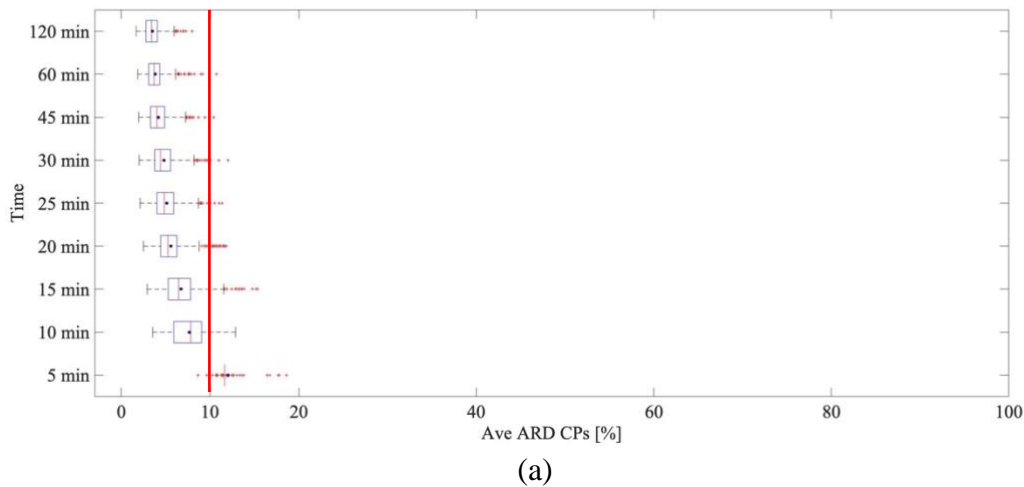
ARD of Characteristic Parameters	DC time length (min)								
	5	10	15	20	25	30	45	60	120
Ave Speed*	1.9	2.4	2.6	2.4	2.5	2.5	2.4	2.5	2.3
Max Speed	11.0	7.2	5.4	4.6	4.1	4.0	4.3	4.4	5.6
SD Speed	10.4	6.8	6.9	5.2	4.6	4.9	4.9	4.1	3.1
Max a+	0.7	4.2	1.8	1.5	0.9	0.6	0.2	0.1	0.0
Max a-	37.6	10.7	7.4	4.7	3.4	2.1	0.8	0.4	0.0
Ave a+	11.6	4.6	4.2	3.9	4.0	3.9	3.1	2.5	2.0
Ave a-	14.4	11.0	8.5	6.2	6.5	6.3	5.3	4.6	3.5
SD a+	6.9	6.2	7.0	5.9	4.9	4.7	3.9	3.3	2.5
SD a-	25.2	14.8	11.0	7.4	7.1	7.3	5.9	5.3	3.9
% Idling*	1.7	2.7	2.5	2.5	2.5	2.4	2.5	2.5	2.5
% a+	3.6	5.2	5.6	4.4	4.0	3.6	3.3	3.0	2.9
% a-	10.8	9.2	7.9	6.6	6.0	5.9	5.3	5.5	6.3
% cruising	11.0	13.4	12.8	10.6	9.8	8.6	7.0	6.1	4.8
Accel/km	6.8	11.3	12.4	11.4	9.3	9.3	8.3	8.3	9.3
RMS	16.2	5.6	5.4	4.3	4.4	3.9	3.6	3.1	3.2
PKE	19.0	6.4	7.0	5.7	5.5	4.8	4.3	3.9	3.3
SAPD	8.0	5.9	4.9	3.4	2.8	2.5	1.9	1.5	0.8
VSP	3.0	6.4	5.9	6.8	6.5	6.1	6.0	6.0	6.4
KI	28.6	11.1	8.9	8.6	8.6	7.8	6.3	6.0	4.8
SFC*	1.9	2.8	2.7	2.6	2.4	2.4	2.3	2.4	2.3
EI CO2	8.3	7.2	6.2	4.4	4.1	4.3	3.5	3.0	2.4
EI CO	15.1	11.7	11.8	9.3	7.9	8.4	7.0	6.0	4.9
EI NOx	21.5	8.8	8.1	7.7	7.3	7.5	6.9	7.3	7.6

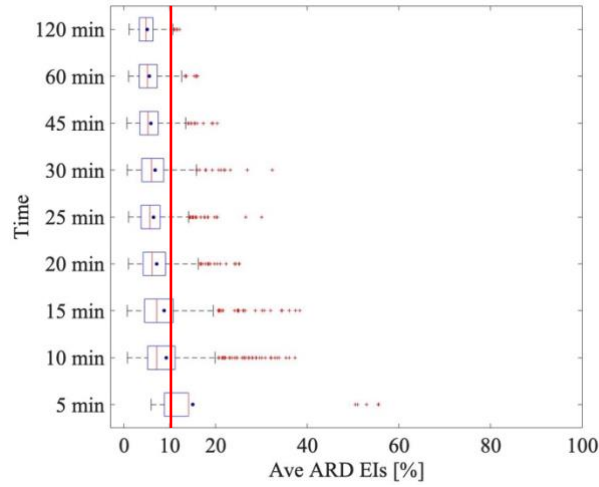
In the Figure 6.2a, we observed that DCs with a time duration below 15 minutes present the highest values of \overline{ARD}_{CP} ($>12.3\%$). For a time duration of 20 minutes the \overline{ARD}_{CP} were below 10% ($\approx 9\%$). The increase of the driving cycle time duration decreases the \overline{ARD}_{CP} values. Then, the lowest result of the \overline{ARD}_{CP} is obtained at 120 minutes ($\approx 4\%$). However, a driving cycle of 120 minutes of duration is not feasible from the economic point view in the type approval test, as we explained before. The increase of the time duration also decreases the \overline{IQR}_{CP} . Driving cycles with a time duration higher than 25 min present \overline{IQR}_{CP} results below 5%.

Short DCs, with time duration below 10 minutes, are not capable to represent the local driving patterns of the region Urban 1, then the \overline{ARD}_{CP} of the characteristic parameters is higher. On the other hand, long DCs, with time duration above 45 min, are capable to represent the local driving patterns. The latter is confirmed with the low values of \overline{ARD}_{CP} of the characteristic parameters. DCs with a time duration between 20 to 30 minutes present medium-low values of \overline{ARD}_{CP} with a reasonable time length. This analysis was extended to the emissions \overline{ARD}_{EI} obtaining similar results. Figure 2b showed that a time duration of 20 minutes, made the \overline{ARD}_{EI} tends to decrease below 10%.

Considering the number of CPs below 5%, the \overline{ARD}_{CP} , \overline{ARD}_{EI} , \overline{IQR}_{CP} , and \overline{IQR}_{EI} results, for the Urban 1 region we recommend a DC with a time length not below of 25 min. This time duration guarantees average ARDs below 6.43%, while IQRs remain below 6.03%, which means that the proposed DCs well represent the driving patterns of the study region.

For the Urban 2, in Figure 6.3a we observe a similar behavior respect to the Urban 1. DCs with time duration below 5 min present \overline{ARD}_{CP} above 10%. The \overline{ARD}_{CP} tends to decrease when the DCs time duration increases. Moreover, the Figure 6.3b show that DCs with time duration above 10 min present \overline{ARD}_{EI} values around 10%. With this result we could conclude that the driving cycle for the region Urban 2 should have a time duration above 10 min.





(b)

Figure 6.3 (a) Average ARD and average IQR of characteristic parameters for different driving cycle time duration. (b) Average ARD and average IQR of emissions for different driving cycle time duration, for the region Urban 2

In the case of the region Urban 2, we suggest DCs with a time duration not below 20 min. This time length assures DCs with \overline{ARD}_{CP} , and \overline{ARD}_{EI} below 7.15%, while \overline{IQR}_{CP} , and \overline{IQR}_{EI} remain below 7%.

6.4 Conclusions

In this study we analyzed the effect of time duration on the generation of driving cycles that truly represent the local driving patterns, and reproduce the fuel consumption, and tailpipe emissions for two urban regions located in a flat and densely populated regions with different traffic conditions. Driving cycles with time duration of 5, 10, 15, 20, 25, 30, 45, 60 and 120 minutes were built using a common trip database and the Micro-trip method. Nineteen characteristic parameters were used to compare the local driving patterns respect to the proposed driving cycles. This comparison was extended to the emissions of CO₂, CO and NO_x and for the different time durations. In the region Urban 1, DCs with time duration below 10 minutes, presented an average \overline{ARD}_{CP} higher than 14%, while long DCs with time duration above 45 min, presented the \overline{ARD}_{CP} lower than 4.5%. The average \overline{ARD}_{EI} showed the same tend to decrease when the driving cycle time length increase. We propose that the driving cycle for this type of fleet and for this specific urban region has a time duration of 25 minutes. For this time duration we observe that DCs presented values of \overline{ARD} and \overline{IQR} equal or below 6.43%. This analysis was extended to the region Urban 2, which presented average \overline{ARD}_{CP} and average \overline{ARD}_{EI} below 10% for DCs with a time length higher than 10 min. For this region we propose DCs with a time length not below to 25 min. This time length assures to have DCs for the region Urban 2 with \overline{ARD} and \overline{IQR} equal or below 67.15%. Driving cycles with this time duration are feasible to implement in the type approval test. More data

needs to be collected in more regions and with different vehicle fleets to validate the proposed analysis.

7 Development of telemetry equipment for monitoring fuel consumption and vehicle operating variables

Abstract: the interest in studying the use patterns of internal combustion, hybrid and electric vehicles under real operating conditions, has led to the development of local driving cycles. These cycles are commonly used to calculate the mechanical performance, the energy and environmental impact produced by the operation of a fleet of vehicles in a region. To develop a local driving cycle, the vehicle operating data is acquired under real driving conditions. The amount and quality of the gathered data influence the representativeness of the proposed local driving cycle. For the development of a driving cycle, it is necessary to record the operating data from the trip of the vehicle with a sampling frequency equal or greater than 1 Hz. Traditional methods for constructing driving cycles, such as Micro-trips (MT) or Markov Chains Monte Carlo (MCMC), require speed and time values as input data. However, the Energy-Based Micro-trip (EBMT) method requires not only speed data but also energy consumption data. Some of the vehicle monitoring devices available in the market do not allow to record and access data on speed and energy consumption with the required sampling frequency. This study presents the development of telemetry equipment to record the fuel consumption and operating variables of a vehicle under real driving conditions with a frequency of 1 Hz. The operating scheme of the equipment, the elements integrated into its development, and the data analytics process are presented in detail. The fuel consumption tests carried out for the equipment validation showed a coefficient of determination R^2 of 98.54% between the readings of the telemetry equipment and the gravimetric tests.

Keywords: on-board diagnosis (OBD), fuel consumption, vehicle speed, telemetry, gravimetric test.

Frequent symbols and acronyms

Symbol	Description	Units
<i>OBD</i>	On-board diagnosis	
<i>RD</i>	Relative difference	%
MT	Micro-trip	
MCMC	Markov Chain Monte Carlo	
EBMT	Energy based micro-trip	
\dot{m}_{air}	Air mass flow	g/s
\dot{m}_{fuel}	Fuel mass flow	g/s

7.1 Introduction

Pollutant emissions, high energy consumption, accident levels, and mobility problems produced by the exponential increase in the number of vehicles, are the main reasons for seeking to monitor and to analyze the operation of public and private road transport systems. Currently, developments associated with the Internet of Things (IoT), big data, and information and communication technologies (ITC) facilitate the possibility to remotely record the operation of large vehicle fleets, as well as private passenger vehicles.

All end-user energy sectors are being impacted by digitalization technologies. Specifically, in the transport sector, new vehicles are built to be more and better connected internally and externally, making them "smarter", increasing their levels of safety and efficiency. The digitalization of transport and electric mobility could drastically change the schemes of how we transport people and goods [70].

The digitalization of transport essentially corresponds to the concept of "intelligent transport systems" (ITS), which implies: the deployment of sensors for data collection; use of communication technologies to allow remote control; and the application of advanced analytics to improve system operations, security, efficiency, and service, as well as to reduce costs [71].

In the research processes, data collection plays a fundamental role due to its relationship with the quality of the result, which is influenced by the reliability, representativeness, homogeneity, and consistency of the data that has been collected [3]. Collecting and remotely accessing large amounts of vehicle operation data under real driving conditions becomes a benefit for studying and understanding, through local driving cycles, the driving patterns of a region that influence the fuel consumption and vehicle emissions. For the construction of local driving cycles, researchers have essentially identified four steps: i) the selection of the study region, ii) the collection of the vehicle operating data, iii) the construction of the driving cycle, and iv) the assessment of the cycle representativeness [3].

In the vehicle operation data collection phase, speed and time are normally recorded, being the input information required by stochastic methods such as Micro-trips (MT) [24], [40], [43] and Markov Chain Monte Carlo (MCMC) [1], [44], [45] to propose synthetic driving cycles. Speed and time data are also used by the deterministic method such as the Trip Based method (TBM) [2] to select one of the monitored trips as a driving cycle. In recent years, the Fuel-based (FB) method [60] and the Energy-based micro-trip (EBMT) method [72] have proposed to collect, in addition to speed and time, data on the energy consumption of the vehicle. These data guarantee the representativeness of driving cycles with respect to driving patterns and the reproducibility of energy consumption and vehicle emissions of the studied region.

The state of art indicates that two methods have been used to collect operational data from a vehicle fleet, the chase car method, and the on-board measurement method [3]. In the first approach, an instrumented vehicle follows a target vehicle on a predetermined route. The speed-time data used in the LA92, LA01, and the Manila driving cycle were collected

through the chase car method [3]. Although the implementation cost of the chase car method could be more efficient, it has drawbacks in terms of the achieved data sample size. On the other hand, in the on-board measurement approach, each vehicle of the fleet is instrumented to collect second-by-second data. The data used for the development of the ARTHEMIS driving cycles and the Australian Composite Urban Emissions Drive Cycle were collected by this method [3]. Although the on-board measurement allows to collect a large amount of data, the implementation costs and the time required to filter and analyze a large amount of data can be a disadvantage.

Both methods of data collection for the construction of driving cycles are based on the monitoring and storage of information from instrumented vehicles. In some cases, the access to the registered data is done through the equipment installed in the vehicle. While in other devices the collected data is sent through the GPRS communication data network to a storage server.

Currently, different devices are capable of monitoring the operation of vehicle fleets. However, there is no universal device that can be used in all types of vehicles, since there are restrictions due to the configuration of the connection port or the languages used in the communication between the device and the computer of the vehicle. Devices such as the ELM 327 microcontroller allows the storage of the operation data of a vehicle and to access them manually and "offline" through a computer or a mobile phone. Once the operation data of the vehicle is accessed, the user can send it to a server or email. On the other hand, it is possible to use devices that do not require human intervention for the collection, storage, and transmission of data. Azuga, for example, is a system used to register the localization and operation of the vehicle events such as average and high speed, aggressive accelerations and braking. Devices like Bitbrew and Aytomic allow to customize their information platforms. Although the aforementioned device options offer remote access to vehicle fleet operating information, their approach is oriented to the logistical control of the fleet, and not to determine the energy and environmental impact of the vehicles. Likewise, the sampling frequencies and the access and visualization schemes of the collected data are not suitable for the energy and environmental analysis of the fleet.

This study presents the development of a telemetry equipment to automatically monitor, store, transmit, and analyze the fuel consumption and operating variables of a vehicle operating under real driving conditions. The design of this equipment, the type of operation to be monitored, the variables that are recorded, and the information management, are based on the requirements to build driving cycles using the EBMT. The equipment is capable to operate continuously and transmit vehicle operation data without user intervention. Vehicle operation data is acquired with a sampling frequency of 1 Hz and is subsequently stored on a Raspberry PI 3 B + card. A protocol for transmitting the collected data to a Dropbox account is activated frequently. In this way, the CSV files that contain the operation data of the vehicle can be analyzed remotely. These files are the input data required by the EBMT method for the construction of local driving cycles.

7.2 Materials and method

7.2.1 Description of the telemetry equipment

Three different types of devices for monitoring and tracking vehicle fleets are identified on the market. However, none of the equipment that was analyzed was designed to collect detailed information on the operation of the fleet to carry out an energy and environmental analysis using local driving cycles. To face this issue, the telemetry equipment obtains different intrinsic signals from the vehicle synchronously, organized, and with a frequency of 1 Hz. The system is based on On-Board Diagnosis (OBD) technology and was programmed with Python to acquire the signals presented in Table 7.1.

Table 7.1 Measured and calculated signals through the telemetry equipment.

Signals	Units	Type of signal	Uncertainty	Measuring principle
Speed (SPD)	km/h	Measured	$\pm 10\%$ of the output signal	Hall effect sensor
Engine speed (RPM)	Revolutions / minute	Measured	± 0.5 mm	Hall effect sensor
Manifold absolute pressure (MAP)	kPa	Measured	± 2.38 kPa	Variation in electrical resistance as they are subjected to the air vacuum pressure in the intake manifold or manifold
Intake air temperature (IAT)	K	Measured	$\pm 9.93\%$ of the output signal	The resistance of the temperature sensor changes depending on the intake-air temperature. As the temperature increases, the resistance is reduced, which reduces the voltage at the sensor
Latitude (LAT) and longitude (LON)	Degree	Measured	± 2.5 metros	Satellite triangulation
Engine Load	%	Calculated		
Altitude	m.a.s.l	Calculated		
Air mass flow (\dot{m}_{air})	g/s	Calculated		

Fuel mass flow (\dot{m}_{fuel})	g/s	Calculated
--	-----	------------

LAT and LON data are established through a digital geolocation sensor neo6mv2. This sensor delivers the vehicle location with a position accuracy of 2.5 meters at 5 Hz. On the other hand, the signals of SPD, RPM, MAP, IAT, and LOAD are signals that are acquired directly from the sensors of the vehicle through the OBD. Due to the sampling frequency of 1 Hz, the mass flow of intake air (\dot{m}_{air}) is calculated. Then, using the stoichiometric air-fuel ratio (AFR) the mass flow of fuel (\dot{m}_{fuel}) is established. Equations 7.1 and 7.2 present the calculation of (\dot{m}_{air}), and (\dot{m}_{fuel}), respectively.

$$\dot{m}_{air} = \left(\frac{RPM * MAP * \eta_{vol} * Engine_capacity}{2 * 60 * (273 + IAT) * R_{air}} \right) * 1000 \quad (7.1)$$

$$\dot{m}_{fuel} = \frac{\dot{m}_{air}}{ARF_{stch}} \quad (7.2)$$

In Equation 7.1, the air mass flow is calculated from the RPM, MAP, and IAT, the volumetric efficiency (η_{vol}), the engine size, and the particular air gas constant R, which has a value of $0.287 \frac{kJ}{kg \cdot K}$. Equation 7.2 presents the calculation of the fuel mass flow (\dot{m}_{fuel}) from the air mass flow (\dot{m}_{air}) and the stoichiometric air-fuel ratio. For this particular case, a value of 14.13 was used considering the fuel used is E8 (92% gasoline and 8% ethanol). We use this approach due to in positive ignition engines the operating dose is closer to stoichiometric point. However, this method does not consider the operation in transient states, which can produce inaccuracy on the final results. In the case of the volumetric efficiency (η_{vol}), the value used varies as a function of the RPM and the manifold pressure registered. The volumetric efficiency table was obtained from a vehicle with a 1.6 L and four cylinders engine [73]

Table 7.2 Volumetric efficiency for different values of RPM and Manifold pressure

		RPM									
		<=1800	2000	2200	2400	2600	2800	3000	3200	3400	3600
Manifold pressure [kPa)	0	0.57	0.68	0.70	0.69	0.68	0.68	0.72	0.74	0.76	0.81
	30	0.57	0.68	0.70	0.69	0.68	0.68	0.72	0.74	0.76	0.81
	35	0.64	0.75	0.77	0.76	0.75	0.75	0.79	0.81	0.83	0.88
	40	0.63	0.74	0.76	0.75	0.74	0.74	0.78	0.80	0.82	0.87
	42.5	0.65	0.76	0.78	0.77	0.76	0.76	0.80	0.82	0.84	0.89

45	0.63	0.74	0.76	0.75	0.74	0.74	0.78	0.80	0.82	0.87
50	0.63	0.74	0.76	0.75	0.74	0.74	0.78	0.80	0.82	0.87
55	0.64	0.75	0.77	0.76	0.75	0.75	0.79	0.81	0.83	0.88
60	0.60	0.71	0.73	0.72	0.71	0.71	0.75	0.77	0.79	0.84
65	0.57	0.68	0.70	0.69	0.68	0.68	0.72	0.74	0.76	0.81
70	0.52	0.63	0.65	0.64	0.63	0.63	0.67	0.69	0.71	0.76

The entire system is controlled by a robust methodology partitioned into three operating algorithms. The three algorithms are: i) connection, ii) acquisition, and iii) transmission. The algorithms are independent, but they interact with each other for the correct operation of the telemetry equipment. The operation and interaction between algorithms can be seen in Figure 7.1.

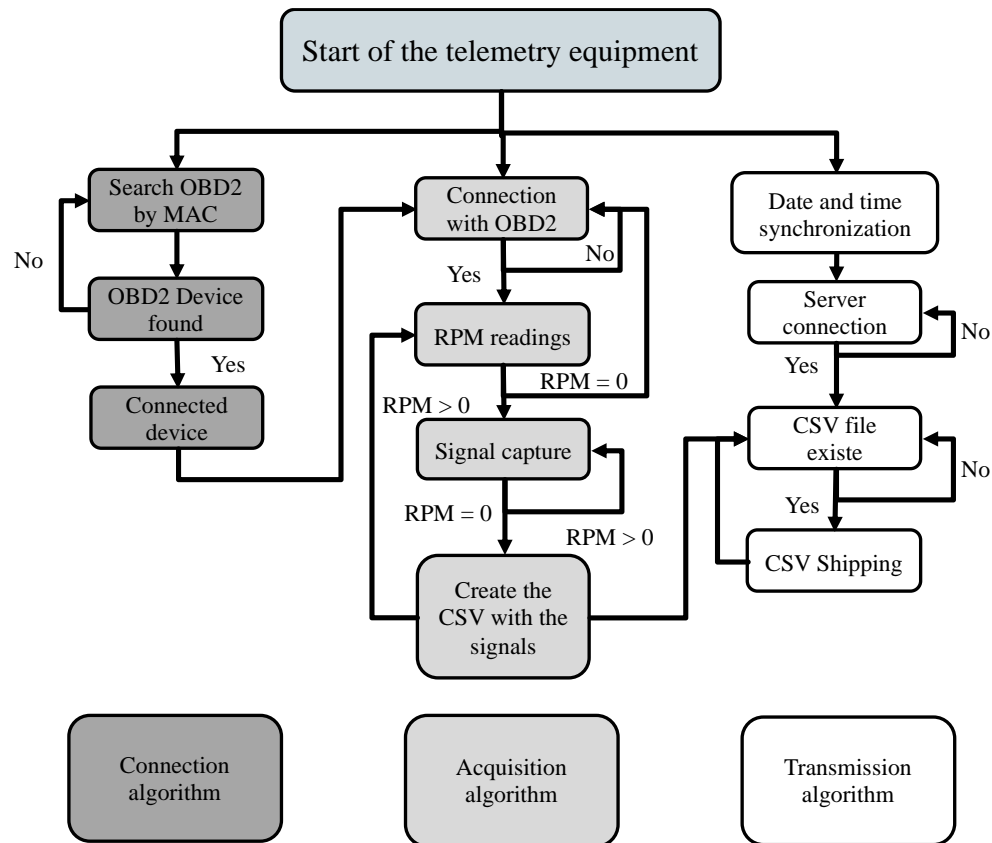


Figure 7.1 Control methodology of the telemetry equipment

The system initiates and deploys the three control systems starting with the connection algorithm. This algorithm is programmed to search for an OBD module through Bluetooth communication, which has a predetermined MAC address. The algorithm scans nearby

devices every two seconds to find and connect to the OBD. Failure to find a device would imply the repetition of the entire process.

The second control algorithm is the acquisition algorithm, which starts with an infinite loop that only ends when an OBD module is found in the device list of the system. After the OBD module is detected, it begins to monitor the RPM, if it detects that the speed of the engine speed is zero, the whole process is repeated from the beginning. On the other hand, if the RPM is greater than zero, the five signals from the engine and the two geolocation signals are captured and organized as a vector. This process is iterative at a frequency of 1Hz until the engine speed is zero again, which indicates that the vehicle was turned off. When the vehicle shuts down, a CSV file is generated. This file contains the measured and calculated signals, which are organized in a column. The file is named with a vehicle identifier, date, and time, which avoids overlapping or replacing files. Finally, the file is moved to a specific location so that it is manipulated by the transmission algorithm and the RPM monitoring process is restarted. It should be noted that the acquisition algorithm bases its operation on the fact that it is inefficient to acquire signals from a vehicle that is switched off.

The last section is the transmission algorithm, which is in charge of sending all the generated files to the cloud. The algorithm starts with an update of the device date and time. When a stable communication channel is established, the stored files predetermined location begins to be monitored. If recent files are found in this location, the algorithm uploads them to the cloud using a General Packet Radio Communication protocol (GPRS). Once all files are uploaded, the default location continues to be monitored every 5 seconds while waiting for new files.

7.2.2 Elements integrated into the telemetry equipment

The equipment must be inside the vehicle, so it must be portable, small, and operating automatically, i.e., decoupling its operation from the action of the driver. To achieve this, the telemetry equipment is made up of three different components as shown in Figure 7.2.

The telemetry equipment is made up of the OBD device, which acquires the signals from the computer of the vehicle and through Bluetooth communication transmits the data to a control system. A Raspberry PI 3 B + (RPI3B) was chosen as a control system for the automation of the entire process. The RPI3B has different peripheral ports, 1 GB of RAM, and supports up to 32 GB of storage, which would allow continuous data to be stored for more than 10 years. The RPI3B operates using a Linux-based operating system and it is responsible for deploying the Python-based acquisition methodology. Finally, a 3G technology Huawei e303 USB transmission system is connected to the RPI3B, which allows connectivity and data transmission in an organized and non-encrypted way to a cloud. It should be noted that the entire monitoring system is powered directly by the battery of the vehicle. No configuration, adaptation or alteration of the electrical system of the vehicle is necessary since the OBD port provides the necessary power.

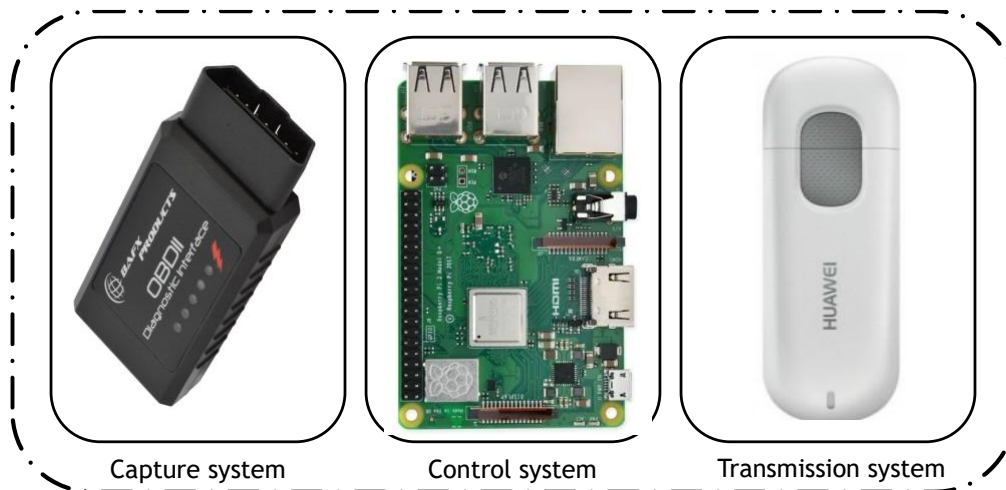


Figure 7.2 Components of the telemetry equipment

7.2.3 Used vehicle to test the telemetry equipment

The developed telemetry equipment was installed in a light passenger vehicle to validate its operation. The technical characteristics of the vehicle are presented in Table 7.2. Likewise, the equipment was installed in 3 other vehicles from different automakers and models. However, the equipment operation was only achieved in one of them, because the connection of the equipment with the vehicle depends on the communication compatibility of the OBD system used. In this sense, before installing the telemetry equipment in a large fleet of vehicles, the compatibility of the OBD system must be verified. This compatibility can be done through the use of a mobile phone application like Torque Pro.

7.2.4 Method to validate the speed signals

The telemetry equipment was designed to deliver speed values with a sampling frequency of 1 Hz. This speed is recorded directly from the computer of the vehicle, which in turn is acquired through the sensor located on the wheels of the vehicle. Recorded speed data is critical to building a driving cycle. The speed readings obtained through the device were compared with the speed data of the vehicle obtained under the WLTC 3a driving cycle simulated in a chassis dynamometer. The graphic results of this comparison are presented in Figure 7.3. Yet, an analysis based on the determination coefficient R^2 , is developed to assess the similarity between the data registered of speed by the telemetry equipment and the WLTC 3a speed data.

Table 7.3 Technical datasheet of the used vehicle

Vehicle characteristics	Type or value
Type of fuel	Gasoline
Ignition system	Distributorless ignition system (DIS)

Engine capacity (cm ³)	1558
Bore (mm) & Stroke (mm)	79 & 81.5
Number of cylinders	4
Number of valves	16
Maximum power (hp)	103 @ 6000 rpm
Maximum torque (N m)	144.91 @ 3600 rpm
Compression ratio	9.5:1
Transmission	Mechanical of 5 gears
Curb weight (kg)	1040

7.2.5 Method for validating energy consumption records

The developed equipment calculates and delivers energy consumption every second. In the case of an internal combustion engine, energy consumption can be expressed as a function of the volumetric flow or mass flow of fuel. A comparison was proposed between the values delivered by the telemetry equipment ($\dot{m}_{fuel-eq}$) and the direct measurement of the mass of fuel consumed by the vehicle, which is called the gravimetric test ($\dot{m}_{fuel-gra}$). This comparison was developed to validate the equipment readings and was performed through the relative difference, which is calculated using Equation 7.3.

$$RD_{fuel} = \left| \frac{\dot{m}_{fuel-eq} - \dot{m}_{fuel-gra}}{\dot{m}_{fuel-gra}} \right| \quad (7.3)$$

Before carrying out the tests, the balance measurement was verified with reference masses of 1 kg, 2 kg, and 5 kg. The results of this verification are presented in Table 7.3.

Table 7.4 Verification of values reported by the scale using mass

Values reported by the scale (g)							
Mass of reference (g)	1st read	2nd read	3rd read	4th read	5th read	Average	Standard deviation
1000	1000	999.5	999.5	1000	1000	999.8	0.27
2000	2000	1999.5	2000	2000	2000	1999.9	0.22

2000	2000	2000	2000	2000	2000	2000	0.00
5000	5000.5	5000	5000	5000	5000	5000.1	0.22

Twenty-seven operating conditions were used to compare the results obtained with the telemetry equipment with respect to those obtained with the gravimetric test. Some of these conditions were simulated using a chassis dynamometer, while others were performed under real driving conditions on urban and suburban routes. These operating conditions were proposed to identify any particular condition of vehicle operation that could generate less accurate results. The set of operating conditions that were evaluated are presented in Table 7.4.

Table 7.5 Set of driving conditions used to test the telemetry equipment

Test	Number of repetitions	Type
30 km/h	1	Steady state & under warm-up phase
30 km/h	4	Steady state
50 km/h	4	Steady state
70 km/h	4	Steady state
Random	4	Transient
Real world conditions	3	Transient & urban conditions
Real world conditions	1	Transient & sub-urban conditions
Idling	1	Steady state - 30 min
Idling	1	Steady state - 60 min
Driving cycle	3	Transient & Low and medium phase of WLTC Class 3a
Driving cycle	1	Transient & Low, medium, high and extra high of WLTC Class 3a

The coefficient of determination R^2 is used to assess the correlation between the values delivered by the telemetry equipment and those measured in the gravimetric test. The slope of the equation relates the measured fuel mass values with those delivered by the equipment.

7.2.6 Construction of the driving cycle through the Energy Based Micro-trip (EBMT) method

After confirming that the fuel consumption values registered by the telemetry equipment are similar to the ones measured under the gravimetric test, the data of the real-world condition trips are used to construct the local driving cycle.

The selected method to construct the driving cycle is the Energy Based Micro-trip (EBMT) method which was explained in chapter 4 (Driving cycles that reproduce driving patterns, energy consumptions and tailpipe emissions). This method constructs driving cycles using the micro-trips procedure and using as the assessment criteria the energy consumption on top of characteristic parameters calculated from the speed time data. The preliminary steps, prior to constructing the local driving cycle, are to identify the main characteristic parameters (Chapter 5 - Main characteristic parameters to describe driving patterns), and to define the time length of the driving cycle (Chapter 6 - Relationship between the time duration of a driving cycle and its representativeness result). In the results section the obtained driving cycle is presented.

7.3 Results

Figure 7.3 presents the speed values collected by the telemetry equipment related to the speed data of the driving cycle WLTC 3a. This cycle presents 4 different phases of operation according to the reached vehicle speeds. We can see that in the low-speed area (time less than 580 seconds) and medium speeds area (time between 580 to 1022 seconds) the values reported by both methods are similar. In the high-speed area (between 1022 and 1477 seconds), the maximum speed recorded by WLTC 3a is close to 97 km/h, while that recorded by the telemetry equipment is 92 km/h. These differences could be caused, not only by the equipment, but also by external factors such as human error, or the vehicle's limitations to follow the proposed speed profile, which is associated with limitations in its acceleration capability. These limitations in acceleration are evident in the last phase, called extra high speed, where the speed differences presented by the telemetry equipment (115 km/h) and the driving cycle (131 km/h) are higher.

An overall similarity assessment between the telemetry equipment speed data and the WLTC 3a speed data is performed through the coefficient of determination R^2 . The obtained results indicate that when the vehicle follows the WLTC 3a driving cycle, the speed recorded by the telemetry equipment is similar to the real speed of the vehicle, which is evidenced with a coefficient of determination (R^2) greater than 97%.

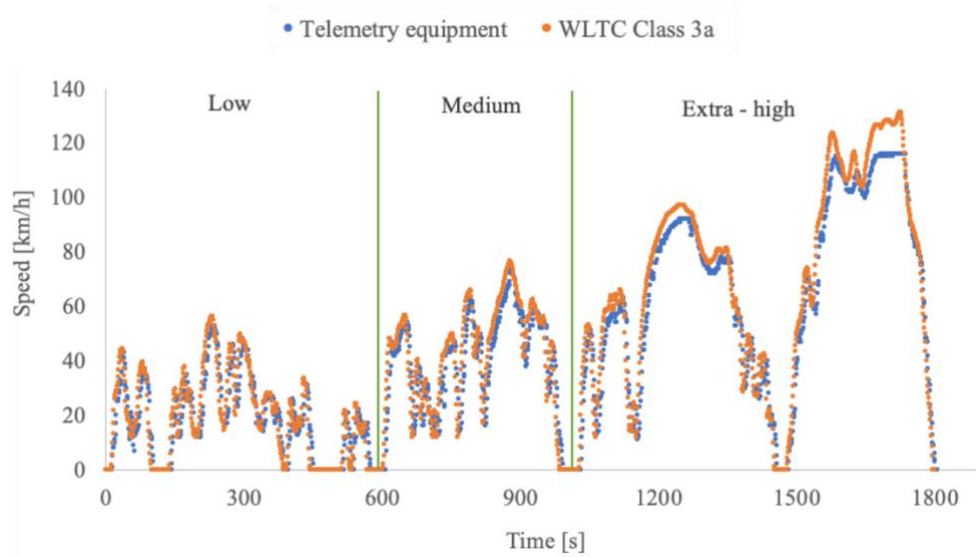


Figure 7.3 Comparison between the speed register by the equipment and the driving cycle data

Furthermore, the results of the fuel mass tests indicate that in 26 of the 27 tests carried out, the values delivered by the equipment are greater than those measured under the gravimetric method. Only in the test at a constant speed of 30 km/h during the vehicle warm-up period, higher fuel consumption was measured in the gravimetric test. On average, the difference between the values delivered by the equipment is 9.74% greater than those measured through the gravimetric test. The results of the tests carried out are presented in Table 7.5

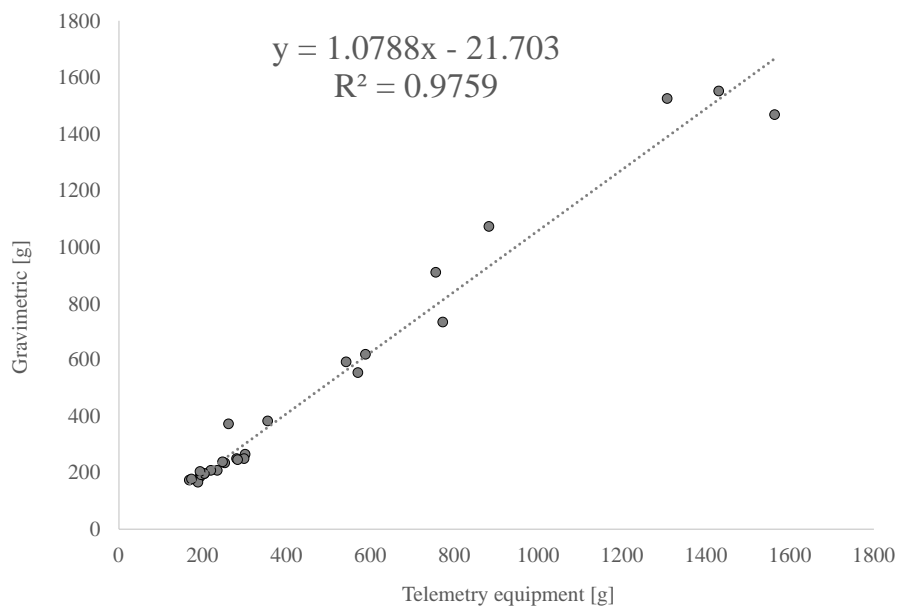


Figure 7.4 Coefficient of determination analysis between the telemetry equipment and gravimetric test results

Table 7.6 Comparison between the fuel consumption reported by the telemetry equipment respect to gravimetric test results

Conditions of the driving test	Test	Gravimetric [g]	Telemetry equipment [g]	Relative difference
Constant speed on a chassis dynamometer	30 km/h -1 (Warm-up phase)	373.00	261.41	30%
	30 km/h -2	193.90	204.56	5%
	30 km/h -3	184.20	194.95	6%
	30 km/h -4	164.30	189.49	15%
	30 km/h -5	190.30	198.82	4%
	50 km/h -1	231.40	255.04	10%
	50 km/h -2	235.90	248.31	5%
	50 km/h -3	206.20	235.51	14%
	50 km/h -4	205.80	221.45	8%
	70 km/h -1	264.00	303.46	15%
	70 km/h -2	249.20	299.94	20%
	70 km/h -3	248.10	282.65	14%
	70 km/h -4	245.40	284.25	16%
Random speed and acceleration change tests on dynamometer	Random 1	195.20	204.74	5%
	Random 2	171.60	168.85	2%
	Random 3	176.60	175.45	1%
	Random 4	201.50	195.54	3%
Tests under real driving conditions	Rotonda Condina (route 1)	1520.00	1309.67	14%
	Circunvalar y terminal (route 2)	1070.00	883.69	17%
	Av. Sur - San Fernando - Av. 30 de Agosto (route 3)	1550.00	1431.75	8%
	Circunvalar Pinares Terminal (route 4)	910.00	755.79	17%
Test under idling conditions	Idling during 30 min	380.00	357.66	6%
	Idling during 60 min	730.00	772.60	6%
Test using driving cycle on a chassis dynamometer	WLTC 3a long	1466.00	1563.94	7%
	WLTC 3a short 1	588.75	542.43	8%
	WLTC 3a short 2	614.80	590.41	4%
	WLTC 3a short 3	551.80	570.83	3%

The analysis through the calculation of the coefficient of determination R^2 presented a result of 98.56%, which indicates that the values delivered by the telemetry equipment are similar to the values measured under the gravimetric method. This means that having only the data delivered by the telemetry device and applying the regression model presented in the equation in Figure 7.4, we could accurately calculate the real fuel consumption values. The results of the coefficient of determination R^2 are presented in Figure 7.4. Likewise, we observe that the slope of the regression model proposed is equal to 0.9251, which indicates that the values registered with the telemetry equipment are greater than those measured under the gravimetric test. However, the adjustment in order of magnitude is not drastic.

After determining the reliability and truthfulness of the fuel consumption data provided by telemetry equipment, we used the trips monitored under real driving conditions to construct a local driving cycle using the Energy Based Micro-trip (EBMT) method. As explained in chapter 4 (Driving cycles that reproduce driving patterns, energy consumptions and tailpipe emissions), the EBMT method constructs a driving cycle using the micro-trips approach, and assessment criteria such as energy consumption and characteristic parameters calculated from the speed time data.

Then, the first step is to define the main characteristic parameters that will join the energy consumption on the list of the assessment criteria. We followed the procedure explained in chapter 5 (Main characteristic parameters to describe driving patterns). Nineteen characteristic parameters (CPs) that describe the driving patterns of the region were used to propose 153 sets of assessment criteria consisting of two elements. Table 7.6 presents the CPs evaluated on this step.

Table 7.7 Characteristic parameters used to describe driving patterns.

Type of parameter	Characteristic Parameters (CPs)		
	Name	Symbol	Units
Speed	Maximum speed	Max Speed	m/s
	Average speed	Ave Speed	m/s
	Standard deviation of speed	SD Speed	m/s
Acceleration	Maximum acceleration	Max Accel	m/s ²
	Maximum deceleration	Max Decel	m/s ²
	Average acceleration	Ave Accel	m/s ²
	Average deceleration	Ave Decel	m/s ²
	Standard deviation of acceleration	SD Accel	m/s ²
	Standard deviation of deceleration	SD Decel	m/s ²
Operational modes (% of time)	Idling	% Idling	%
	Acceleration	% Accel	%
	Deceleration	% Decel	%

	Cruising	% Cruise	%
Dynamics	Number of accelerations per km	Accel/km	km ⁻¹
	Root mean square of acceleration	RMS	m ² /s ²
	Positive kinetic energy	PKE	m/s ²
	Speed-acceleration probability distribution	SAPD	-
	Vehicle specific power	VSP	kW/ton
	Kinetic intensity	KI	1/m
Energy consumption	Specific fuel consumption	SFC	l/km

Due to the stochastic nature of the micro-trips' method, five hundred driving cycles were constructed using each set of assessment criteria. Then, as was explained in chapter 5, the \overline{ARD} and the \overline{IQR} of the CPs, as well as the average relative difference of the specific fuel consumption (ARD SFC) were calculated. Table 7.7 shows the 20 first set of assessment criteria which present the lowest values of \overline{ARD} .

Table 7.8 Sets of assessment criteria with lowest values of \overline{ARD} .

CP1	CP2	Ave_ARD	Ave_IQR	ARD SFC
Ave Speed	SD Speed	6.48	6.52	4.59
Ave Speed	Max Decel	6.99	7.08	4.46
Ave Speed	SD Accel	7.05	6.37	4.55
Ave Speed	%_idling	6.74	6.92	5.82
Ave Speed	%_Cruise	6.59	6.51	3.89
Ave Speed	RMS	6.31	5.50	4.92
Ave Speed	PKE	6.73	6.45	3.66
Ave Speed	KI	6.41	5.77	3.35
SD Speed	%_idling	6.26	5.41	4.98
SD Speed	%_Cruise	6.80	7.12	4.99
SD Speed	VSP	6.25	5.89	3.93
Max Decel	VSP	6.96	7.16	4.19
SD Accel	VSP	6.87	6.01	4.57

CP1	CP2	Ave_ARD	Ave_IQR	ARD SFC
%_idling	VSP	6.12	5.18	5.22
%_idling	KI	5.87	5.56	4.15
%_Cruise	VSP	6.44	5.70	3.91
%_Cruise	KI	6.75	7.02	5.53
RMS	VSP	6.22	5.52	4.66
PKE	VSP	6.65	6.58	3.56
VSP	KI	6.57	5.79	3.40

From Table 7.7 we identified that CPs with the highest frequency are average speed and VSP (both with 8 times), followed by the kinetic intensity, standard deviation of speed, % of time in idling, and % of time in cruise (4 times). From these results we decided to apply the EBMT method using as assessment criteria the Average Speed, the VSP, and the fuel consumption. Moreover, we decided to add to the criteria the percentage of time in idling since the micro-trips approach does not reproduce well this externality of the driving patterns.

Once the main assessment criteria of the EBMT method are identified, the next step is to define the time duration of the local driving cycle. The methodology to identify is explained on chapter 6 (Chapter 6 - Relationship between the time duration of a driving cycle and its representativeness result). We have analyzed the following time durations: 5, 10, 20, 30, 45, 60, 90 and 120 minutes. The suitable time length of the driving cycle will best represent the driving patterns of the studied region. For each time duration we built 500 driving cycles and then the \overline{ARD} and the \overline{IQR} of the CPs were computed. The results for different time durations are showed in Figure 7.5 and Table 7.8

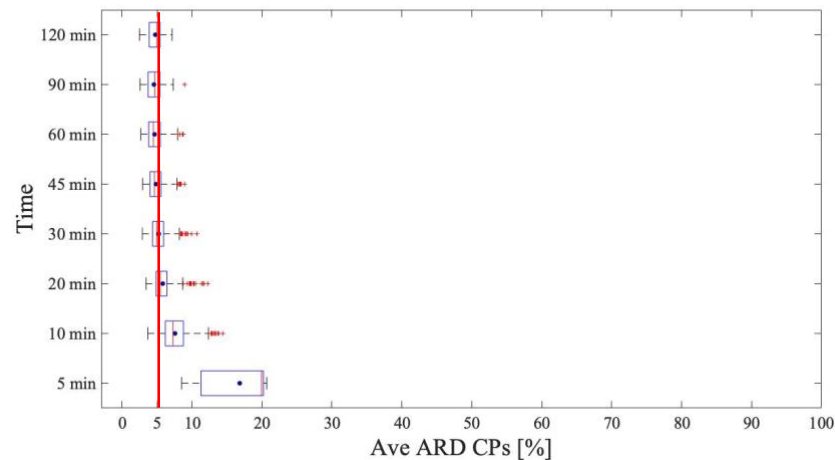


Figure 7.5 \overline{ARD} and the \overline{IQR} of the CPs for different time lengths of driving cycles

Table 7.9 \overline{ARD} and the \overline{IQR} number results for different time lengths of driving cycles

Time length (Minutes)	Ave_ARD	Ave_IQR
5	16.80	11.47
10	7.60	7.27
20	5.78	5.14
30	5.23	4.56
45	4.82	4.83
60	4.66	4.57
90	4.59	4.31
120	4.77	4.07

From Figure 7.5 and Table 7.8 we observe that when the time duration of the driving cycle increases, the \overline{ARD} and the \overline{IQR} of the CPs decrease. For driving cycles with time lengths of 5 minutes the \overline{ARD} is 16.80% while for driving cycles with time lengths of 120 minutes the \overline{ARD} is 4.77%. Moreover, we observe that driving cycles with time lengths equal or higher than 20 minutes, the \overline{ARD} tends to stabilize between 4.5% and 6%. Then, from these results we select as time length for driving cycles a value of 20 minutes.

At this point we have set-up the requirements to construct the local driving cycle through the EBMT. We defined the main assessment criteria to evaluate the proposed driving cycles (Average speed, VSP, % of time in idling, and specific fuel consumption). Also, we established the time duration of the driving cycle in 20 minutes. Due to the stochastic approach of the EBMT, we built 500 driving cycles. Then, we calculated the \overline{ARD} of the characteristic parameters for each driving cycle and we selected the driving cycles with lowest values of \overline{ARD} . The values for the \overline{ARD} of the characteristic parameters range between 3.525% and 12.53%. Table 7.9 presents the characteristic parameters for the driving patterns and for the first five driving cycle with the lowest values of \overline{ARD} . Figure 7.6 presents the speed-time profile of the selected driving cycles.

The proposed local driving cycles developed by the EBMT presented characteristic parameters that are close to the ones of the driving patterns. Any of these driving cycles represents the driving patterns of the study region. The next step, out of the scope of this work, is to validate if a light-duty vehicle driven under this driving cycle is able to follow the speed profile and the proposed accelerations. Likewise, to calculate the fuel consumed by the vehicle in the execution of the driving cycle.

Table 7.10 Characteristic parameters of the five local driving cycles and driving patterns

Cycle No.	83	196	277	308	371	Driving Patterns
Time [s]	1294	1211	1201	1312	1204	2694 (Average)
Distance [m]	7209	6850	6634	7296	6721	15545 (Average)
Max Speed	15.83	15.83	15.28	15.83	15.83	16.81
Ave Speed	5.57	5.66	5.52	5.56	5.58	5.57
SD Speed	4.69	4.57	4.71	4.79	4.48	4.69
Max Accel	1.83	1.81	1.83	1.81	1.81	1.90
Max Decel	-1.78	-1.78	-1.94	-1.94	-1.78	-1.93
Ave Accel	0.50	0.49	0.52	0.50	0.50	0.50
Ave Decel	-0.55	-0.54	-0.56	-0.52	-0.54	-0.54
SD Accel	0.29	0.31	0.31	0.30	0.30	0.31
SD Decel	0.36	0.35	0.35	0.38	0.36	0.34
% Idling	24.27	24.53	24.56	24.77	25.50	24.71
% Accel	30.14	29.89	29.14	28.96	29.32	27.01
% Decel	27.05	27.17	27.56	27.74	27.24	25.37
% Cruise	18.55	18.41	18.73	18.52	17.94	17.40
Accel / km	16.65	15.77	15.68	16.59	16.37	16.80
RMS	0.47	0.46	0.48	0.46	0.46	0.45
PKE	0.37	0.36	0.37	0.37	0.36	0.38
VSP	1.03	1.04	1.02	1.04	1.01	1.04
KI	1.85	1.87	1.85	1.75	1.91	1.90
SFC	0.11	0.12	0.11	0.11	0.12	0.12

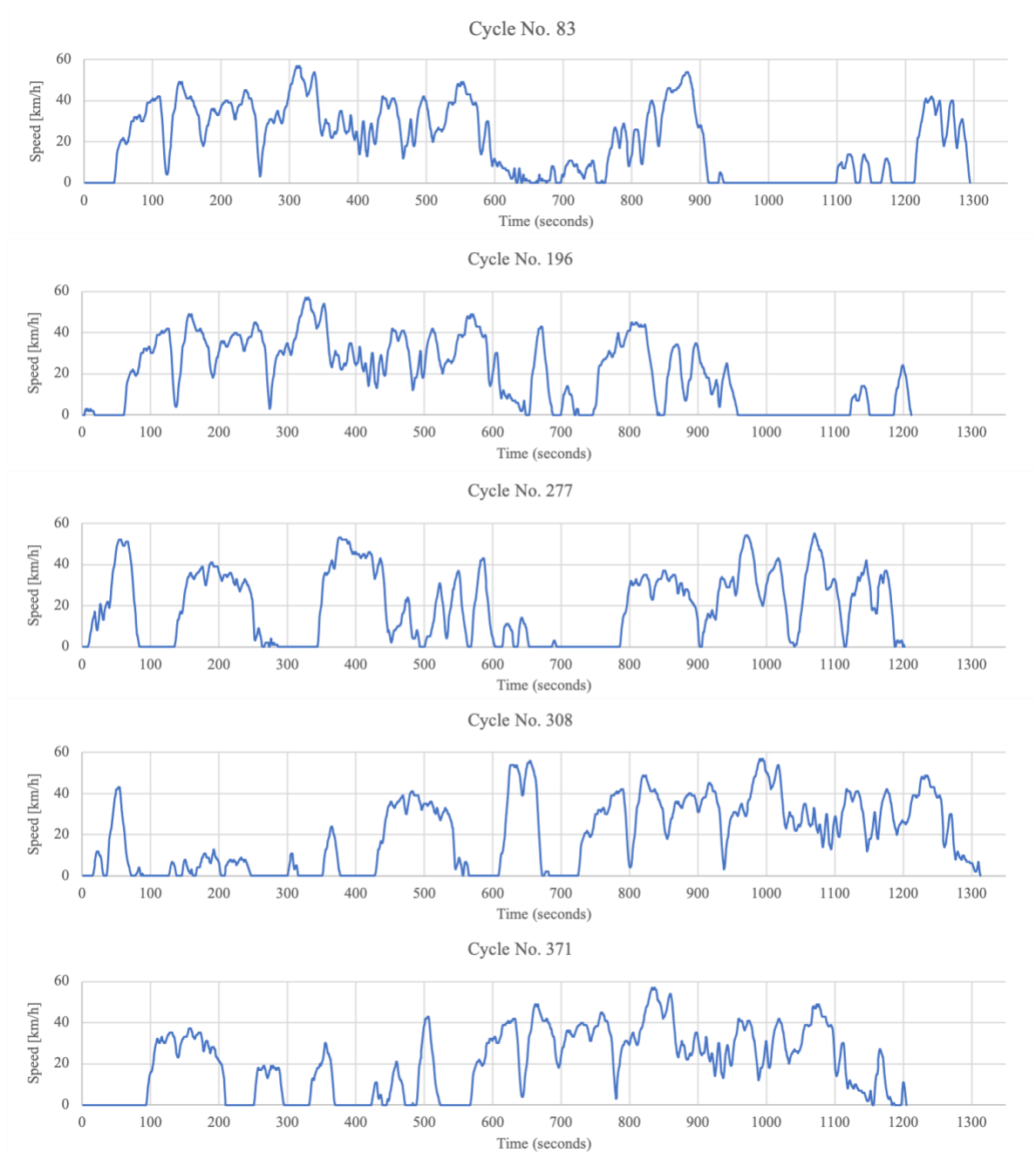


Figure 7.6 Five driving cycles proposed for Pereira

7.4 Conclusions

This study presents the development of a telemetry equipment that registers the location of the vehicle, its longitudinal speed, engine speed, intake manifold pressure, inlet air temperature, percentage of engine load, the mass flow of air and the mass flow of fuel. The equipment was designed to record the mentioned variables with a frequency of 1 Hz.

The equipment available on the market for fleet monitoring do not operate with the required sampling frequency or have restrictions on access to information on their platforms. An on-board diagnosis (OBD) device, a neo6mv2 geolocation sensor, a Raspberry PI3B + data storage and management system, and a Huawei e303 USB transmission system was integrated into the developed telemetry equipment. This equipment was developed to monitor the operation of a fleet of vehicles under real driving conditions, and record speed and fuel consumption data that serve as input for the development of local driving cycles under the Energy-based micro-trip (EBMT) method.

To validate the speed and fuel consumption data recorded by the telemetry equipment, it was installed on a light passenger vehicle. The instrumented vehicle was tested on different operating conditions that included tests at different constant speeds, tests at idling, tests with random speeds and accelerations, and tests on a dynamometer following a driving cycle. The obtained results indicate that when the vehicle follows the WLTC 3a driving cycle, the speed recorded by the telemetry equipment is similar to the real speed of the vehicle, which is evidenced with a coefficient of determination (R^2) greater than 96%. To validate the energy consumption readings, the fuel mass values delivered by the equipment were compared with those measured by gravimetric test for the same set of trips. For this comparison, the coefficient of determination R^2 presented a result of 98.56%, which indicates that the values delivered by the telemetry equipment are similar to the values measured under the gravimetric method. However, the positive results in this phase of the project must be validated in other vehicles from automaker and models, and with different motorization technologies.

The trips data monitored under real driving conditions were used to construct a local driving cycle using the EBMT method. Then, following the procedure explained in chapter 5 and 6, we identified the average speed, VSP, % of time in idling and specific fuel consumption as the assessment criteria for evaluating the proposed driving cycles. Also, we established that the time duration of the driving cycle might be $20 \text{ min} \pm 2 \text{ min}$. Finally, these results were used to construct 500 driving cycles and the first with the lowest values of \overline{ARD} are presented. Theoretically, these driving cycles best represent the driving patterns and the energy consumption of the study region. Nevertheless, the proposed driving cycles must be evaluated on a chassis dynamometer test in order to validate if a driven light-duty vehicle is able to follow the speed profile and the proposed accelerations.

8 General discussion

The energy and technological model of the road transport sector presents high consumption of energy resources, as well as direct impacts on climate change and air quality. In this sense, understanding and optimizing the operation of vehicles under real driving conditions is essential to reduce emissions and energy consumption of the vehicle fleet.

Local driving cycles are tools to describe and analyze the driving patterns of a region. Local driving cycles are used for different purposes such as optimization of the powertrain of vehicles, the generation of fuel consumption values and emission factors to establish accurate emission inventories adjusted to the realities of the study regions. The use of local driving cycles also allows reducing the existing difference between the fuel consumption perceived by users and the one reported by vehicle manufacturers from the type approval tests. The state of the art indicates that this difference can vary between 9% and 60% depending on the model year and the vehicle technology.

Therefore, there is a need not only to use local driving cycles but also to improve their level of representativeness. This means to increase their capacity to express the driving patterns of a region. The construction process of a local driving cycle requires the following steps: (i) to collect a large amount of operational data from a fleet of vehicles, (ii) to select a method for constructing the driving cycle, and (iii) to evaluate the representativeness of the proposed driving cycle. We identified that the methods for the construction of driving cycles can be categorized in stochastic and deterministic methods. Micro-trips (MT) and Monte Carlo Markov Chains (MCMC) are part of the analyzed stochastic method whereas the Trip-based is the deterministic method analyzed. Usually, the representativeness of the driving cycles generated by the mentioned methods is measured using metrics associated with the kinematics of the vehicle which are defined as characteristic parameters (CP). There is no unique set of CPs to assess the representativeness of a driving cycle. The selection of the CPs is based on the experience of the researcher and according to the study region. However, after analyzing the main driving cycles developed in the world, it is concluded the most used CPs are the average speed and the percentage of time idling. This review of the state of art also identified the absence of a method to define the suitable time duration of the local driving cycles.

We concluded that the current process to construct local driving cycles seeks to assure the representativeness in terms of driving patterns. However, this process does not guarantee the similarity in terms of energy consumption and vehicle emissions. This research redefines the concept of a driving cycle as a time series of speed that represents the driving patterns of a region, and reproduce the energy consumption and the emissions of all vehicles with the same technology driven in the study region. To support this new concept, this project develops a methodology to construct local driving cycles based on fuel consumption and emissions.

For the development of the methodology proposed by this research project, a database was provided by Energy and Climate Change research group of Tecnológico de Monterrey. This database contains the information of the vehicle trips made in 8 months by a fleet of 15 buses that traveled in the TOL-MEX route that connects Mexico City with the city of Toluca. The route contains two flat urban regions with different traffic conditions, and one sub-urban

region with mountainous topography. In this database we can find trips with data of speed, fuel consumption and CO₂, CO and NO_x emissions, and with sample frequency of 1 Hz.

The initial step of this research project was to propose a deterministic method in which the trip with the closest fuel consumption to the average fuel consumption of the sampled trips, is selected as the driving cycle. We defined this repeatable and reproducible method the Fuel-based (FB) method. We hypothesized that using the FB method, the proposed driving cycle represents the driving patterns of a given region. This means that the characteristic parameters of the driving cycle (CP*s) are the same or similar to the characteristic parameters of the driving patterns (CPs). The level of similarity was measured in terms of the relative difference between CPs and CP*s. For flat regions, we obtained relative differences results below than 15% for CPs related with speed and acceleration, which are directly influenced by the driver. These results confirmed our hypotheses. However, the percentage of time in idling presented the highest relative difference since it is considered as an external factor, which in the case of the mountain region reaches up to 80% of relative difference.

The performance of the FB method had to be validated. For this reason, in the second step of this project research the FB method is compared with the MT and MCMC methods. In the three methods, their capability to construct local driving cycles was measured in terms of (i) representing the driving patterns, and (ii) reproducing the fuel consumption and emissions generated by a vehicle in the study region. The comparison of the three methods was performed based on 23 CPs used previously by different researchers in the construction of driving cycles. It is not possible to make a direct comparison between the CP*s of a driving cycle generated by the FB method and the CP* of the driving cycles generated by the MT or MCMC methods, due to their stochastic nature. This means that the driving cycles proposed by MT and MCMC, change every time the methods are applied. For this reason, the MT and MCMC methods were applied 1000 times, reporting the trend of the CPs through the average relative difference (ARD) and their dispersion through the inter-quartile range (IQR). The results indicated that in the four regions analyzed, 83% of the CPs obtained with the FB method presented an ARD below 10%, while the MT method and the MCMC method presented 69% and 20% of the CPs with ARD below 10%, respectively. We concluded that the FB method presented the best results to represent the driving patterns, and to reproduce the fuel consumption of the study regions. The MT and the FB methods presented the best performance of the three analyzed methods. However, the FB method, as a deterministic method, can generate too long driving cycles to be implemented in a type approval test, or too short to represent the driving patterns of the studied region. Under this situation, the MT has opportunities for improving and to represent the fuel consumption and vehicle emissions of the study region. In this step we also proposed a methodology to evaluate the representativeness of a driving cycle developed by stochastic methods, which is based on the calculation of the average relative difference (ARD) and the inter-quartile range (IQR). These indicators were used in the subsequent analyzes of this investigation.

To improve the representativeness of the driving cycles obtained by the MT method, we proposed to implement as the assessment criteria the energy consumption and a set of CPs, specifically the average speed and the percentage of time in idling. These two CPs were selected because they have been the most used by other researchers in the development of driving cycles. This proposal was denominated as the Energy-Based Micro-trip (EBMT) method. The EBMT method differs from the traditional MT method by its ability to represent

local driving patterns, and simultaneously reproduce energy consumption and tailpipe emissions. The driving cycles proposed by the EBMT method were compared with the cycles generated using three reference cases: i) Average speed and percentage of time in idling (traditional MT method), ii) specific fuel consumption (SFC), and iii) Average speed and percentage of downtime, SFC and CO, CO₂ and NO_x emission. The performance of EBMT method and reference cases were calculated based on the fuel consumption ARD (ARD_{SFC}), the average ARD of the CPs (\overline{ARD}_{CPs}), and the average ARD of emissions (\overline{ARD}_{EIs}). The driving cycles constructed by the EBMT method represents the driving patterns with $\overline{ARD}_{CPs} < 7.66\%$ and reproduce energy consumptions with $ARD_{SFC} < 2.69\%$ and tailpipe emissions with $\overline{ARD}_{EIs} < 5.36\%$. The traditional MT method showed $\overline{ARD}_{CPs} < 8.85\%$, $ARD_{SFC} < 9.64\%$, and $\overline{ARD}_{EIs} < 9.81\%$. The benefits in terms of representativeness are evident when using EBMT instead MT when constructing local driving cycles

We found that there are different sets of CPs used to assess the representativeness of the driving cycles. However, it is unknown which is the set of CPs that generate driving cycles with the best level of representativeness. This problem was addressed in this phase of the research project. Then, nine-teen CPs were used to build 1140 sets of 2 and 3 CPs. We observed that idling time, the standard deviation of the positive acceleration, and average speed were the most recurrent CPs. Therefore, we concluded that they are the ones that must be included in the MT method as assessment parameters to obtain DCs that represent the driving pattern and that reproduce the real energy consumption and tailpipe emission of the vehicles. This result agrees with the fact that average speed and the percentage of idling time are the CPs most frequently used by researchers for constructing DC. This work also shows that a third CP (the standard deviation of the positive acceleration) should be included. Alternatively, kinetic intensity or vehicle specific power can be used for the same purpose.

During the development of the research, we identified that the time duration of the driving cycle is an additional factor that impacts its representativeness. This factor has not been studied in-depth since in most cases the driving cycle time duration is established by the researchers based on their experience and vehicle traffic data. The time duration of each driving cycle is unique due to its direct relation to the local operating conditions of the vehicles. A time duration for the DC must be defined to allow the vehicle operation under its normal operating temperature and to properly represent the local driving pattern, the energy consumption and the vehicle emissions. To understand how the time duration of the driving cycle affects its representativeness results we took a first approach building DCs with a time durations of 5, 10, 15, 20, 25, 30, 45, 60 and 120 minutes using the MT method. We found a direct relation between the time duration of driving cycle and its capability to represent the local driving patterns and to reproduce the energy consumption and emissions. In the study regions we observed that DCs with short time duration (less than 10 minutes) presented higher values of \overline{ARD}_{CPs} than long DCs with time duration above 30 to 45 minutes. The \overline{ARD}_{EIs} showed the same tend to decrease when the driving cycle time duration increases. This analysis could be used as a methodology to define the suitable time duration of a driving cycle for a specific region.

At the end of this research, a complementary work was carried out focused on the development of a telemetry equipment to record the fuel consumption, speed and operating time of a vehicle under real driving conditions with a sampling frequency of 1 Hz. Design requirements of this telemetry equipment respond to the needs to develop local driving cycles

using the EBMT method. Alternatively, the operation database could be used to carry out different studies in eco-driving, the identification of traffic spots, the design of alternatives powertrains, among other research related to the vehicle energy efficiency. Nowadays, on the market we can find devices with the ability to monitor vehicle fleets remotely. However, the focus of these devices is the control and logistics of the fleets, and not for determining the energy and environmental impact of the vehicles. Additionally, it should be mentioned that there is no universal device that can be used in all types of vehicles. We found restrictions in the geometry of the connection port, and in the language of communication with the vehicle, and restrictions in the variables that can be delivered by the car. In the development of the telemetry equipment, an OBD device, a Raspberry PI 3B + card and a Huawei e303 transmission system were integrated. To validate the speed and fuel consumption data recorded by the telemetry equipment, it was installed on a light passenger vehicle. The instrumented vehicle was tested on different operating conditions that included tests at different constant speeds, tests at idling, tests with random speeds and accelerations, and tests on a dynamometer following a driving cycle. The recorded speed and fuel consumption were compared respect WTLC 3a speed data and fuel gravimetric test, achieving in both cases coefficients of determination R^2 above 97%. These results indicate that the values delivered by the telemetry equipment are similar to the real readings.

A first approach to implement the EBMT method were proposed using the trips data monitored under real driving conditions. We used as assessment criteria the average speed, VSP, % of time in idling and specific fuel consumption and the time duration of the driving cycle on $20 \text{ min} \pm 2 \text{ min}$. Due to the stochastic nature of the EBMT method, we constructed 500 driving cycles, and the ones with the lowest values of \overline{ARD} were selected. However, the proposed driving cycles must be evaluated on a chassis dynamometer in order to validate if a driven light-duty vehicle is able to follow the speed profile and the proposed accelerations.

Further work is required to expand the applicability of the acquired outputs and the EBMT method in different regions with different traffic conditions, with relevant variations in altitude, and with different and heterogenous types of vehicle technology, including hybrid and electric vehicles. On the other hand, despite the good results obtained in the development of the telemetry equipment, it is required to continue with the validation tests of the equipment. Then, it is recommended to install it in a medium to large size vehicle fleet in order to establish a data management process. Moreover, as an opportunity to expand the research in driving cycles, we recommend analyzing how to integrate mathematical data analysis techniques such as wavelets. We consider that this type of analysis could help to understand the changes in the driving patterns at local level and their relationship with the driving behavior and with traffic externalities.

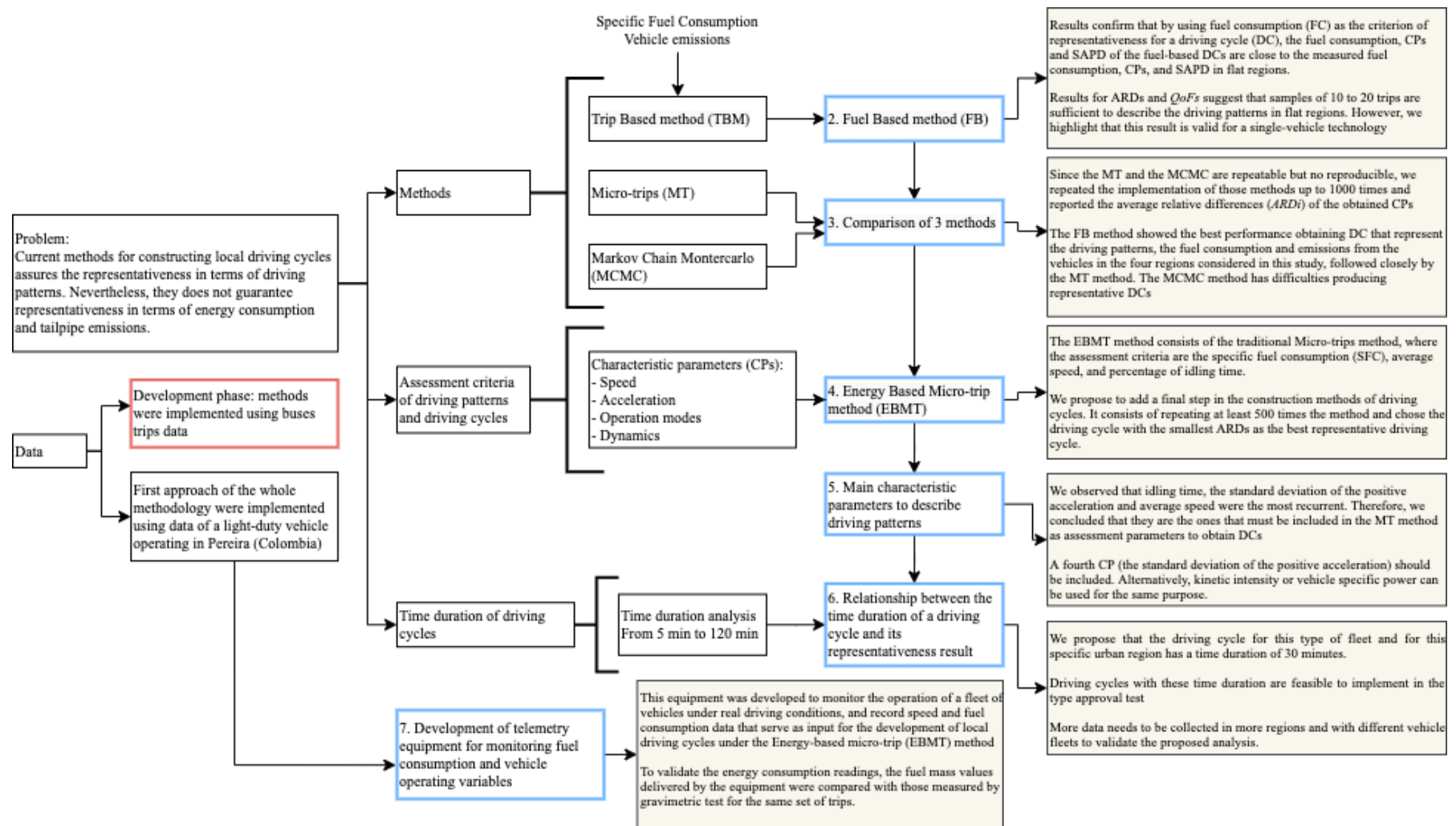


Figure 8.1 Methodology and main outputs of the thesis by chapter

References

- [1] X. Zhang, D. J. Zhao, and J. M. Shen, “A synthesis of methodologies and practices for developing driving cycles,” in *Energy Procedia*, 2011, vol. 16, no. PART C, pp. 1868–1873, doi: 10.1016/j.egypro.2012.01.286.
- [2] H. Y. Tong and W. T. Hung, “A framework for developing driving cycles with on-road driving data,” *Transp. Rev.*, vol. 30, no. 5, pp. 589–615, 2010, doi: 10.1080/01441640903286134.
- [3] U. Galgamuwa, L. Perera, and S. Bandara, “Developing a General Methodology for Driving Cycle Construction: Comparison of Various Established Driving Cycles in the World to Propose a General Approach,” *J. Transp. Technol.*, vol. 05, no. 04, pp. 191–203, 2015, doi: 10.4236/jtts.2015.54018.
- [4] EEA, “Improving Europe’s air quality – measures reported by countries,” Copenhagen, 2018. [Online]. Available: <https://www.eea.europa.eu/themes/air/improving-europe-s-air-quality>.
- [5] IEA, “CO₂ emissions from fuel combustion,” Paris, 2018. doi: 10.1670/96-03N.
- [6] IEA, “Energy Efficiency Indicators: Highlights,” Paris, 2016. doi: 10.1017/CBO9781107415324.004.
- [7] UPME, “Plan de Acción Indicativo de Eficiencia Energética 2017-2022,” 2016.
- [8] CONPES, *Política para el mejoramiento de calidad del aire*, no. Política para el mejoramiento de la calidad del aire. 2018, pp. 61–62.
- [9] U. Tietge, P. Mock, V. Franco, and N. Zacharof, “From laboratory to road : Modeling the divergence between official and real- world fuel consumption and CO₂ emission values in the German passenger car market for the years 2001 – 2014,” *Energy Policy*, vol. 103, no. November 2016, pp. 212–222, 2017, doi: 10.1016/j.enpol.2017.01.021.
- [10] L. Ntziachristos *et al.*, “In-use vs. type-approval fuel consumption of current passenger cars in Europe,” *Energy Policy*, vol. 67, no. 2014, pp. 403–411, 2014, doi: 10.1016/j.enpol.2013.12.013.
- [11] G. O. Duarte, G. A. Gonçalves, and T. L. Farias, “Analysis of fuel consumption and pollutant emissions of regulated and alternative driving cycles based on real-world measurements,” *Transp. Res. Part D Transp. Environ.*, vol. 44, pp. 43–54, 2016, doi: 10.1016/j.trd.2016.02.009.
- [12] Q. Gong, S. Midlam-Mohler, V. Marano, and G. Rizzoni, “An Iterative Markov Chain Approach for Generating Vehicle Driving Cycles,” *SAE Int. J. Engines*, vol. 4, no. 1, pp. 1035–1045, 2011, doi: 10.4271/2011-01-0880.
- [13] N. E. Ligterink and A. R. A. Eijk, “Update analysis of real-world fuel consumption of business passenger cars based on Travelcard Nederland fuelpass data,” 2014. doi: 10.13140/RG.2.1.3212.5040.
- [14] U. Tietge *et al.*, “From Laboratory To Road A 2017 update of official and ‘ real-world ’ fuel consumption and CO₂ values for passenger cars in Europe,” 2015.
- [15] G. Fontaras, N. G. Zacharof, and B. Ciuffo, “Fuel consumption and CO₂ emissions from passenger cars in Europe – Laboratory versus real-world emissions,” *Prog. Energy Combust. Sci.*, vol. 60, pp. 97–131, 2017, doi: 10.1016/j.pecs.2016.12.004.
- [16] Ministre de l’environnement de l’énergie et de la mer, “Contrôles des émissions de polluants atmosphériques et de CO₂,” Paris, 2016.

- [17] M. Tutuianu *et al.*, “Development of the World-wide harmonized Light duty Test Cycle (WLTC) and a possible pathway for its introduction in the European legislation,” *Transp. Res. Part D*, vol. 40, pp. 61–75, 2015, doi: 10.1016/j.trd.2015.07.011.
- [18] A. Ashtari, E. Bibeau, and S. Shahidinejad, “Using large driving record samples and a stochastic approach for real-world driving cycle construction: Winnipeg driving cycle,” *Transp. Sci.*, vol. 48, no. 2, pp. 170–183, 2014, doi: 10.1287/trsc.1120.0447.
- [19] E. G. Giakoumis, *Driving and engine cycles*. 2016.
- [20] M. Knez, T. Muneer, B. Jereb, and K. Cullinane, “The estimation of a driving cycle for Celje and a comparison to other European cities,” *Sustain. Cities Soc.*, vol. 11, pp. 56–60, 2014, doi: 10.1016/j.scs.2013.11.010.
- [21] H. Wang, X. Zhang, and M. Ouyang, “Energy consumption of electric vehicles based on real-world driving patterns: A case study of Beijing,” *Appl. Energy*, vol. 157, pp. 710–719, 2015, doi: 10.1016/j.apenergy.2015.05.057.
- [22] Q. Wang, H. Huo, K. He, Z. Yao, and Q. Zhang, “Characterization of vehicle driving patterns and development of driving cycles in Chinese cities,” *Transp. Res. Part D Transp. Environ.*, vol. 13, no. 5, pp. 289–297, 2008, doi: 10.1016/j.trd.2008.03.003.
- [23] S. H. Kamble, T. V Mathew, and G. K. Sharma, “Development of real-world driving cycle : Case study of Pune , India,” *Transp. Res. Part D*, vol. 14, no. 2, pp. 132–140, 2009, doi: 10.1016/j.trd.2008.11.008.
- [24] W. T. Hung, H. Y. Tong, C. P. Lee, K. Ha, and L. Y. Pao, “Development of a practical driving cycle construction methodology: A case study in Hong Kong,” *Transp. Res. Part D Transp. Environ.*, vol. 12, no. 2, pp. 115–128, 2007, doi: 10.1016/j.trd.2007.01.002.
- [25] L. C. Belalcazar, H. Acevedo, M. Ossess, and N. Rojas, “Construcción De Los Ciclos De Conducción De Bogotá Para La Estimación De Factores De Emisión Vehiculares Y Consumos De Combustible,” 2015.
- [26] J. Agudelo, A. Agudelo, and R. Moreno, “Ciclos de conducción de vehículos livianos y motocicletas para el Valle de Aburrá,” 2017.
- [27] A. Hurtado, “Ciclos de conducción para el AMCO,” 2015. .
- [28] M. A. Pouresmaeili, I. Aghayan, and S. A. Taghizadeh, “Development of Mashhad driving cycle for passenger car to model vehicle exhaust emissions calibrated using on-board measurements,” *Sustain. Cities Soc.*, vol. 36, no. September, pp. 12–20, 2018, doi: 10.1016/j.scs.2017.09.034.
- [29] N. H. Arun, S. Mahesh, G. Ramadurai, and S. M. Shiva Nagendra, “Development of driving cycles for passenger cars and motorcycles in Chennai, India,” *Sustain. Cities Soc.*, vol. 32, no. May, pp. 508–512, 2017, doi: 10.1016/j.scs.2017.05.001.
- [30] U. Galgamuwa, L. Perera, and S. Bandara, “Development of a driving cycle for Colombo , Sri Lanka : an economical approach for developing countries,” *J. Adv. Transp.*, no. September, pp. 1520–1530, 2016, doi: 10.1002/atr.
- [31] A. Esteves-booth, T. Muneer, H. Kirby, J. Kubie, and J. Hunter, “The measurement of vehicular driving cycle within the city of Edinburgh,” *Transp. Res. Part D Transp. Environ.*, vol. 6, pp. 209–220, 2001.
- [32] M. André, “The ARTEMIS European driving cycles for measuring car pollutant emissions,” *Sci. Total Environ.*, vol. 334–335, pp. 73–84, 2004, doi: 10.1016/j.scitotenv.2004.04.070.
- [33] J. Brady and M. O’Mahony, “Development of a driving cycle to evaluate the energy economy of electric vehicles in urban areas,” *Appl. Energy*, vol. 177, pp. 165–178,

- 2016, doi: 10.1016/j.apenergy.2016.05.094.
- [34] K. Brundell-Freij and E. Ericsson, "Influence of street characteristics, driver category and car performance on urban driving patterns," *Transp. Res. Part D Transp. Environ.*, vol. 10, no. 3, pp. 213–229, 2005, doi: 10.1016/j.trd.2005.01.001.
 - [35] E. Ericsson, "Independent driving pattern factors and their influence on fuel-use and exhaust emission factors," *Transp. Res. Part D Transp. Environ.*, vol. 6, no. 5, pp. 325–345, 2001, doi: 10.1016/S1361-9209(01)00003-7.
 - [36] H. Achour and A. G. Olabi, "Driving cycle developments and their impacts on energy consumption of transportation," *J. Clean. Prod.*, vol. 112, pp. 1778–1788, 2016, doi: 10.1016/j.jclepro.2015.08.007.
 - [37] D. Huang, H. Xie, H. Ma, and Q. Sun, "Driving cycle prediction model based on bus route features," *Transp. Res. Part D Transp. Environ.*, vol. 54, pp. 99–113, 2017, doi: 10.1016/j.trd.2017.04.038.
 - [38] J. Ko, D. Jin, W. Jang, C. L. Myung, S. Kwon, and S. Park, "Comparative investigation of NOx emission characteristics from a Euro 6-compliant diesel passenger car over the NEDC and WLTC at various ambient temperatures," *Appl. Energy*, vol. 187, pp. 652–662, 2017, doi: 10.1016/j.apenergy.2016.11.105.
 - [39] T. J. Barlow, S. Latham, McCrae I S, and Boulter P G, ! *REFERENCE BOOK OF DRIVING CYCLES FOR USE IN THE MEASUREMENT OF ROAD*. 2009.
 - [40] N. Tamsanya and S. Chungpaibulpatana, "Influence of driving cycles on exhaust emissions and fuel consumption of gasoline passenger car in Bangkok," *J. Environ. Sci.*, vol. 21, no. 5, pp. 604–611, 2009, doi: 10.1016/S1001-0742(08)62314-1.
 - [41] J. Pavlovic, B. Ciuffo, G. Fontaras, V. Valverde, and A. Marotta, "How much difference in type-approval CO2 emissions from passenger cars in Europe can be expected from changing to the new test procedure (NEDC vs. WLTP)?," *Transp. Res. Part A Policy Pract.*, vol. 111, pp. 136–147, May 2018, doi: 10.1016/j.tra.2018.02.002.
 - [42] Q. Shi, Y. B. Zheng, R. S. Wang, and Y. W. Li, "The study of a new method of driving cycles construction," *Procedia Eng.*, vol. 16, pp. 79–87, 2011, doi: 10.1016/j.proeng.2011.08.1055.
 - [43] S. H. Ho, Y. D. Wong, and V. W. C. Chang, "Developing Singapore Driving Cycle for passenger cars to estimate fuel consumption and vehicular emissions," *Atmos. Environ.*, vol. 97, pp. 353–362, 2014, doi: 10.1016/j.atmosenv.2014.08.042.
 - [44] J. D. K. Bishop, C. J. Axon, and M. D. McCulloch, "A robust , data-driven methodology for real-world driving cycle development," *Transp. Res. PART D*, vol. 17, no. 5, pp. 389–397, 2012, doi: 10.1016/j.trd.2012.03.003.
 - [45] J. Lin and D. A. Niemeier, "An exploratory analysis comparing a stochastic driving cycle to California's regulatory cycle," *Atmos. Environ.*, vol. 36, no. 38, pp. 5759–5770, Dec. 2002, doi: 10.1016/S1352-2310(02)00695-7.
 - [46] S. Shi *et al.*, "Research on markov property analysis of driving cycles and its application," *Transp. Res. Part D Transp. Environ.*, vol. 47, pp. 171–181, 2016, doi: <https://doi.org/10.1016/j.trd.2016.05.013>.
 - [47] J. I. Huertas, J. Díaz, D. Cordero, and K. Cedillo, "A new methodology to determine typical driving cycles for the design of vehicles power trains," *Int. J. Interact. Des. Manuf.*, vol. 12, no. 1, pp. 319–326, 2018, doi: 10.1007/s12008-017-0379-y.
 - [48] J. Liu, X. Wang, and A. Khattak, "Customizing driving cycles to support vehicle purchase and use decisions: Fuel economy estimation for alternative fuel vehicle users," *Transp. Res. Part C Emerg. Technol.*, vol. 67, pp. 280–298, 2016, doi:

- 10.1016/j.trc.2016.02.016.
- [49] National Academic of Science, *Highway Capacity Manual 2010*. Washington DC, USA, 2010.
 - [50] J. I. Huertas, G. Andrés, and Á. Coello, “Accuracy and precision of the drag and rolling resistance coefficients obtained by on road coast down tests,” *Proc. Int. Conf. Ind. Eng. Oper. Manag.*, pp. 575–582, 2017, [Online]. Available: <http://ieomsociety.org/bogota2017/papers/97.pdf>.
 - [51] J. L. – B. Vilnis Pirs, Žanis Jesko, “Determination methods of fuel consumption in laboratory conditions,” vol. 1, pp. 154–159, 2008.
 - [52] SAE, *Fuel Consumption Test Procedure - Type II*. 2012, pp. 1–50.
 - [53] R. Günther, T. Wenzel, M. Wegner, and R. Rettig, “Big data driven dynamic driving cycle development for busses in urban public transportation,” *Transp. Res. Part D Transp. Environ.*, vol. 51, pp. 276–289, Mar. 2017, doi: 10.1016/j.trd.2017.01.009.
 - [54] J. Huertas, M. Giraldo, L. Quirama, and J. Díaz, “Driving Cycles Based on Fuel Consumption,” *Energies*, vol. 11, no. 11, p. 3064, 2018, doi: 10.3390/en11113064.
 - [55] G.-H. Tzeng and C. June-Jye, “Developing a Taipei Motorcycle Driving Cycle for Emissions and Fuel Economy,” *Transp. Res. Part D*, vol. 3, no. 1, pp. 19–27, 1998.
 - [56] Environmental Protection Agency, “Determination of PEMS Measurement Allowances for Gaseous Emissions Regulated Under the Heavy - Duty Diesel Engine In - Use Testing Program,” 2008.
 - [57] M. Giraldo and J. I. Huertas, “Real emissions, driving patterns and fuel consumption of in-use diesel buses operating at high altitude,” *Transp. Res. Part D Transp. Environ.*, vol. 77, no. October, pp. 21–36, 2019, doi: 10.1016/j.trd.2019.10.004.
 - [58] B. Mashadi, Y. Amiri-Rad, A. Afkar, and M. Mahmoodi-Kaleybar, “Simulation of automobile fuel consumption and emissions for various driver’s manual shifting habits,” *J. Cent. South Univ.*, vol. 21, no. 3, pp. 1058–1066, 2014, doi: 10.1007/s11771-014-2037-x.
 - [59] M. Montazeri-Gh and M. Mahmoodi-K, “Optimized predictive energy management of plug-in hybrid electric vehicle based on traffic condition,” *J. Clean. Prod.*, vol. 139, pp. 935–948, 2016, doi: 10.1016/j.jclepro.2016.07.203.
 - [60] I. Huertas, L. F. Quirama, M. Giraldo, and J. Díaz, “Comparison of Three Methods for Constructing Real Driving Cycles,” *Energies*, vol. 12, no. 4, p. 15, 2019, doi: 10.3390/en12040665.
 - [61] R. E. Kruse and T. A. Huls, “Development of the federal urban driving schedule,” *SAE Tech. Pap.*, 1973, doi: 10.4271/730553.
 - [62] H. Steven, “Development of a Worldwide Harmonised Heavy-duty Engine Emissions Test Cycle,” 2001.
 - [63] H. Xie, G. Tian, H. Chen, J. Wang, and Y. Huang, “A distribution density-based methodology for driving data cluster analysis: A case study for an extended-range electric city bus,” *Pattern Recognit.*, vol. 73, pp. 131–143, 2018, doi: 10.1016/j.patcog.2017.08.006.
 - [64] F. An, M. Barth, J. Norbeck, and M. Ross, “Development of comprehensive modal emissions model: Operating under hot-stabilized conditions,” *Transp. Res. Rec.*, no. 1587, pp. 52–62, 1997, doi: 10.3141/1587-07.
 - [65] S. R. Kancharla and G. Ramadurai, “Incorporating driving cycle based fuel consumption estimation in green vehicle routing problems,” *Sustain. Cities Soc.*, vol. 40, no. September 2017, pp. 214–221, 2018, doi: 10.1016/j.scs.2018.04.016.
 - [66] EEA, “Explaining road transport emissions. A non-technical guide,” 2016. doi:

10.2800/71804.

- [67] D. G. C. Moreno, “Metodología para minimizar el consumo de combustible en autobuses, que sirven rutas fijas, mediante la reconfiguración del tren motriz,” Instituto Tecnológico y de Estudios Superiores de Monterrey, 2015.
- [68] L. Berzi, M. Delogu, and M. Pierini, “Development of driving cycles for electric vehicles in the context of the city of Florence,” *Transp. Res. Part D*, vol. 47, pp. 299–322, 2016, doi: 10.1016/j.trd.2016.05.010.
- [69] G. Amirjamshidi and M. J. Roorda, “Development of simulated driving cycles for light, medium, and heavy duty trucks: Case of the Toronto Waterfront Area,” *Transp. Res. Part D Transp. Environ.*, vol. 34, pp. 255–266, 2015, doi: 10.1016/j.trd.2014.11.010.
- [70] “IEA 2017 - Digitalization & Energy.pdf,” 2017.
- [71] U.S. DEPARTMENT OF TRANSPORTATION, “History of Intelligent Transportation Systems,” 2016. doi: 10.21608/kjis.2018.2741.1000.
- [72] L. F. Quirama, M. Giraldo, J. I. Huertas, and M. Jaller, “Driving cycles that reproduce driving patterns , energy consumptions and tailpipe emissions,” *Transp. Res. Part D*, vol. 82, p. 102294, 2020, doi: 10.1016/j.trd.2020.102294.
- [73] G. De Nicolao, R. Scattolini, and C. Siviero, “Modelling the volumetric efficiency of IC engines: Parametric, non-parametric and neural techniques,” *Control Eng. Pract.*, vol. 4, no. 10, pp. 1405–1415, 1996, doi: 10.1016/0967-0661(96)00150-5.